Oscillatory Behaviour and Strategy to Reduce Drilling Vibration

A thesis submitted for the Degree of Doctor of Philosophy

By

Suriani Binti Che Kar

Brunel University London

College of Engineering, Design and Physical Sciences

Department of Mechanical, Aerospace and Civil Engineering

April 2017

Declaration

This thesis titled "Oscillatory Behaviour and Strategy to Reduce Drilling Vibration" is submitted for the Degree of Doctor of Philosophy in the Department of Mechanical, Aerospace and Civil Engineering, College of Engineering, Design and Physical Sciences at Brunel University London.

I, Suriani, the undersigned, hereby declare that the research work in this thesis was carried out in accordance with the Regulations of Brunel University London. The work presented in this thesis is original, except where indicated in the text by special reference. The research has not formed the basis for any submission of any other degree. The views expressed in this thesis are those of the author.

The above–titled thesis has not been presented to any other University for award either in the United Kingdom or overseas.

Signed: Date: 30th April 2017

Suriani Binti Che Kar

Publications Based on this Research

(Che Kar, Esat, Alkhamees, et al. 2016) 'Drill String Dynamic : Improving the drilling performance by optimizing the speed limit and study the resonance of the experimental drill string system', *2nd International Conference on Mechanical and Control Engineering (ICMCE 2016)* at Bandung, Indonesia 18-19th March.

(Che Kar, Esat, Mohd Farid Woo, et al. 2016) 'Drill String Dynamic: Improving the drilling performance by study the resonance of the experimental drill string system using 2 contact points of friction force of breaking system', *7th International Conference on Mechanical and Aerospace Engineering (ICMAE)* London, United Kingdom, 18-20th July.

(Che kar Binti & Esat 2016) 'Drill String Dynamic' *Brunel Research Student Conference* (2016). London, United Kingdom, 25-26th June.

(Che Kar et al. 2017) 'Drill String Dynamic Improving the Drilling Performance by Optimizing the Speed Limit and Study the Resonance of the Experimental Drill String System', *Journal of Engineering and Applied Science* Volume 12 Issues 15 2017.

Abstract

Drill String dynamic behaviour during the oil drilling operation, was a major source for the failure of the Bottom Hole Assembly (BHA). The behaviour produced torsional vibration, which underpins the stick slip phenomena. Besides threatening the safety of the oil drilling process, such failure cause interruptions in the drilling operations and incurred high maintenance cost to the oil drilling company. This issue can be resolved with the implementation of the optimum control mechanism while operating the drill string. In this research, an optimum control mechanism was proposed to suppress the torsional vibration as well as mitigate the risk of stick slip phenomenon from occurring. The mechanism was proposed through a series of rigorous research strategies i.e. updated-mathematical equation modelling, experimentation and simulation. As the first step, a mathematical equation model describing system dynamics was derived to set the parameter of investigation. Representing the freedom torsional of the two degrees - conventional vertical drill string, the model was used to predict the frictional Torque On Bit (TOB) through non-linear friction force, denoting the ground-formation behaviour during drilling activity. Using a velocity feedback system, the drill-string oscillation was reduced while gradually increasing its velocity via gain scheduling method – allowing fast response to load disturbance. To avoid the motor torque from exceeding the maximum threshold, a Weight On Bit (WOB) was introduced. This approach remarks the novel contribution of this research. Next, an experiment on the preliminary test rig within a controlled laboratory set up was conducted. The rotary drill rig was assembled to identify the dynamics (i.e. parameters) of an individual part of the drill string. The results obtained were then applied in the drill string operation experiment, to identify the optimum control mechanism that can avoid the torsional vibration. To enable triangulation of results, a simulation was conducted by applying the same parameters obtained from the test rig experiment in the model– which is the optimum control mechanism that was proposed in this research to minimise torsional vibration, as well as reducing the chance of drill-string failure due to stick-slip phenomenon.

Acknowledgement

TABLE OF CONTENTS

List of Figures

List of Tables

List of Abbreviations

PWM	Pulse width Modula
IDE	Integrated Development Environment
SISO	Single Input Single Output
MISO	Multi-Input Single-Output
MCU	Micro Control Unit
ROP	Rate Of Penetration
WOB	Weight On Bit
TOB	Torque On Bit
BHA	Bore Hole Assembly
MWD	Measurement While Drilling
IDE	Multi-Platform
DVMCS	Drilling Vibration Monitoring & Control System
BACK-EMF	Back - Electromotive Force

List of Notations

g   Vibration amplitude

RPM   Rotational speed

(t)   Time

A   Current flow

W   Power input

V   Voltage input

º   Degree

f   Frequency

ω   Angular Velocity

Chapter 1

Scope of the Thesis

1.1 Purpose and Scope

The depth of the drill string has complicates its measurement, thus impedes the development of optimum controller that is able to reduce vibrations. The situation has resulted into serious issues, particularly on efficiency, reliability and safety of the drilling operation, which has become a concern for the oil industry. This has become a motivation for this research. Hence, this study attempts to introduce a controller system that is able to prevent the stick slip phenomenon, by reducing the torsional vibration.

To do so, this research defines the drill string system, developed through numerical simulation – describing the vital dynamics and exhibiting torsional vibrations. The torsional vibration has become the main research focus, where the system was modelled as a pendulum. This model studies the friction forces that were created due to the bit-rock interaction. Considering various drill string parameters, the results of the experimental test rig indicates varying parameters such as mass, stiffness and constant damping of the string contribute towards torsional vibration. Assuming all of the frictions being liner, these parameters were verified during simulation and experiment conducts, in order to design the controller, which was proposed as the research findings. The main advantages of this proposed non-linear controller is its ability to reduce the torsional vibration, which is the key to mitigate stick-slip phenomenon. As advocated earlier, the constant occurrences of such phenomenon potentially lead to critical issues such as drilling inefficiency, unreliability and threat to safety (Dwars, 2015; Runia et al., 2013). The establishment of this finding offers solution towards such issues, by eliminating the stick slip phenomenon.
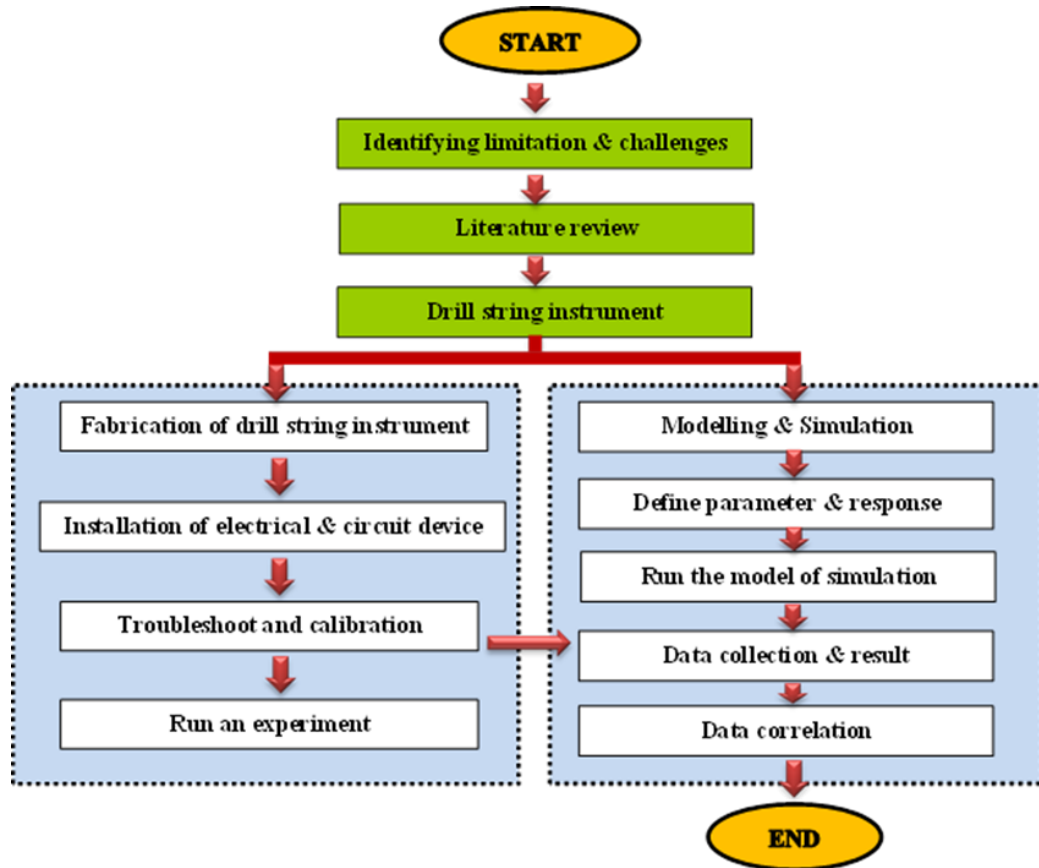
Figure 1.1: Research flow chart

1.2 Research Objectives

Avoiding drill string failure is of paramount important. Therefore, it is important to know how to identify such failure through certain indicators i.e. vibration types, consequences, symptoms and the coupling modes.

As the drill string system becoming more complex, a more advance method such as computer simulation is needed to tackle such complexity. Based on the dynamical system and mathematical modelling, the software allows the construction of a more precise analysis of the drilling systems. However, to enable such precise analysis, the software needs an up-to-date mathematical modelling capability, as the existing models are limited. Such model was based on construction of trajectories numerical integration of differential equations describing dynamical systems, hindering a broader investigation of stability and oscillations of the drilling systems, Figure 1.1 described details of a schematic of the research plan. The research introduced with a comprehensive literature review to understand the vibration behaviour and the purpose

of the research. Hence, this study proposes a state of the art simple model, yet featuring complex effects.

The frequency of failure occur at drill string assembly has become one of the most common problems in oil and gas industry entailing other implications, particularly cost. Such implications were objectively measured in a few studies, especially by (Horbeek et al. 1995) and (Shokir 2004), discovering the facts as shown in Figure 1.2.

1985
• 45% drill string failures due to deep well drilling problems

1991
• Shell Expro loses more than US $ 2MM loses within two months

1992
• Shell Expro develop a "Drill String Prevention Quality Improvement Project" to provide assistance.

1994
• Shell expo losses were reduced to less than US $1MM (improved performance by 55% i.e. US $8.5MM savings)
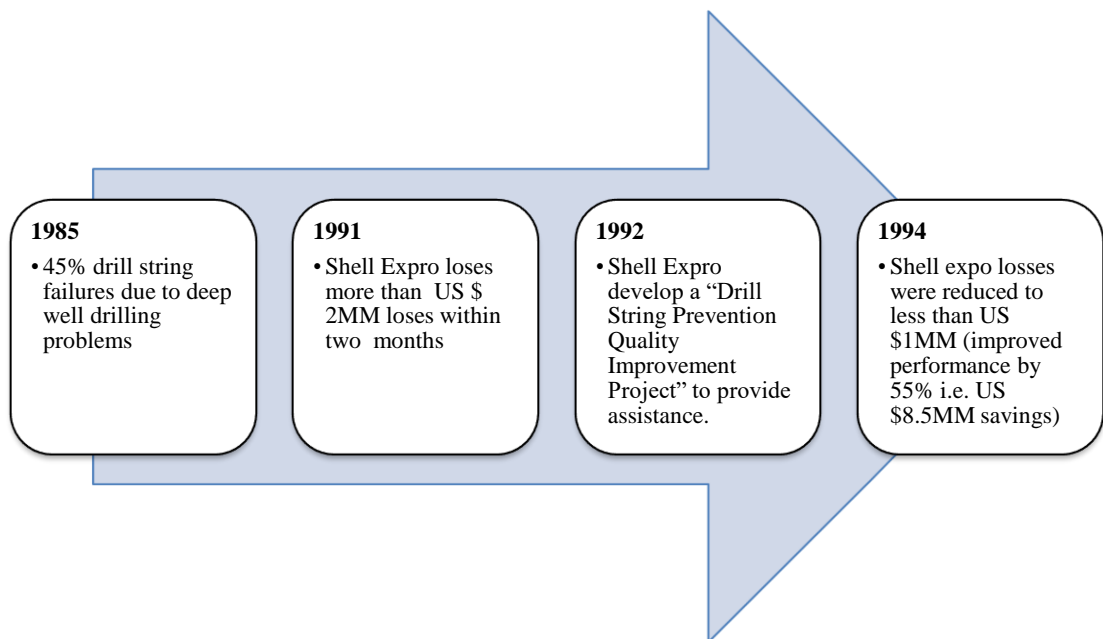
Figure 1.2: Drill String Cost Failure

The studies found that each failure cost the company US $106, 000, and 1 out 7 drill rigs was at risk of failure. Therefore, the issue of drill string failures was proven to be extremely critical.

The drill string failures are potentially caused by many, particularly due to torsional vibrations. The torsional vibrations or stick slip phenomena are due to the non-linear interaction between the bit and the rock, known as stick slip event – which possibly exacerbate a sudden stop of the drill rotation.

Based on these arguments, the objectives of this study are as the followings:

1) To develop a lumped (simple) parameter model that will be used to describe torsional model.

2) To incorporate the 'bit-rock interaction' effect in the lumped parameter model developed in (1), in identifying the bit-rock interaction effects on the drill string – since the frictional torque appears on the system. The model consists of two ends i.e. upper and lower extremities that dynamically create the 'bit rock interactions', which is the root cause of stick-slip phenomena affecting the drill string failure. Therefore, it is pivotal for the bit rock interaction to be accounted for in the model.

3) To identify strategies to minimise the stick-slip phenomena that will reduce the risk of drill string failure, using system simulations in order to highlight the proposed strategies.

4) To analyse control strategies that were identified in (3) in order to propose the optimum control mechanism.

Chapter 2

Preview of Research

2.1 Introduction

Drilling is one of the most expensive operations in oil and gas exploration. Drilling costs increase during exploration in more hostile, more-complex well program, deeper well and environment pressure (Bourgoyne et al. 1986). A lot of experimental researches about drill string dynamics have been done by researcher since the 1950s.

For the past few decades, extraction of fossil fuel from the boreholes has been a fast growing field as the importance of the petroleum industry increased. Most of the fossil fuels resources become a major contribution source of energy, which is very importance to our daily use. In order to provide such unlimited demand and reserve of fossil fuel the effectiveness of oil rig should be improved to maximize the exploration of the fossil fuel. Oil well drilling involves drilling through kilometres of rock to access the reservoirs (Petzet 2009), Transocean Ltd's Deepwater Horizon ultradeepwater semisubmersible drilled Tiber true vertical depth is about 10.69 km measured depth.

Increasing the performance and avoiding failure which are very costly relates to the time taken in drilling. Drilling vibration is one of the main cause of performance loss due to bit wear, mass imbalance, and frictions of column and borehole wall (Dunayevsky et al. 1993a), or between bit and drilling surface, pipes disconnections, borehole disruption and also time constrain for drilling might involve to reduce to economic loss. By focusing on the dynamic behaviour of the drilling equipment, especially in drill string, and expanding development of control technology will potentially offer solution for the development of controlling software that enables automation adaption to the drilling process. These control approaches has been tested

and proven to reduce the induced vibration especially in the torsional vibration because of stick slip phenomenon which are the main interrupt to drill string failure

Many researches have conducted tests to tackle the vibration problem during the drilling process. Three main vibration modes can be observed in the drilling processes which are lateral, axial, and torsional, each vibration giving different type of problems and damages. Each vibration separates into specific phenomenon such as bit bounce, whirl and stick slip, those phenomena which as a result of the vibrational modes have such a damaging effect on the drilling process. The rotary drill system has been controlled by many methods in order to reduce the presence of vibration. (Gonzalez-Garcia et al. 2011) mention as three method to detect the vibration which are sensor, surface sensor, and post-run inspection.

The interaction between contact bit and rock formation may results in unstable rotational speed movement at the BHA while top drive rotary speed is constant. Non-linear relationship results in oscillations namely stick slip phenomena. This motion comes due to the difference between static and kinetic friction; when Torque On Bit exceeds the force required to overcome the torsional stiffness in the string is sufficient to result in a zero velocity, while the top drive still rotates with a constant speed. Torsional energy is built up within the string until it exceeds the torque on bit, the bit rotates reaching speeds in excess of the top drive due to the energy released in the string. These stick slip event are started by the bit rock interaction and downhole friction which provides the torque on bit. Torsional vibrations promote many negative consequences, such as fatigue to drill collar connection, damage the drill bit, thus slowing down the drilling operation, prolonging the overall drilling process.

The destruction or mitigation of these vibrations can be done actively or passively, by control and monitor the Measurement While Drilling (MWD). Some methods are introduced and can be used to avoid vibrations, this can be achieved by decreasing WOB and increasing Angular Velocity at the upper part while varying WOB and this may mitigate the torsional vibrations which give impact to drilling performance, quality of the borehole wall and damaging of the components. These two common types control techniques are fully and semi-automated drilling systems.

In the late 19th Century active damping technique was one of the methods introduced to overcome the problem of the stick slip in drill strings. (Al-Hiddabi, S.A. et al. 2003) Nonlinear controller was also introduced to minimise the oscillations of the vibration, meanwhile (Abdulgalil & Siguerdidjane 2005) have developed a PID and back-stepping control technique used to measure error as result between measured variable with desired set point. A more detailed elaboration is presented in the literature review.

The nonlinear relationship between bit velocity and Torque On Bit (TOB) with inconsistences in rock formations, effect of drilling fluid and constantly changing dynamics properties and borehole wall interaction, which mean the dynamic models are required to investigate analyse and design suppression methods.

2.2   Vibration Induced to Drill String Failure

Vibration in drilling is a major cause of component failures, with more than a dozen potential failure mechanisms. However, many factors may play parts in its failures by a specific mechanism as showed at Figure 2.2 and Figure 2.3 for an example. The failure mechanisms includes, Drill pipe tube fatigue, BHA connection fatigue, Torsion, Tension, Sulphide Stress Cracking (SSC), Combination tension/torsion, collapse, split box, weld related failure, stress corrosion cracking (SCC), connection leak, frictional heating and galling. Those failure modes are accountable for the vast majority of drill string failure. Thus (Fearnley 2011) when the drill pipe tube fatigue combine together with BHA connection fatigue account for 80% of all drill string failures. Although drill bit and drill string are very complex motions this motion can be with three basic vibration modes. Figure 2.1 shows three basic vibration modes, torsional (stick sip), axial (longitudinal) and lateral (transverse).

The harsh nature of drilling oscillations to be subject to the direction of vibration occurs. Torsional vibrations leading cause effect threaded pipe connections, meanwhile axial vibrations damaging effect on the Bottom Hole Assembly (BHA). Direction of drilling may cause drilling oscillations and torsional vibrations that can damage threaded pipe connections. On the other hand, the axial vibrations potentially harm the BHA components (e.g. down hole, drill collar, drill bit), while the lateral

vibration leads to the propagation of fatigue (e.g. induced fissures in screwed joints) (Saldivar et al. 2015), torsional (i.e. stick slip) motion causing by twist-off and torque.
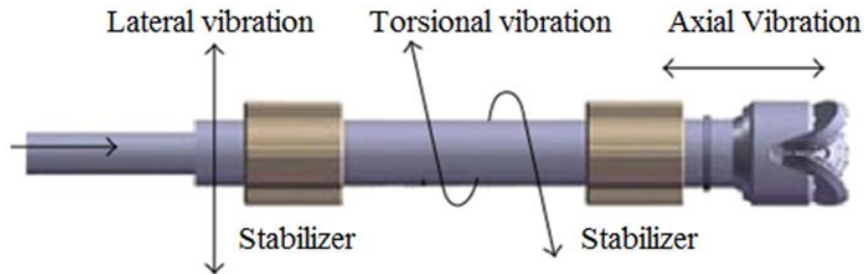
Figure 2.1: Illustrated of vibration behaviour (Ren et al. 2016)

Overall view of drill string system is shown in Figure 2.4 and described in Table 2.1. The main part of drilling system is called the drill string and it can be up to 1000 to 8000m long, BHA include drill bit and drill collar. Other than BHA, drill string system also consists of drill pipe sections, typically around 10 meter (Saldivar et al. 2015), drill collars used to stabilize the drill bit, drill bit which is cutting part to break through the rock formation usually we called as a bit. The drill string is rotated through a motor placed on top of the Kelly. The drill string pipe must be hollow to enable the injection of the drilling fluid by a mud pump, in extracting the removed rock.
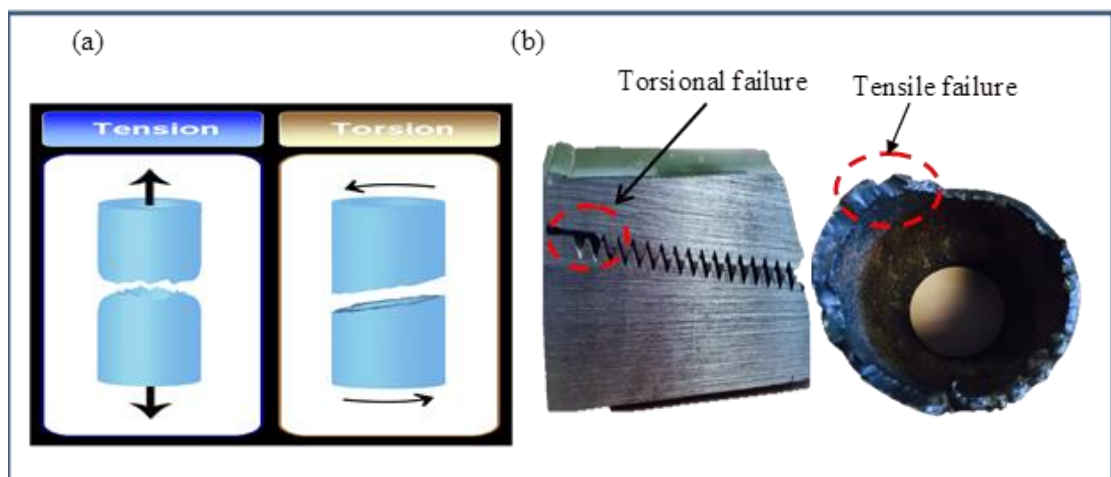
Figure 2.2: Torsional failure and Tensile Failure

(a)   Source: Pegasus Vertex, Inc. – (Liu 2012)

(b)   Source: Course training manual Rev.4 – (Fearnley 2011)

Figure 2.3: Drill string separation and drill string washout (Fesmi Abdul Majeed 2013)
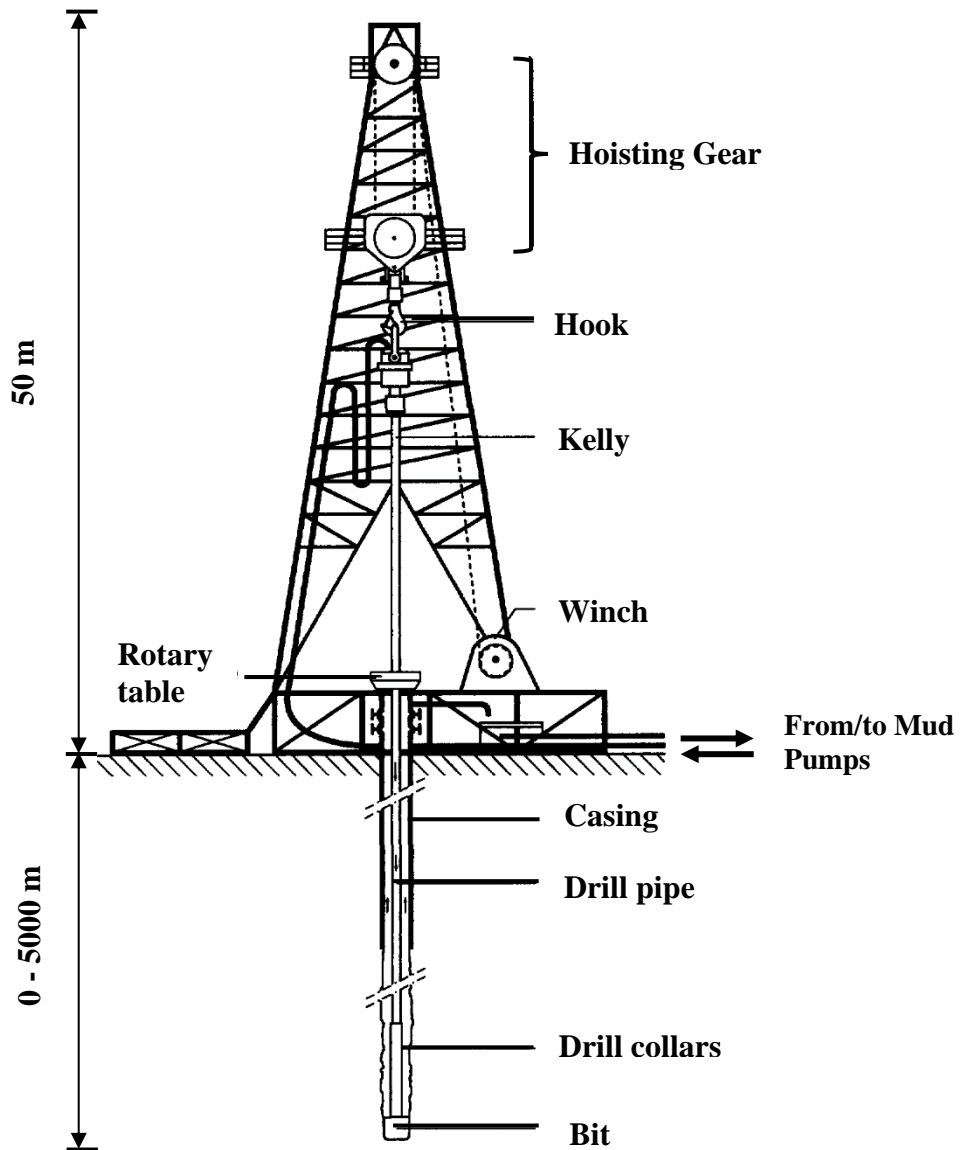
Figure 2.4: Basic components of an oil well drilling rig (Jansen 1993)

Table 2.1: Description of the drilling system component (Saldivar et al. 2015)

No	Part	Description
1	Top extremity	The rig consists of several part of rotating equipment. The turntable which is place at the surface of ground is called as rotary table. It drives the entire drill string using power from electric motor.
2	Drill string component	The drill strings are connected to the turntable and consist of drill pipes and drill collars: • **Drill pipe string** Is one of the long shafts which connect to upper part and drill bit. The length is depends to the drilling depth, typically final hole depth can be 1000 to 8000m for ultra-deep drilling. • **Drill collar** The purpose is to give weight on drill string. Drill collar tube length is about 300 to 350 meter long with 40 to 60 tons weight at the bottom hole. The thicker part of the drill collar name is stabilizers and used as protection from well bore friction towards drill string. Drill collar is the most affected part when the lateral vibration induced that because of the drill string failure. • **Drill bit** Is a cutting tool, attached at the end of the drill string. Fixed cutter tools are used to cuts the rock while roller cone ones act more by crushing. Diamond used as agent to cutter. Most of vibration and shock affect the drill bit which cause decreasing of rate of penetration.

3	Measurement while drilling (MWD)	This tools used accelerometers and magnetometers for measured wellbore inclined and azimuth. other than this MWD also can measure:
		  i. Drill string speed
		  ii. Downhole temperature
		  iii. Weight on bit (WOB)
		  iv. Torque on bit (TOB)
		  v. Mud flow volume
		
		There are three technique to measures and transmitted data to the surface:
		
		i Mud pulse telemetry technology,
		Where a valve varies the flow of the drilling fluid depends to the information to be transmitted. The bandwidth can be up to 40bps.
		
		ii electromagnetic telemetry,
		This one is different part to the drill string sections which

		is generates voltage, and where all the data are transmitted through digital modulation; its offers data rates of up to 10 bps. *iii. wired drill pipe,* Wired drill pipe technology transmitted the date through electric wires, wired drill pipe yield data rates upwards of 1Mbps.
4.	Logging while drilling (LWD)	Typically used for measuring geological characteristics like density, porosity, resistivity, acoustic-calliper, inclination at the drill bit, magnetic resonance, and formation pressure. The information is not directly transmitted to the surface but its keep to local memory, and extracted when the LWD tool is brought to the surface.

2.3 Literature Review

As the outcome of a research that was conducted by (Texter et al. 1949), the American Petroleum Institute has made a recommendation to avoid the "critical rotary speed" (American Petroleum Institute 1987, 1989). Based on this, a review on existing literatures was conducted to discuss about the general perspective of vibration, including various mode of vibration and their behaviour to the drill string vibration phenomena and narrowed down to a specific study which is natural frequency and their consequences and the resonance of the system. This approach applied in experiment of rotary drill string natural frequency and their resonance intend to destructive failure. In order to reduce number of drill string failure, the study of drill string comes to very high demand and important. Statistic by (Horbeek et al. 1995) and (Vaisberg et al. 2002) an approximation of 45% of all oil rigs failure and damage comes directly from the string itself. Researcher nowadays develop to reduce the failures of the strings according to (Besselink et al. 2011), (Mihajlovic et al. 2004b), (Germay et al. 2009) and (Viguié & Kerschen 2009) estimated that one out of seventh rigs experience such a drill failure shows that the drill string still break.

(Mason & Sprawls 1998) the cause of vibration can effected premature wear and tear of the drilling equipment, and influence of the fatigue failures such as drill pipe tube fatigue or washout failure and twisting (Macpherson et al. 1993) state that the vibrations can also cause significant wastage of drilling energy. Other than that it may

often induce wellbore and stabilities that can worsen the condition of the borehole while reduced the direction of control (Dunayevsky et al. 1993a).

At present, drilling for oil and gas production has introduced new prospects for petroleum professional and engineers try to counter the influence of the vibrations. While latest technology approach has been deployed such problem situation still arise, thus require control method in order to improve perforation processes performance. Since 1994, some efforts have been looking and narrow down to concentrated development of suitable control to reach desired targets. Vibration control means in this situation is to mitigate and minimize system oscillations, in many ways control can be divided by passive, active or semi active. There are three categories of vibration method mitigation which is isolation, cancelation and damping. Vibration isolation includes the avoidance of transmission of vibrations through the system. Vibration damping normally is a term that used to reduce the amount of the energy that produced by the system. When disturbances occur at certain frequencies which are very close to the resonant frequencies, forced vibration damping may not be effective. Meanwhile passive vibration cancellation is achieved by adding the oscillating system with dynamic absorber however active vibration cancellation involves with active elements, sensor and controllers to produce an out phase actuation that remove the disturbance producing the vibration.

2.4   Natural Frequency and Resonances

Free vibration of any moving part or structure means natural vibrations can occur at the frequency called the natural frequency, if one of the structures vibrate and become excited at one of its natural frequencies, then the resonance will take place with resulting increase of oscillation amplitudes.

Drill collar length is the most important in the BHA problem (Dareing 1984). Dareing used mathematical models, applied excitation at the natural frequency and the critical speeds. In his study he proved that axial and torsional vibration modes appear separately. Resonance will exist when the frequency of the string itself is equal to a natural free vibration frequency. Shock absorber proved to minimize the effect of vibration. (Santos et al. 1999) found that operation at critical speeds can cause damaging harmonics, generating high stresses. The main focus on this research is to

reduce drill pipe fatigue failure. Drill string vibration analysis have been developed according to composition, weight on bit, wellbore diameter, distance from the bit, geometry of wellbore, fluid properties. All this account to drill string critical frequencies vibration and easier to estimate drill string stresses and lateral displacements (W. Dykstra et al. 1994), (Besaisow et al. 1990), (Aarrestad & Kyllingstad 1988) and (Aadnoy 1986) This research suggested that drill string rotational speeds in the range of resonances should be avoided. (Cobern & Wassell 2005) classify that all of the vibration occurred in the range 1 Hz to 10 Hz. The project showed the most destructive phenomena is bit whirl dynamic meanwhile backward whirl can be expected reaching until 100 Hz. The total length of the drill string is the key factor that determines the range of the natural frequency (Cobern & Wassell 2005). In (Cobern et al. 2007) Optimal drilling cannot be achieved where the drilling operated below the resonant frequency while vibration can be minimize when the drilling operation plays above the resonant frequency. The drill string vibration and resonant frequency are the major important research and (Bailey et al. 2008) designed the model and studies the critical point that induced the resonant.

There are two approaches to analyse the drill string vibrations which is quantitative approaches is a forced vibration response for whole drill string (W. Dareing & Joe Livesay 1968). In this case mathematical model have been developed for torsional vibration modes and computer can predict based on model developed through downhole drill string measurements vibrations. Therefore this model, forced vibration response is very useful to determine the design criteria and test specifications (Dareing 1984). Another approach is qualitative, basically is a definition by resonance frequencies (J Bailey & Finnie 1960). Mechanical vibration can caused resonance of excitation to a natural frequency. Vibration also can be eliminated by detuning these two frequency axial and torsional mode vibrations. Previous paper (Dareing 1984) study on natural frequency of BHA especially at the collar section was a major factor in control the vibration.

Table 2.2: Drill string vibration type and their consequences Source: Sperry Drilling Service, Halliburton – Drilling evaluation and digital solution 2007 (F.A. Majeed 2013)**.**

Mechanism	Mode of Vibration	Frequency	Consequences
Stick-slip	Torsional	0.1-5 Hz	PDC bit damage, lower ROP, back off and drilling twist offs.
Bit-bounce	Axial	1-10 Hz	Damage to the drill bit cutting structure, bearing and seals. Hoisting equipment may damage in shallow wells.
Bit whirl	Lateral/Torsional	10-50 Hz	Damage to the bit cutting structure. Creates ledges as the weaker rock will be enlarged to a greater diameter than the stronger rock.
BHA (forward and backward whirl)	Lateral/Torsional	5-20 Hz	Causes BHA and down hole tools failure. Increases fatigue rates of these components. Damages drill collar and down hole electronic.
Lateral shocks	Lateral	Irregular Impacts	Causes MWD (Measurement While Drilling) component failures (motor, MWD tool, etc.); localized tools joints and/or stabilizer wear; washout or twist offs, increases average torque.
Torsional Resonance	Torsional	20-350 Hz	Backwards turning of the bit and cutter damage; damage to down hole electronics.
Parametric Resonance	Axial/Lateral	0.1-10 Hz	Create the opportunity for borehole enlargement; Poor directional control whirling.
Bit Chatter	Lateral/Torsional	20-250 Hz	Bit cutter impact damage, Electronic failure; Bit dysfunctions that can lead to bit whirl.
Model Coupling	Lateral/Torsional /Axial	0.1-20 Hz	Cause BHA and down hole tools failures. Increases fatigue rates of these components. Damages drill collar and down hole electronic failure.

2.5   Bit-rock Interaction

It is usually assumed that the big issue leading to stick slip and bit bounce oscillations, one of the mechanisms which are non-linear friction present between two surfaces, cutting device and the wellbore. The presences of the friction into vibration stick slip phenomena, allows the appropriate controls strategy to be to prevent the drill string going to the vibration phenomena. The system model must be subject to a suitable friction law, (Saldivar et al. 2015) study on how to estimate the physical phenomenon between bit and rock due to bit rock interaction laws. The most popular model is the Coulomb friction model; this is widely used because of model simplicity to predict the direction and magnitude between two dry surface contacts. Linkage Physical characteristics and type of lubricant existence must be taken into account to derive. several modelling approaches has been introduce and one of them called Stribeck effect (Stribeck 1902) will present due to unequal geometry of the point contact and where the stick slip phenomenon arises. Karnopp's model with rotating friction model was simulated accurately and also the stick slip phenomena. However, the model does not include the viscous friction effects at higher velocity's, since the stick-slip phenomena of main interest this was believed acceptable for the simulation and considered in the results. The Karnopp's friction model is widely used for practical purposes, for this reason, simplified torque on bit model proposed in Figure 2.5 which described essential dynamic properties (Knüppel et al. 2014).
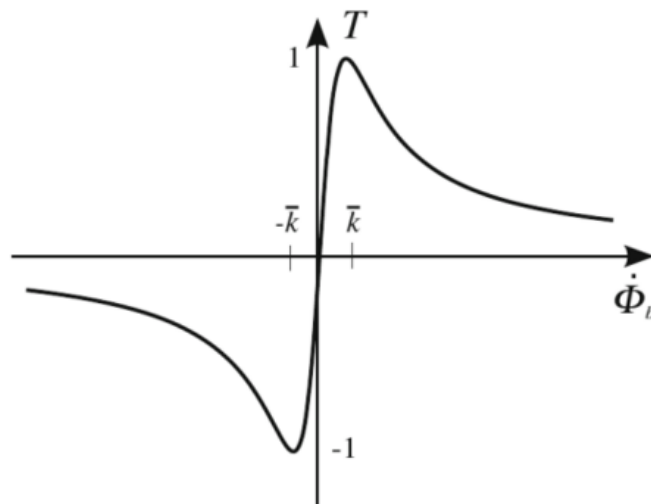
Figure 2.5: Simplified torque on bit model proposed by (Knüppel et al. 2014)

2.6 Friction Modelling

The friction phenomenon has been study for hundreds of years. Leonardo Da Vinci was the first person to create an experiment which proved that the frictional force is proportional to the normal force or load, and the frictional force is independent of the contact surface area. It is a natural phenomenon when two surface is slide against each other (Saldivar et al. 2015). After that in 1699 Guillaume Amontons refined the theory of the friction properties known as Fundamental Laws of Friction (Hutchings & Shipway n.d.) and followed by Charles-Augustin de Coulomb, 1781 (Oliveira 2004).

As we mention earlier, the torsional vibrations can lead to the stick slip phenomenon induced by bit rock interaction. Friction is a natural phenomenon that occurs as the motion which two sliding surface is resistance, the friction phenomena can be divided into static and dynamic friction phenomena, classical models have been developed allowed relative force to overcome the friction at different stages here only there main model will described for a better understanding of the model so that researcher can predict the dynamics state of the system thus enable to an appropriate control techniques to be applied. First model is Coulomb Friction model which was the classic model, whereby friction forces is proportional to the load, opposes the direction of motion and independent to contact surface.
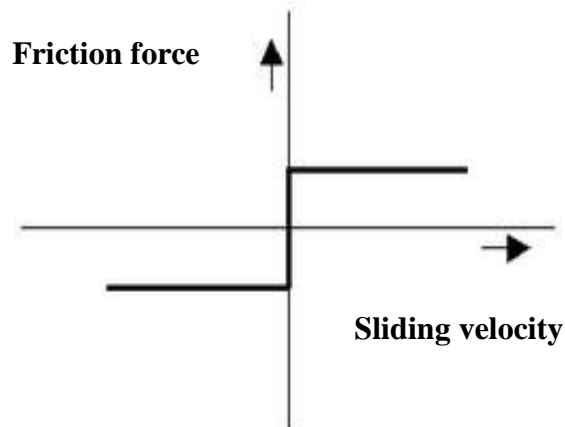
Figure 2.6: The coulomb friction model (Olsson et al. 1998)

Coulomb model Figure 2.6, are the combinations of static and kinetic friction which are the normal force is proportional to the friction and how much force is required to induce relative motion between the two different moving surfaces (Popov 2010).

Second model is viscous friction describe by friction induce associated with the velocity between two moving surfaces. Osborne Reynolds introduced the theory of fluid film lubrication because lubricant is a agent which can reduce friction forces and wear. In different situations viscous friction combined together with coulomb friction therefore the combination is used to represent the dynamics better. The last model we will discuss here is the stiction model, stiction friction or high static friction is a common problem to overcome the adhesion and deformation. The static friction force need to start the movement is more than kinetic friction force its just to keep the motion maintained.

The major factor for friction force induced adhesion including surface roughness described in the coulomb friction model. The classical friction components combination can be at any different way see Figure 2.6 and Figure 2.7 combined (Olsson 2001). All of model describes is represent the bit-rock interaction.
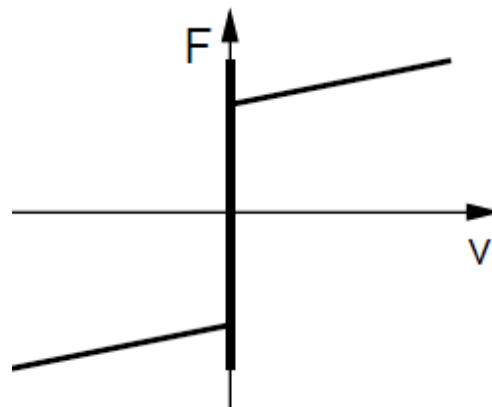
Figure 2.7: Stiction plus coulomb and viscous friction (Olsson et al. 1998)

2.7 Data Acquisition and Monitoring

A proper drilling operation requires certain tools for supervising, analyzing, displaying, recording and also retrieving information. Acrcording to (Azar & Samuel 2007). The main parameters to be developed and monitored are included, the mud flow rates, the hook load, depth of the well, the pump strokes, the weight on bit, the hoisting speed, and also density, temperature properties and salinity.

In real drilling operation monitoring tools will help to identify the problems related to the drill string vibrations such as well kick and pipe sticking. A suitable drilling

performance is such a proper maintainence of the Weight On Bit (WOB), the rotary speed and the flow rates of the drilling mud. The monitoring and control are very imoportant for the entire drilling operations. At present, the expertise only concentrating on monitoring, recording, analysis, storage, and recovery of drilling data and it is part of the drilling operation process routine. Control and monitoring methods have involved over the years. Here are some of the description or sequential review of the main technique of sensing and supervising the drilling data.

Developed in the 1960s by Bailey and Finnie (Bailey & Finnie 1960) and (J Bailey & Finnie 1960), from the Shell Development Company the most popular of study on drill string vibration, (Leine et al. 1998) were carried out by using a surface measurement while drilling, to measure torque, axial force, rotation, and also axial displacement.

In 1968, Esso Research Company study on down hole recording equipments to measure downhole forces and motions for internal and external (Deily et al. 1967), The equipment also can measure axial, torsional and bending forces and moments for internal and axial, lateral and angular accelerations for external pressures.

In 1986, the research more to improving drilling perfornmance through a better knowladge of the dynamic phenomena handled by French oil company EIL-DYNAFOR research project, Dynamètre used as device measuring tension, torque and accelerations in three directions at the top of drill string.

1980s, (MWD) Measurements while Drilling systems were developed. The significant for resercher is to save time by obtaining formation evaluation and drilling optimization data while drilling operation, and also can reduce failures. (Aarrestad & Kyllingstad 1988) study on coupling between bit torque and axial load at the bit the research developed by Aarrestad and Kyllingstad of Rogaland Research Institute. In the late 1980's. Cook et al. proposed the first real-time downhole Root Mean Square (RMS) which is to measure forces, accelerations and fluid pressures. The *Institute Français du Pétrole* introduced by modelled TRAFOR system consists of a downhole measurement sub (*Télévigile)*, (*Survigile*) is a surface measurement device. The signal of the Télévigile and Survigile are obtained by a computer and synchronized. The Télévigile is connected to the surface equipment to measure WOB, TOB,

accelerations in three directions and bending moments in two direction are measured meanwhile this tools also can measure torque, tension, and rotary speed at the surface. The advantage of the TRAFOR system is the capability to measure into downhole and surface data at real time.

In (Besaisow et al. 1990) introduced ADAMS (Advanced Drill string Analysis and Measurement System) which measures only surface data, the surface had a large spectral content and introduce diversity descriptions of the peaks that were observed.

In (Dubinsky et al. 1992) describe a historical overview of Russian, European and American research based on surface monitoring of downhole vibrations. The Russians objective was to optimize the performance of turbines by the 1970s, after that they coming out with a method to detect stick slip vibrations exists though using a turbine by inspecting the auto-spectral density of the surface axial accelerations. Meanwhile in the United States the objective of their researcher was to minimize the drill string failures. The author suggested that downhole to be able to observe. New technology has allowed the development of innovative systems for measuring and controlling the drilling data. Drilling Vibration Monitoring & Control System (DVMCS) is one of the technology solutions that both can measure and monitor the downhole drilling environment, also able to control the damping drilling-induced vibrations. The experimental result for design and modelling shown in (Cobern & Wassell 2005). Data acquisition devices (sensors) can be wired or wireless. Normally most sites used wired sensors, however their cost is very high and they may not be suitable for harsh conditions, meanwhile they also very hard to used and difficult to maintain, because of these difficulty and costly, so the research keen to develop of the sensor equipment taking into account of benefits in cost, easy to use, flexible and accessibility.(Li & Zou 2011), the design of the wireless for data acquisition try to minimize a low power consumption single chip and up final result they coming out with the new data transmission chip. One of the advantages comes from this system is consistency, practical, high transmission rate, cutting cost and low power consumption characteristics. In (Adejo et al. 2013), make a survey on the wireless sensor network applications furthermore, in their discussion on it performance results obtain from the case studies also on the upcoming prospect and their challenges. A current field study in which BHA vibrations were measured by using new available bit control and

monitoring device is elaborated in (Ledgerwood III et al. 2013) the objective on this research is to understand the main source of the PDC bit damage, which is predict will happen when the stick slip phenomenon exists.

2.8 Data Transmission Methods-MWD
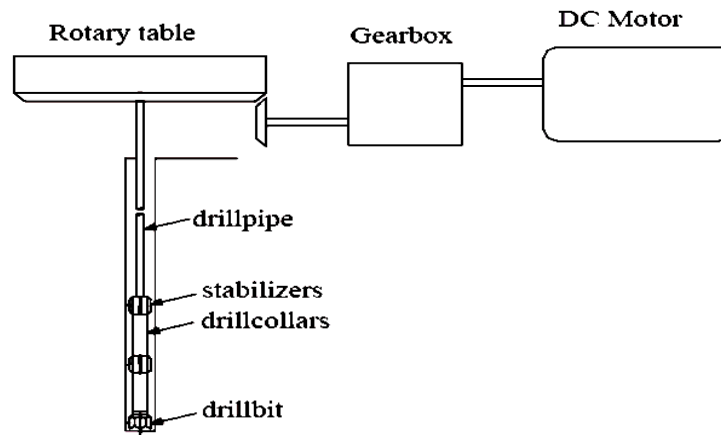
Figure 2.8: Power transmission system (Ahmadian et al. 2007)

Transmission and sensing are very important factors to be taken into consideration Figure 2.8, in order to justify the investigation of the control using downhole sensing for both experimentally and numerically. The efficiency of control and method depends completely on the advantageous information available, which can be used to modify the drilling parameters and to reduced or mitigate undesirable vibrations. Surface sensors will estimate the downhole, therefore current transmission have limited their chances of obtaining real time downhole data, hence this will verify how difficult and limits the effectiveness of the controller according to the complex dynamics of the system.

There are some methods to transfer bottom information to the drilling operator; the most popular are: (i) Mud-pulse telemetry (MPT), the information transmits via the mud that passes through the drilling pipes, it is a binary coding nature passes through the drilling pipes the data is represented by pressure (Jeffryes et al. 2001). MPT technology offers cost-effective data transmission and band widths of up to 40 bits/s, the method becomes less effective with increasing well depth and the rate of transmission is low around 1.5 bps -3 bps at a depth of 35,000ft to 40,000ft (Spracklen & Aslam 2013); (ii) Acoustic waves, acoustic transmission is an effective method to

deliver the pulses to the top extremity, the transmission rate is about 6 bps which does not vary with depth, and acoustic waves are produced by torsional reductions produced by magneto restrictive rings set inside the drill string (Drumheller 1992). However, both methods still present the problem of delaying transfer signals directly between the real time measurements to the surface through the channel; (iii) Wired drill pipe (WDP) technology, is an advanced method, capable to transmit high-resolution data speeds of up to 57,000 bps (Lawrence et al. 2009), it delivers real-time visibility of the drilling process, borehole and formation data which achieving control strategies to improve the real-time.

It is well known that industrial process are seriously improved and currently Halliburton manufactures a commercial high bandwidth wired drill string (Lawrence et al. 2009) which is IntelliServ® network system, it was widely used on a large offshore development in North West Australia. A similar system was used (Poletto et al. 2014) to monitor drill bit seismic profiles. Therefore, with advance technology, could well be adapted to provide downhole data through the system to surface to control and monitor system performance. Apart from that, data transmission, sensing methods are also to be considered. Torsional vibration can be acquired through strain measurements and twist angle between upper and lower extremities. (Tian-shou & Ping 2015) Research on a system that capable to operate in downhole conditions at depths of several thousand meters, and suggest the measured data is also one of the methods to analyse the drill string vibrations. The purpose of the research was to investigate the difference between real time data and estimated values; as a result showing that the real time values were higher than predicted by logging this is included in WOB and TOB.

2.9 Control Strategies to Reduce Drilling Vibrations

Most of the torsional vibrations occur as torque fluctuations; therefore most of the methods proposed employed vibrations dampening by include an opposing torque to match that represented by the bit rock interaction. The following sections will discuss current efforts of suppressing those vibrations, and then follow the same theory of vibration mitigation.

2.9.1 Angular Velocity Regulation

A simple technique to tackle the problem of the angular speed regulation in (Canudas-de-Wit et al. 2008), the parameter model describing the drill string torsional dynamic such varying torque on bit created from the bit-rock interaction which mean results in velocity fluctuations at the rotary table, (Navarro-López & Suárez 2004) apply an angular velocity regulation law into fully coupled vibrations of actively controlled drill strings while maintaining a constant rotary table and bit velocity proposed on their study. In this law, it keeps the torsional vibration toward zero and shows the rotary table velocity feedback as insufficient to maintain constant downhole velocity and torsional vibration cannot be controlled unless an effective state observer is designed can predict bit velocity.

2.9.2 Torque Feedback

Christoforou & Yigit, (2003) used torque feedback controllers to maintain a constant rotary speed while reducing torsional vibrations. This system estimated torque value at rotary table to adjust the velocity provided. This method includes a proportional integral controller which to regulate the velocity and introduce two different algorithms for prevent back-spinning and auto-tuning of the controller purposed. The method purposed was validated experimentally in a laboratory setup and on an actual oil drilling field. The investigation presented an effective damping of the leading torsional vibrations, with the torsional harmonic wave being dampened on the upper extremity, instead of being a fed back to the bit. However, this method requires accurate measurement of the torque and in real situation, drilling is very difficult. It is concluded that optimal drilling performance will sufficiently damped into the drill string vibrations.

2.9.3 Soft Torque Control

The soft torque, introduced by Halsey, Kyllingstad, & Kylling (1988) is also one of the control approach widely used in the field drilling to tackle the torsional vibration. Shell Offshore Inc. initially developed with modified versions was introduced. The method reduces the need for downhole torque measurement of estimation; instead the torque is computed through the motor current. The purpose of the controller is a stand

speed controller with a high pass filtered torque signal. First soft torque method was used in 1990 in Mobile bay. This approach was introduced significantly eliminating the torque flection and stick slip event when varying hard rock formations coupled for directional drilling verified troublesome with high torque and frequency stuck pipes. In order to reduce drill string vibrations proper tuning of the controller is required (Runia et al. 2013).

2.10 PID Control

Recently, PID control was used for all areas and 90% used PID control strategies in process control system. The most common control method used to mitigate torsional oscillation is PID controlled system, therefore (Puebla & Alvarez-Ramirez 2008), (Canudas-de-Wit et al. 2005), (Navarro-Lopez & Suarez 2004) and (Pavone & Desplans 1994) apply this method for a proportional integral derivative (PID) controller subject to monitor speed of rotary table to reduced stick slip, But the implementation of PID control method is very limited due to the existence of high non linearity in the drilling process. It is a control looped feedback mechanism which consists with three main component Proportional gain, Integral gain and Derivative gain. The function is reduced by adding proportional gain to minimize the error such as simple ON/OFF control, (Tucker & Wang 1999), (Slotine & Li 1991) and (Isidori 1989). PID as we known is nonlinear control system and it was a referring to fundamental methods since 25 years ago. The main purpose of this method is nonlinear feedback control changes into a linear time-invariant system, and from the newly set the system is manage to reduce the stick slip phenomenon in drill string.

Institute Français du Pe'trole, They derived parameters for a proportional integral-derivative (PID) controller to control the speed that can cause stick slip. TRAFOR used to derive a model of the drill string which is can simulate stick slip.

The elaboration about control method have been discussed, used control method to mitigate torsion oscillation, therefore review for control method was performed to justify and investigate it.

2.11 Adaptive Control

PID control strategy has been developed by (Fubin et al. 2010) to minimize the stick slip of the drill bit. The main purposed of these control method is to improve system output to input and follows by dynamics response. Canudas-de-Wit et al. (2008) proposed control law called Drilling Oscillation Killer (D-OSKILL). The main purpose of D-OSKILL is to eliminate stick slip phenomena by using a vertical force WOB as an additional variable. Li, Zhang, & Rasol (2011) also proposed the same control law by developing a time varying sliding mode adaptive control for the mathematical model for the rotary drilling system. However this control law can be improved by adding with additional adaptive observer which is to estimate the unknown states. However, no researchers have been successful in reducing drill bit vibrations with developing an adaptive control. Hence it is still an opportunity to explore by developing a control law which can efficiently reduce the drill string vibrations resume the normal drilling operation.

2.12 Vibration Induced Failure

2.12.1 Torsional Vibration (stick-slip)

Normally torsional vibration is a different rotational speed between upper and lower part of the drill string, (Al Dushaishi 2012) torsional vibration appears when upper drill string rotational speed is not parallel between the drill bit. Torsional mode vibration can lead to many failures and stick slip induced most failure during drilling process (Khulief & Al-Sulaiman 2009). The lower part of BHA store kinetic energy when the drill bit stand still to the rock thus, angular velocity has been created during this phenomena. (Van Campen & Keultjes 2002) rate of penetration (ROP) happen when the rotating of drill string alternatingly experiencing sticking and slipping.

In rotary drilling with constant speed, it is very complicated to translate into a steady rotational motion of the bit (Brett 1992) thus large amplitude fluctuations during a significant fraction due to drilling time. Stick slip is also known as self-excited rotational motion phenomena. Skaugen (1987) it is non-uniform oscillation behaviour, causing very high rotation speeds. Torsional vibration can cause damage on drill bit, and induced fatigue to the drill collar connections necessarily, thus slowing down the

overall drilling operation process. Previous researcher have studied stick slip vibrations, thus this phenomenon required accurate modelling during investigation. Figure 2.9 shows the simplified two degree of freedom torsional model of the conventional vertical drill string (Navarro-Lopez & Suarez 2004). Torsional pendulum described by a lumped parameter model and represent into BHA of the drill string.

Many studies have been using a model to investigate the bit-rock interaction and the relationship to torsional vibration. Torsional vibration can be investigated when the lumped parameter model order reduced by simplifies the drilling dynamics. In 1991 researcher started to used torsional pendulum model to investigate the effect of rotary speed, viscous damping, rotary speed and also natural frequency on the stick slip vibrations. Jansen & Steen, (1995) investigated the torsional pendulum and the method has been adding the electrical analogy describing the top drive (Lin & Wang 1991). Research on an integral high order sliding mode control system for stick slip suppression, particularly focusing on stick slip phenomena recently being intensified, such as the work of Hernandez-Suarez, Puebla, Aguilar-Lopez, & Hernandez-Martinez (2009).

As discussed earlier, the main factor that can cause stick slip phenomenon is more about downhole characteristics like whole conditions, formation and significant drag. Stick slip vibrations have their own range frequency under 2 Hz. It occurs when the bit stalls in the formation while the rotary table still rotates. When torsional energy trapped or reaches a level so that the bit can no longer stay, and the bit comes to loose, rotating and whipping at very high speeds. This phenomenon stick slip can generate a torsional wave starting from the string till rotary top system and wave back to drill string and drill bit because a fixed end to the drill string and so that the wave is reflects back to down. It can repeated stall again and automatically the torsional wave cycle keep exists (Navarro-Lopez & Suarez 2004). The most typical environment for stick slip is aggressive PDC bits and high WOB, when the downhole frictional torque reaches the rotary torque (Azar & Samuel 2007). The stick slip is most frequently stirring and destructive vibration mode.

2.12.1.1 Recognition Guideline

The indicators that suggest the presence of torsional vibration are: increase up to 20% of the torque at upper limits, significant variations of the drill string angular velocity, clogging of the rotary table and top drive, unmatched top and bottom angular velocities, unscrew the pipe joints, increased of the torque of screwed joints, and others.

2.12.1.2 Disadvantageous and Consequences

Problem associated with the existing of stick slip behaviour are: rate of penetration reduction, BHA components breakage, impact-induced bit damage, screwed joints rupture, PDC bit damage, connection over torque, drill string twists-off, and extra.
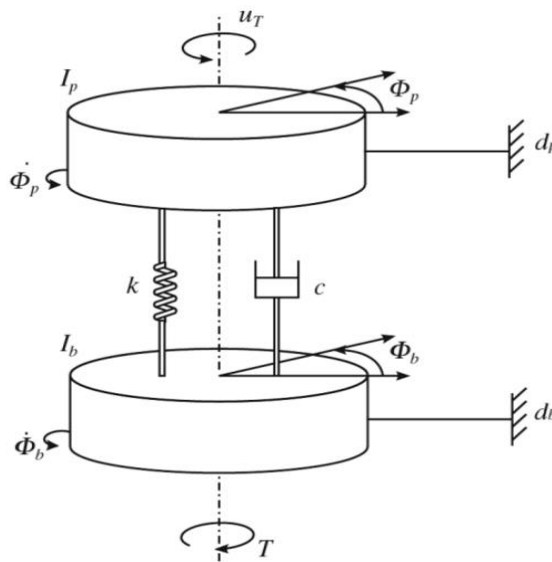
Figure 2.9: Lumped parameter model of a rotary drilling rig

2.12.2 Axial Vibration (bit-bounce)

(Al Dushaishi 2012) Longitudinal vibration (axial) exists while drilling thus interaction between the drill bit and rock surface. Bit-bounce takes place when axial vibrations occur and can cause damage to the drill bit, bearing and also cutting tools. (Saldivar et al. 2013), the high speed level that induced by stick-slip exists in torsional phenomena can excited severe axial vibrations in the BHA assembly which may induce the drill bit to spasmodically lose contact between the rock formation beat the

drill surface with enough force. In drilling situation, for certain cases the bit periodically come loose and this phenomena known as "bit-bounce". This phenomenon can cause periodic displacement at the drill bit.

It is a longitudinal drill string vibration resulting in a repetitive loss of contact between the bit and the drilling surface as known as bit bounce phenomenon; this is normally persuaded by the torsional drilling oscillations. The phenomenon actually happen when formation of the rock has change the characteristic by significant of Weight on Bits fluctuations also contribute to the existence of bit-bounce. We can identify the axial mode vibration if one or more of the characteristics are observed such as irregular movements of the drill sting along the string, significant fluctuation of the WOB. The effect factor of the axial mode vibration can reduce the rate of penetration (ROP) and also can cause damage to the bit cutter, bearings, drill string, and downhole tools and in axial vibration the range of typical frequency between 1 and 10 Hz.

2.12.3 Lateral Vibration (whirling)

Drill string whirl (particularly forward and backward) known as lateral vibration or bending of the part of the drill string pipe (Schlumberger, 2010). It is very destructive that because might be no indication at the surface of wellbore wall. The impact of bit whirl also can make the borehole wall larger which means the size for soft rocks greater than hard rocks. Lateral vibrations have their own range of frequencies around 20-250 Hz by Sperry Drilling Service, Halliburton 2007 (F.A. Majeed 2013) compared to torsional vibrations, lateral vibration lead to washout and parametric resonance counterpart the borehole enlargement and got higher frequencies so that it is very difficult to predict based on the surface measurement.

The coupling between axial and lateral vibrations will divided by two different of bending, Linear bending and also parametric coupling, (Dunayevsky et al. 1993b) discussed more to parametric coupling study between axial forces and bending vibrations. Meanwhile linear coupling is not simply occurring when axial vibration exists at straight string beam. The main source of linear coupling is comes from initial bend/ deformation of BHA (Van Campen & Keultjes 2002), (Draoui 1996), and (K. Vandiver et al. 1990) also study more about drill collar whirling and the linear

coupling between the weight on bit fluctuation and bending vibration of an initial curved of the BHA drill string.

Lateral vibration is sometimes very hard to predict at the surface since it may be able to reduce. However, magnifications of harmonies in the harmonics in the frequency domain an increase of the torque on the bit at the top of the drill string suggest the presence whirling. Whirling phenomenon able to reduce the rate of penetration, create an eccentric borehole, might also cause damages on the components such as, bits, stabilizers, pipe joints, MWD equipment, twist-off and washout other impact factor can induced the premature wear of the bit.

2.13 Vibration Modelling Control

In modelling there are two different parts to investigated phenomena in the drill string. (Wiercigroch et al. 2015) low dimensional dynamical models which is normally concentrated on a few part s or dominant modes and the other one is whole part with full scale continuous models and used finite element analysis as a main methods. Torsional pendulum model is one of the approaches to investigate the drill string system (Jansen & Van den Steen 1995) and (Yigit & Christoforou 1998) are the researchers who had study about the non- linear model and relationship of bit rock interaction and coupling together axial and torsional modes of vibrations. There are two main issue when low-dimensional models ability to mimic two important characteristics which is length of the drill string were increases during the process and the other one is all the vibration exists along drill string composed of connected between drill pipe and drill collars. (Liu et al. 2014) a multi-dimensional lumped parameter model introduced by (Balachandran 2001) to overcome the problem occurred.

There are some popular techniques to eliminate axial vibrations divide by two categories by software and hardware solving. In software solution the resonance effect is also a source of bit bounce phenomena. This effect exists when the rotary speed is close to the natural frequencies, each velocity they called critical. In order to escape the resonance, angular velocity must be selected properly. In (Chunjie & Tie 2009) proposed a method to find the natural frequency on the axial vibration by developed the algorithm using the programming language Delphi, meanwhile in this research

FFT (Fast Fourier Transform) algorithm in MATLAB are using to analyse the natural frequency. the strategy is choose to be effective in minimizing the string deform and purposely in fatigue of the drill string by optimizing the drilling parameters such as by reducing the Weight on Bit on the upper rotary disk, and also by increase the angular velocity also one of the main reason to avoided the bit bounce phenomenon occur. The second category is hardware solution; the technique is implemented sub device while an aggressive drill bits applying through the operations. (Azar & Samuel 2007) noted that during drilling proses, by modified of the hardware such as of less aggressive bits the result is more effective in order to achieve the elimination of axial vibrations comparing the technique of modifying the drilling parameters in software solution.

The following techniques solution also to avoid the whirling phenomena from lateral vibration same as axial solution techniques they divided by two categories (Azar & Samuel 2007) in software solution; resonance as known as irregular movement which leads to self-excited high magnitude vibration, researcher also investigate the natural frequency of the system by applying the finite element platform. Thus according to study avoiding the critical speeds should be considered only a part of the vibration mitigation process. Through hardware solving; BHA eccentricity and buckling are the famous causes of the lateral vibration in order to avoid the whirling phenomena. In the other hand some strategy are used to avoid the lateral vibration are by modifying the parameters such as by increases the angular velocity and reduce the Weight On Bit or in the real operation implementing instead roller reamers (Stroud et al. 2012). By optimize the BHA configuration one of the alternative way to eliminate the vibrations.(Wu et al. 2010), stated that the bit at BHA interactions can be reduced through the analysing the optimum zone which is obtained by pre estimation the critical WOB rotations per minute triggering drilling vibrations. The values are representing the boundaries of the different conditions for an example the maximum torque by rig and minimum ROP by operators.

According to Schlumberger there are two main types of vibration models which are frequency and time domain in frequency domain models, like static model is a fast running to compute BHA parts and all the information or result used to compute the natural frequency. Normally in static model user is ask to select the excitation sources

and a critical rpm is computed for each source, but interaction between borehole wall and drill string is not taken into consideration, while critical speed rpm is a surface rotational speed at which of natural frequencies.

Vibration control technique can be used for minimize or maximized vibrations force in drill string. Drill string failures normally is a main part of large dynamic force, it is very useful if we get more understanding about maximum of force levels to increase the rate of penetration without damaging the component of the drill string. There are four basic technique for reduce magnitude of mechanical vibration (Dareing 1984) first change natural frequency, change forcing frequency, increase or apply mechanical damping, and fourth is eliminate source of excitation, thus this all give alternatives for operational control techniques.

2.14 Investigating Drill String Vibrations

2.14.1 Experiment Set-Up

Experimental set-ups (pre-drilling analysis) are very important to support and verify result findings this allows better understanding of the parameters and downhole dynamics and also understand as how vibrational modes can be induced and typical set-up features which have proved valuable in best replicating the drilling phenomenon.

Many researches have been conducted to study the drill string dynamic. For instance, Mihajlović, Wouw, Rosielle, & Nijmeijer (2007) study on interaction between the friction-induced vibration and self-sustained later vibrations in drill string rotor dynamic experimental setup. In this experiment they discussed the response of a rotor subject to a friction force applied along the direction with clamped at the bottom and another mounted is upper part which is mounted to the motor directly. Meanwhile, A. Khulief & A. Al-Sulaiman (2009) focused on the influence of stick slip, weight on bit, wellbore interaction, and drill fluid interaction idea from Mihajlovic is bottom part is clamped at the end. In such study, the string was fixed to a motor and the other one is free at the end. This is the main feature of the present study, which concentrate on both rotor and contact dynamics. The drill string has been studied in various setting experiment which is to examine the rotor response in different frictional forces and driving speeds. In this research the experiment method approach used to identify the

dynamics of the drill string mechanism. The experimental setup is described in Figure 4.2. The accelerometer used to determine the position or direction of the string are describe in, appendices the result gather are presented and explained in section Experimental .

Chapter 3

Simulation and Partial Differential

3.1 Modelling Strategies Allowing the Analysis and Control of Drilling System

This section describes the mechanical model of the test rig presented in mathematical equations, which was used in the simulations.

3.2 System Modelling-Lumped Parameter Model

The use of reduction model for vibration analysis needs to define a simple description of drilling dynamics. Figure 3.1 shows the simplified of two degree of freedom torsional model of conventional vertical drill string as proposed by Navarro-Lopez & Suarez, 2004, simplified as follows:

- The main components of the model are two damped inertias mechanically coupled by an elastic shaft (drill string). Such mechanical system creates infinite natural resonance frequencies, assuming that the drill string is homogenous along entire length and simplified as a single linear torsional spring with stiffness coefficient k.

- Free body diagrams are symbolised as θ_m, θ_u, θ_s, θ_l, representing the displacements of motor, upper disk, string and lower disk, respectively.

- θdot and θdotdot is represent the angular velocities and accelerations for each mass.

- C_m, C_u, C_s, C_l, represent the viscous damping coefficients. C_s is a damping effect of the bearing and encoder at lower part of the string.

- J_m, J_u, J_s, J_l, represent the mass moments of inertia of the motor, upper disk, string and lower disk respectively.

- T_m is the torque delivered by the motor system. T_f is the stick slip oscillations, which are driven by nonlinear friction at near zero bit velocities and thus represent the combined effects of reactive torque on the bit and non-linear frictional forces along the BHA. In general, the electrical behaviour of the motor has to be described in terms of non-linear differential equations that depend on the type of the motor used,

- The electric circuit (upper part of the diagram) represent the motor system, where V_a is armature voltage, the back-electromotive force (back-emf) V_b is linearly related to the rotary table speed, L is the electrical inductance, I is the current in the motor armature and R being the electrical resistance.
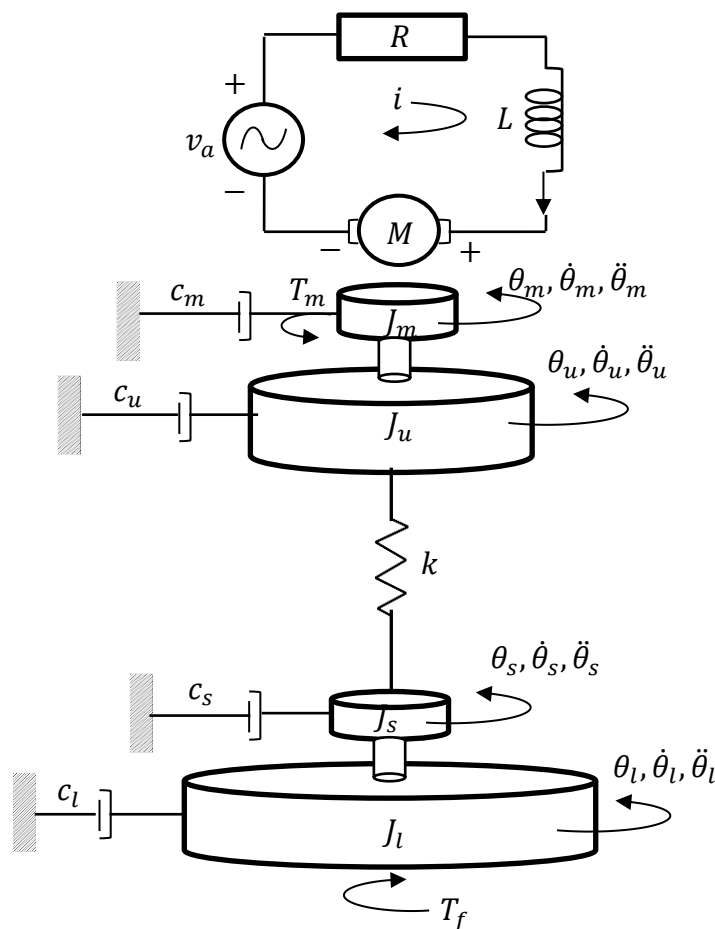
Figure 3.1: Simplified schematic model of the drilling system

$$C_m + C_u = C_1$$
$$C_s + C_l = C_2$$

$$J_m + J_u = J_1$$
$$J_s + J_l = J_2$$

The above model is simplified and described through free body diagram
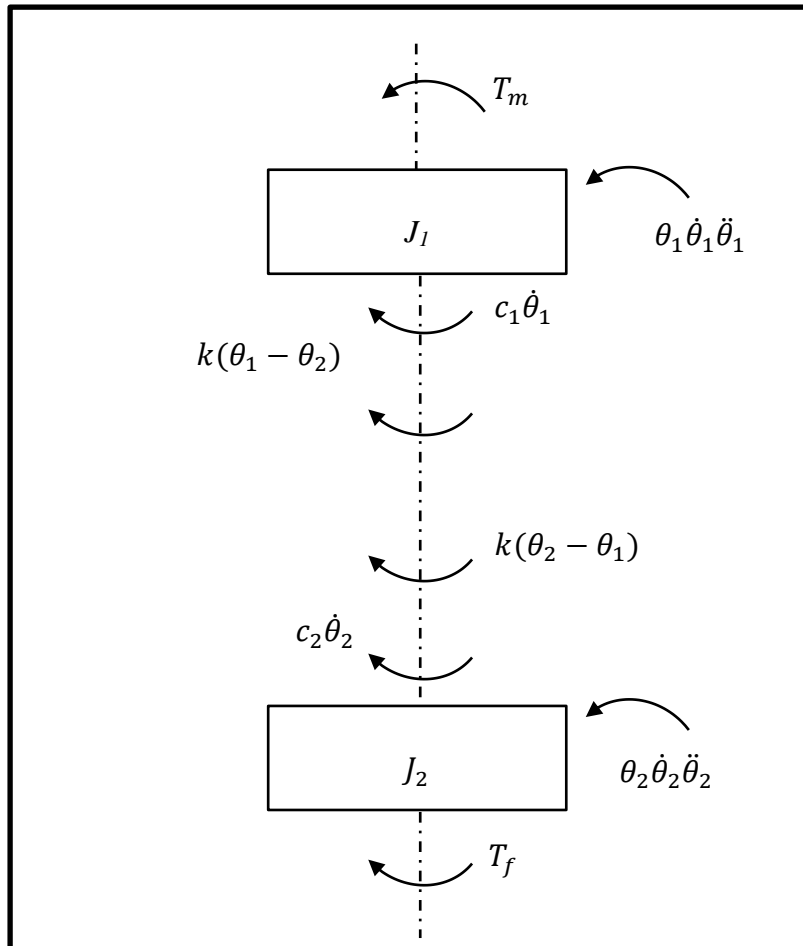
Figure 3.2: Free body diagram of drilling system

Equation of motion of the upper part;

$$J_1\ddot{\theta}_1 + k(\theta_2 - \theta_1) + c_1\dot{\theta}_1 = T_m$$

3.3

The upper part is described by the first order differential equation that may find in equation 3.3, where θdot is the angular velocity and J_1 equivalent of moment of inertia, C_1 is the equivalent viscous damping coefficient of the rotary table, and T_m is torque delivery by the motor.

Equation of motion of the lower part;

$$J_2\ddot{\theta}_2 + k(\theta_2 - \theta_1) + c_2\dot{\theta}_2 + T_f = 0$$

3.4

The mechanical behaviour of the lower part of free body diagram is described in equation 3.4 where J_2 represents the moment of inertia of the lower part, C_2 is viscous damping of the BHA and T_f is nonlinear function which will be referred to be the torque on bit.

The drilling system is essentially converting electrical energy to mechanical energy in equation 3.5 (Halin 2017); and the mechanical electrical equation is modelled as below:

$$v_a = 2Ri + 2L\frac{di}{dt} + k_e\dot{\theta}_1$$

3.5

In the oil drill string, the stick slip oscillations are driven by non-linear friction T_f where represent the combination effect of reactive torque on the bit and nonlinear frictional force along the BHA in equation 3.6 (Saldivar et al. 2015); where k is a positive parameter, representing the constant of the friction top angle of the velocity threshold.

$$T_f = F_b\frac{2\bar{k}\dot{\theta}_2(t)}{\dot{\theta}_2^2(t) + \bar{k}^2}$$

3.6

This describes the essential dynamic of the torque on the bit which associated to stick-slip oscillations, the function equation is multiplied by the friction force on the bit, however some modifications has been made at the lower disk which is friction force F_b is product of *WOB* and the coefficient of the friction between the bit and surface (Karnopp 1985) in equation 3.7 (Saldivar et al. 2015).

$$F_b = \mu_s WOBR_b \qquad\qquad\qquad \textbf{3.7}$$

The magnitude of torque on bit depends on the WOB is the weight on bit and R_b is the bit radius $\boldsymbol{\mu_s}$ is the dry friction coefficient at the bit and surface which in reality, changes depend on the rock type and hardness.

3.3   Lumped Parameter Model Derivation

This section will discuss the most important phenomena observed in oil well drilling. Several unstable dynamics appeared once the bit comes in contact with drilling surface giving rise to the existence of the drill string vibrations. The most popular empirical methods used in practice to eliminate the stick slip vibration are evaluated through numerical simulations of the torsional drilling model. Through mathematical model, fluctuations of the bit velocity which describe the stick slip phenomena can be reproduced. The torsional occurs when a part of the rotating drill string is temporarily held between frictions against the surface, then released. The bit may finally get trapped and then, storing energy in terms of torsion suddenly released.

The control system applied was angular velocity and relative WOB as the feedback signals, the purposed is to maintain a constant bit velocity. The control design was designed with motor speed as the feedback then modified accordingly to tackle the torsional vibration problem by including bit velocity as the feedback signal. Changing the velocity of the bit reduced torsional vibration (Canudas-de-Wit et al. 2005). As the friction increases at the bit then the velocity will decrease thus feeding this back to the previous controller by increasing the motor speed while maintaining a constant velocity and applying opposing forces in the opposite direction. Due to the rotational string and difference in rotation speeds under load, motor torque as a feedback

parameter is not sufficient to reduce the vibration occurring. Finally the WOB regulation was added which uses the motor torque as feedback to reduce the WOB if the torque exceed the maximum motor torque. The WOB regulation was not aimed at reducing the torsional vibrations, by noticing the maximum torque provided by drive motor, in such case the torque on bit reached the torque available at the motor then WOB was reduced preventing the bit velocity reaching lower speeds and stick slip oscillations begin. The model parameters used in simulations as given in Table 3.1 was obtained from the field data.

Table 3.1: Numerical values of the drilling system parameter obtained from field data (Challamel 2000)

Symbol	Description	Values	Unit
J_1	Moment of inertia	79	Kg m^2/rad
J_2	Moment of inertia	89	Kg m^2/rad
C_1	Viscous Damping	425	Ns/m
C_2	Viscous Damping	50	Ns/m
k	Drill string stiffness	473	Nm/rad
k_e	Electromotive Force Constant	0.33	V/rad/sec
k_t	Motor Torque Constant	0.33	Nm/Amp
WOB	Weight On Bit	97347	N
-	Max Motor Torque	12474	Nm
-	Velocity Threshold	0.3	-
-	Friction Coefficien	0.09-0.4	-

In order to analyse the system dynamics and design control for the suppression of the drilling vibration in a successful manner the model was modelled for an actual drilling field (Challamel 2000). The friction coefficient used were replicated and used to represent the varying friction forces experience as a final result of varying rock characteristics. Maximum motor torque is important to WOB regulation, so an AC drilling motor manufactured by General Electric was selected to simulate the simulation. The previous dynamic model equation was therefore combined and stated in state space form and assumed that the variables for this dynamic system are of a continuous time-invariant nature and the equation described below in equation 3.8.

$$\dot{x} = Ax + Bu$$ 3.8

The motor and bit velocities is relative angular displacement between upper part and lower extremities and motor current describe the state variables meanwhile torque on bit and motor voltage as the input variable.

$$\begin{bmatrix} x_1 \\ x_2 \\ x_3 \\ x_4 \end{bmatrix} = \begin{bmatrix} \dot{\theta}_1 \\ \theta_2 - \theta_1 \\ \dot{\theta}_2 \\ I \end{bmatrix}$$

3.9

The following equations represent the derivation of the state space for matrix A and B from the previous equation of motion.

$$\dot{x}_1 = \ddot{\theta}_1 = -\frac{k}{J_1}(\theta_2 - \theta_1) - \frac{c_1}{J_1}\dot{\theta}_1 + \frac{k_t}{J_1}i$$

3.10

$$\dot{x}_2 = \dot{\theta}_2 - \dot{\theta}_1 = x_3 - x_1$$

3.11

3.12

$$\dot{x}_3 = \ddot{\theta}_2 = -\frac{k}{J_2}(\theta_1 - \theta_2) - \frac{c_2}{J_2}\dot{\theta}_2 - \frac{1}{J_2}T_f$$

$$\dot{x}_4 = \dot{I} = \frac{1}{L}v_a - \frac{R}{L}i - \frac{k_e}{L}\dot{\theta}_1$$

3.13

$$\begin{bmatrix} \dot{x}_1 \\ \dot{x}_2 \\ \dot{x}_3 \\ \dot{x}_4 \end{bmatrix} = \begin{bmatrix} -\frac{c_1}{J_1} & \frac{k}{J_1} & 0 & \frac{k_t}{J_1} \\ -1 & 0 & 1 & 0 \\ 0 & -\frac{k}{J_2} & -\frac{c_2}{J_2} & 0 \\ -\frac{c_2}{J_2} & 0 & 0 & -\frac{R}{L} \end{bmatrix} \begin{bmatrix} x_1 \\ x_2 \\ x_3 \\ x_4 \end{bmatrix} + \begin{bmatrix} 0 & 0 \\ 0 & 0 \\ \frac{1}{J_2} & 0 \\ 0 & \frac{v_a}{L} \end{bmatrix} \begin{bmatrix} T_f \\ f_c \end{bmatrix}$$

3.14

The below equation describe the derivation of the state space matrix C from equations of motion derived before. The outputs of the system are relative angular displacement between upper part and lower part of the BHA, which is used to determine string torsion (multiplying by the string stiffness) and bit angular velocity. The system was assumed as no disturbance, so that Du is equal to zero.

$$y = Cx + Du \qquad \qquad \textbf{3.15}$$

$$y = Cx \qquad \qquad \textbf{3.16}$$

$$y_1 = \theta_2 - \theta_1 = x_2 \qquad \qquad \textbf{3.17}$$

$$y_2 = \dot{\theta}_2 = x_3 \qquad \qquad \textbf{3.18}$$

$$\begin{bmatrix} y_1 \\ y_2 \end{bmatrix} = \begin{bmatrix} 0 & 1 & 0 & 0 \\ 0 & 0 & 1 & 0 \end{bmatrix} \begin{bmatrix} x_1 \\ x_2 \\ x_3 \\ x_4 \end{bmatrix} \qquad \qquad \textbf{3.19}$$

Furthermore, a brief of dynamic physical device used in conjunction with the empirical control methods to reduce drilling vibrations is presented. Figure 3.3 Simulations presented hereinafter are developing using the variable step MATLAB SIMULINK solver.
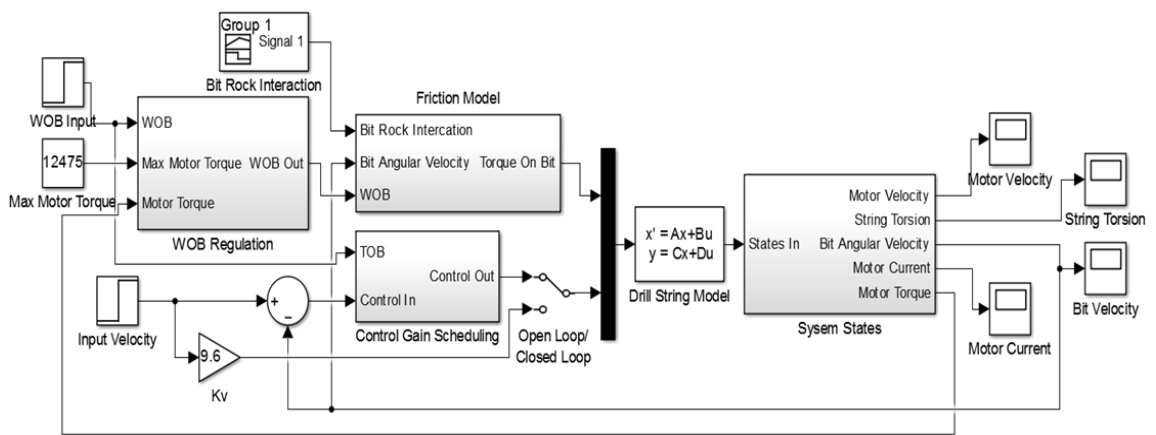
Figure 3.3: Simulink model used for simulating the drilling system and proposed control scheme
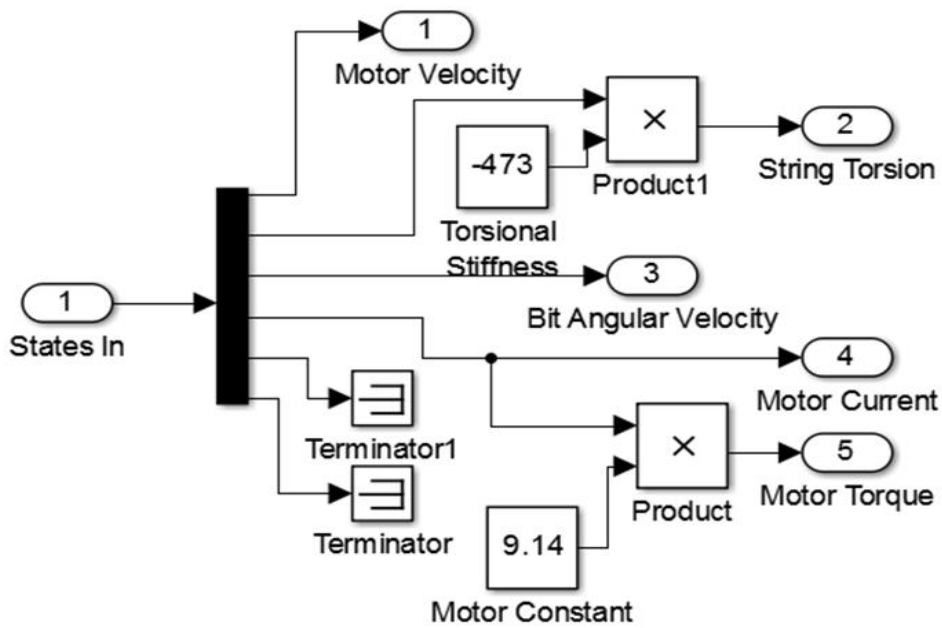
Figure 3.4: Simulink model used to determine motor torque and string stiffness

Figure 3.4 is describing how to calculate the string torsion and motor torque based on parameter in Table 3.1. Figure 3.5 shows the calculation of Torque On Bit (TOB), by using the non-linear friction dynamic model.
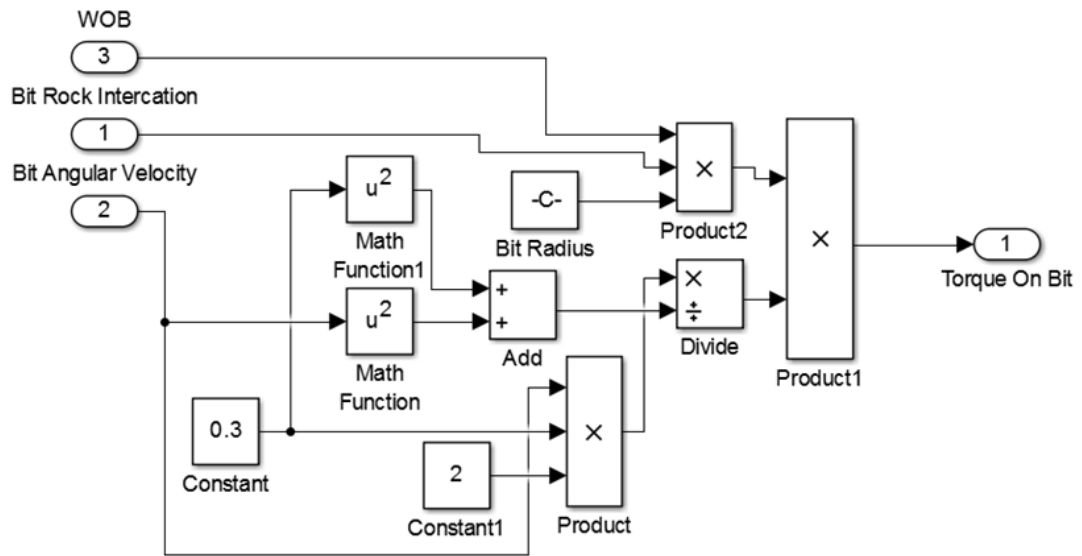
Figure 3.5: Simulink model representing the non-linear friction model

The PID control is developing as gain scheduled PID for the velocity control. In this model more control input required to maintained the velocity such as in this situation, faster response required once load was applied and friction force at the drill bit also increased, but a slower response was needed during initial start-up from zero to desired angular velocity. Simulations were run to optimise the PID gains.
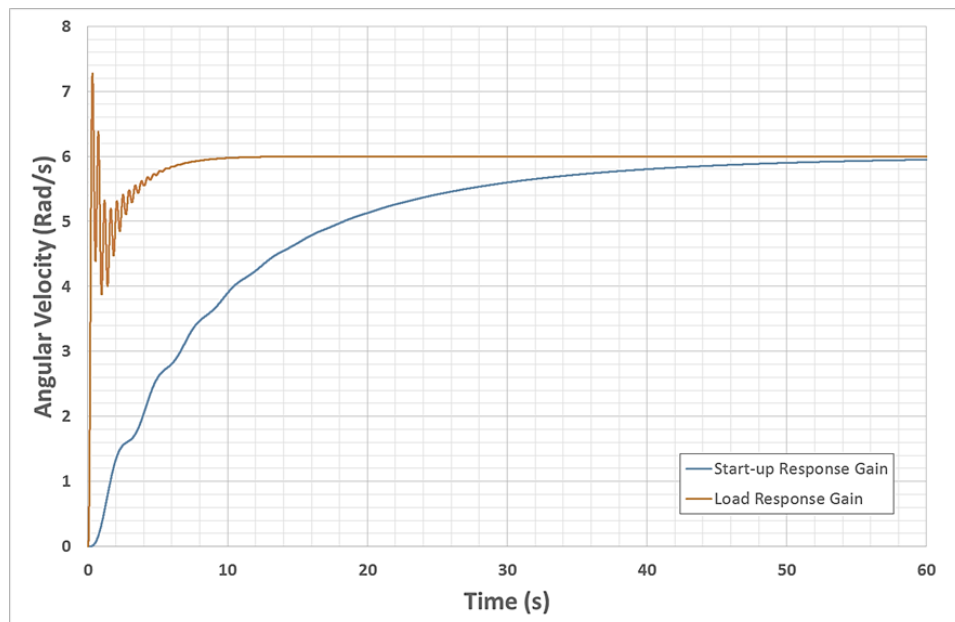
Figure 3.6: Simulation of start-up from 0-6 rad/s for both load gain and start-up gain

The Figure 3.6 above elaborates the angular velocity response start from 0 to 6 rad/s with no load applies, by using tuned for load response and start-up response. The PID was tuned for start-up response showed a regularly increase in speed until approaching 60 seconds set point with minimum lower extremity velocity oscillation, meanwhile the gain tune for load response were applied as the torsional vibrations is observed at the bit resulting the velocity oscillation at 0 to 5 seconds.
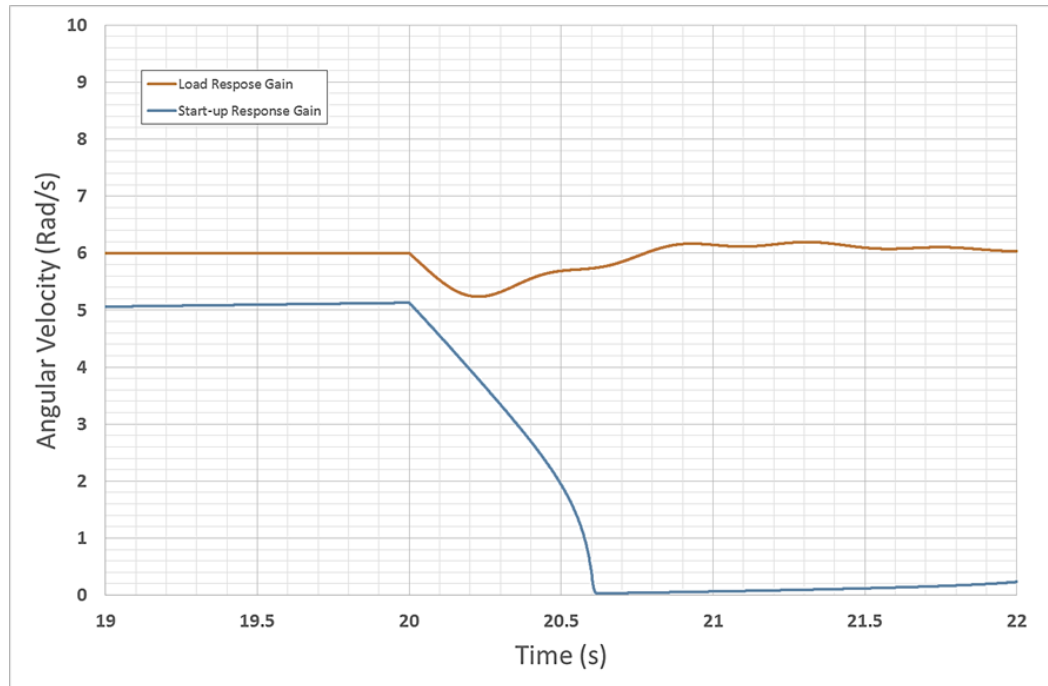
Figure 3.7: Simulation of load disturbance response at cutting velocity, for both load gain and start-up gain

Figure 3.7 shows the response with the load applied at time 20 seconds, the gains tuned for load disturbance appropriate controls of the bit velocity with minimum overshoot, therefore the gains tuned for start-up cannot sustain to maintain the desired velocity and decreased till no rotation was experience at the bit.

In comparison, Figure 3.6 shows that the response with load applied at 20 seconds, the gains tuned the load disturbance sufficiently by controlling the bit velocity with little overshoot, Thus the gains was tuned before did not maintain the desired velocity and reduced till rotation stop.

Hence, a PID gain scheduling was designed which diverse the gain an as depending on the conditions of the model system, for example by not applying any load at the

start up and also add input disturbance load. Figure 3.8 describe about Simulink model that was used to counter this situation. The Torque On Bit (TOB) was used as the scheduling parameter and in the gains itself automatically change as a function of TOB (Torque On Bit). The PID tuning in Simulink auto-tuning is a suitable method to achieve the desired output on this drill string model.
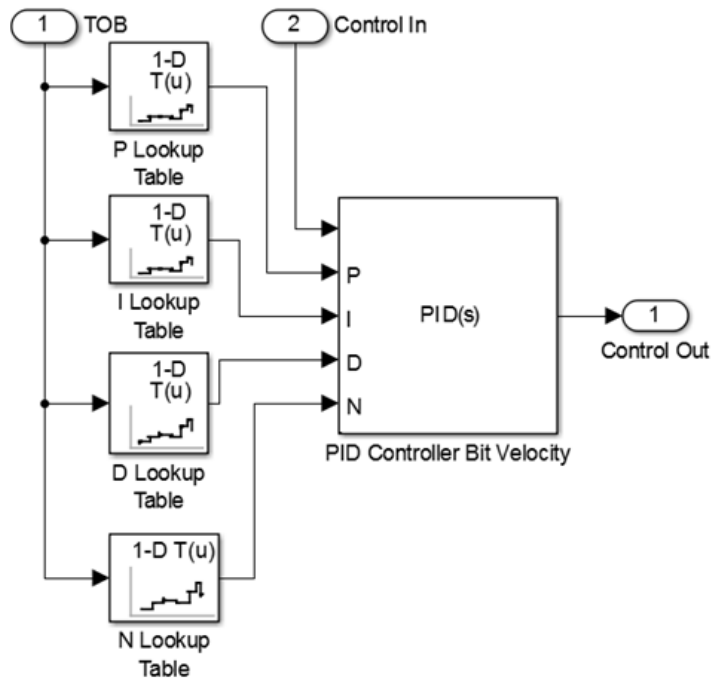
Figure 3.8: Simulink model for PID controller with gain scheduling
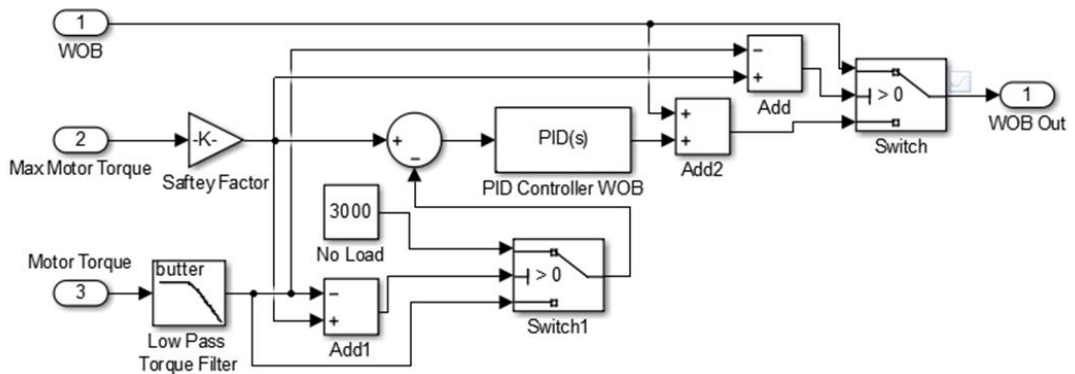
Figure 3.9: Simulink model for WOB regulation control

The Weight On Bit (WOB) regulation control is illustrated in Figure 3.9, the control system was created to reduce the WOB value from the beginning (set point). In order to reduce TOB, the motor torque required to overcome friction force while maintaining the bit velocity. The motor torque feedback had large oscillations which can cause instability for the control system and it was only required to reduce the overall WOB and not interfere with the torque variation. Therefore for final output the torque feedback signal was filtered with low pass Butterworth filter to maintain the bit velocity.
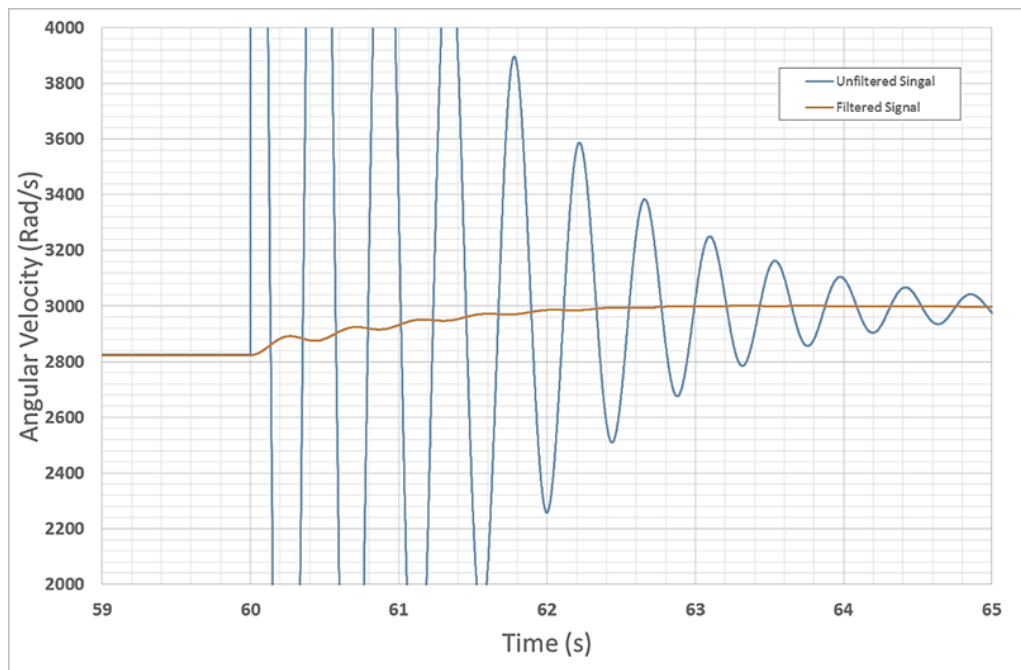
Figure 3.10: Filtered signal using low pass Butterworth

Figure 3.10 result describe of the filtered signal was choose then the large torque oscillations observed and necessary need to adjust the bit speed. Since the aim was not to regulate WOB to maintain bit velocity to react to these torque variations but only for final torque value once the vibrations were reduced.

3.4   Drill String Rotational Stiffness for K

In this research the string rotational stiffness K is obtained by modelling in FEM analysis, the maximum shear stress is determined for a torsion moment which is on the analysis one of end is fixed support at the other. Equation 3.20 is a resultant angle of twist.

$$\theta = \frac{\gamma_{max}L}{r}$$

$$\textbf{3.20}$$

$$K = \frac{T}{\theta}$$

$$\textbf{3.21}$$

Where L is length of the string, meanwhile r is the radius and γ_{max} is the maximum shear stress. The string rotational stiffness K equation 3.21, represent by the ratio of torsion moment to angle of twist, also as represent the maximum allowable torque which resulting to deformation of the shaft it shown at Figure 3.11.
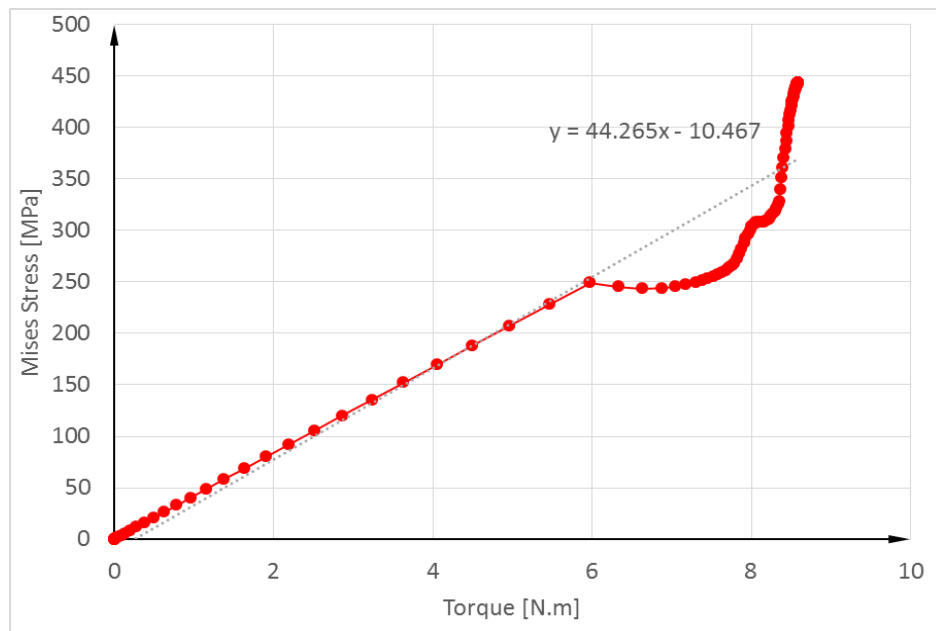
Figure 3.11: Maximum allowable torque

3.5   Data Collection for motor velocity, string torsion and motor torque

This part will discuss about the procedure for simulation purposes, where an angular velocity of 6 rad/s was used for all cases and motor velocity, string torsion and motor torque were recorded in Table 3.2, then simulation were run through;

Table 3.2: Simulation procedure

Feedback	Response	Values	Disturbance
Open-Loop	Applied 2 sec after the initial start-up response has settled	at 6 rad/s	with load
Open-Loop	start from 0 to 6 rad/sec	6 rad/s	no load
Closed-Loop	start from 0 to 6 rad/sec	6 rad/s	no load
Closed-Loop	applied 2 sec after the initial start-up response has settled	at 6 rad/s	with load
Closed-Loop	applied 2 sec and 20 sec after the initial start-up response has settled	at 6 rad/s	with load

In experimental data, three different angular velocities were tested, 5.236 rad/s (50 rpm), 10.472 rad/s (100 rpm) and 15.708 rad/s (150 rpm) with constant load disturbance of 1N (normal force) produce by the brake after desired speed was achieved.

3.6 Simulation – angular velocity for open and closed loop system by SIMULINK solver

This part represents the result acquired from the simulation model based on parameters discussed from literature. Figure 3.12 show the start-up response for motor and bit angular velocity for open and closed loop systems. A constant voltage was included in the open loop system, thus the result for motor velocity shows a very short rise with a large overshoot. At the maximum velocity, which are 3.58 rad/s (34.187 rpm) at bit velocity showed a large oscillations and higher velocity than the desired output, but the desired oscillations were then minimize or reduce at point 16 seconds.

External control aggregate the voltage applied to the motor regularly would have reduced however on this study the aim was to control the drilling system and eliminate operator input, as a solution bit velocity and motor velocity closed loop (feedback) was added to the previous design so as a result, Figure 3.12 shows a much slower and smoother oscillation which mean, it eliminate the oscillation at the bit allowing the increment of the desired drilling rotational velocity. The response on this result with

no load disturbance applied, it means here, representation of the start-up of the drilling rig while allowing the bit to achieve a desired suitable speed before the load applied.
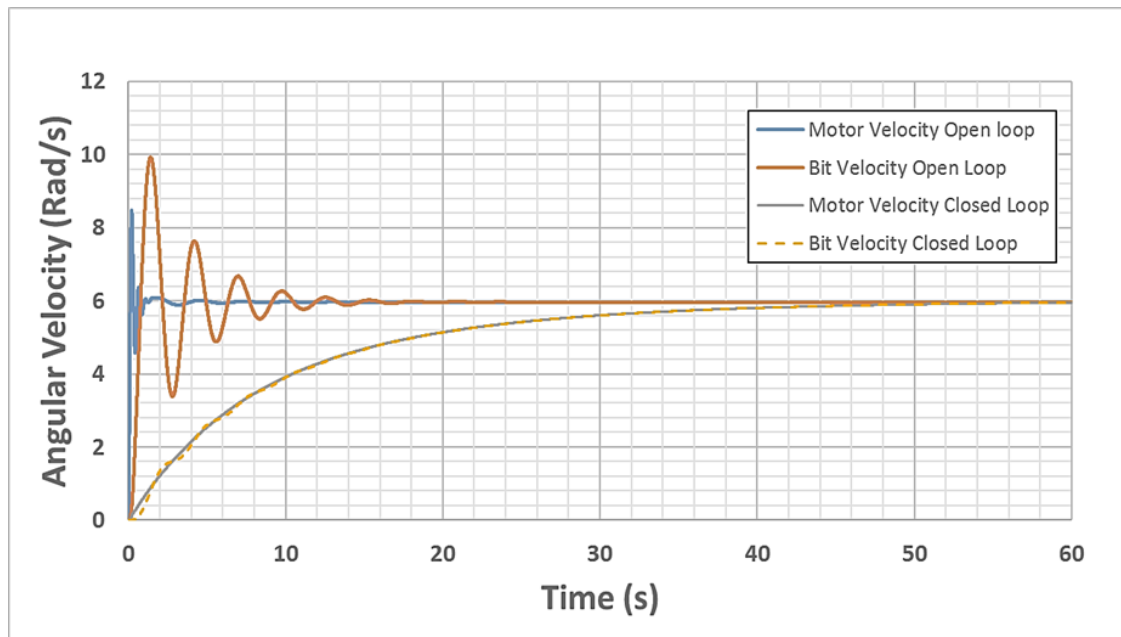
Figure 3.12: Angular velocity versus motor time and bit response in open-loop and closed-loop systems

Figure 3.13 below is about open loop response when WOB on the bit is increased and the interaction between bit and surface formation of the WOB on the bit is increased at the time of 2 seconds with torque on bit is constant. The motor velocity of the bit is decrease with tiny variations. This show that high torsion in the string exists and we can also conclude here that, applied load was not sufficient to cause the bit to stall. The velocity increased near to twice the motor velocity, once the torsional energy stored within the string was enough to exceed the torque on bit, this situation is similar but only effecting as the torsional energy in the string and can caused a rapid decrease for bit to stall and a stick slip event to start. In this case the bit oscillated with a 0.2 Hz frequency speeds achieving more than 4 times than motor. Here also show that continuous as a self-excited (torsional) vibration without any external force variation. Apart from that, it even starts rotating in the opposite direction at 0.12 rad/s (1.146 rpm), during this event the motor velocity shows a small difference and also might not obvious at the surface.
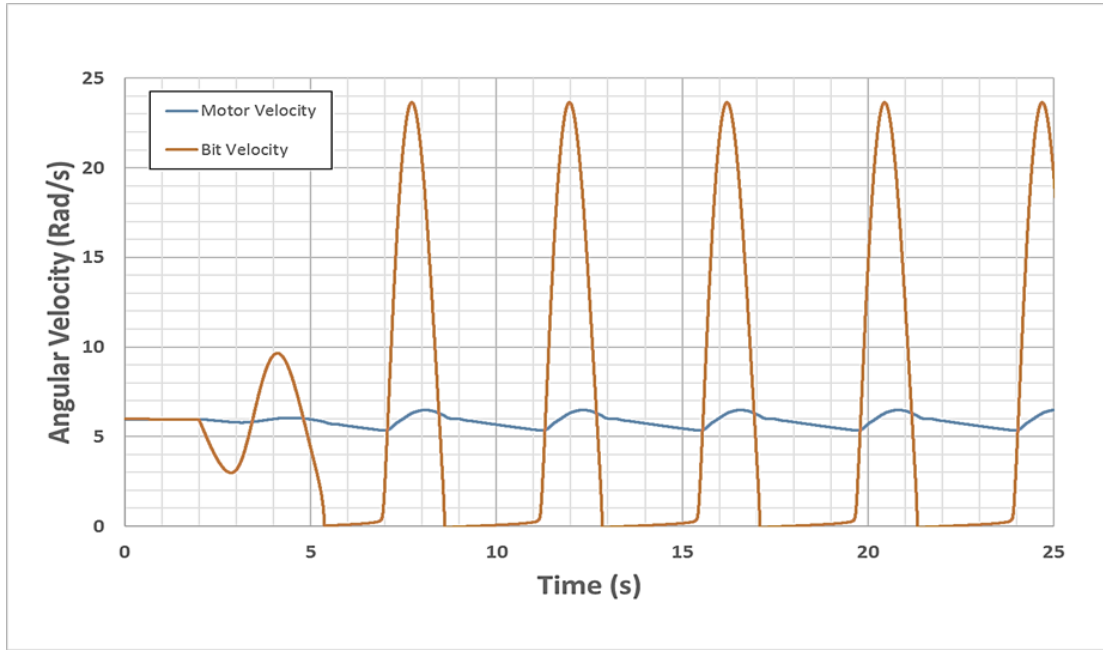
Figure 3.13: Angular velocity verses time for open-loop load disturbance (Bit Rock Interaction)

Figure 3.14 is a direct bit velocity feedback as a control parameter is a sufficiently reduced the bit oscillations entirely, the strategy succeeds in eliminating torsional vibration and the stick slip event is avoided. At motor velocity the oscillation is gradually increased but then returns to the desired velocity. An important reduction of torsional vibrations using the bit velocity as a feedback parameter is observed.
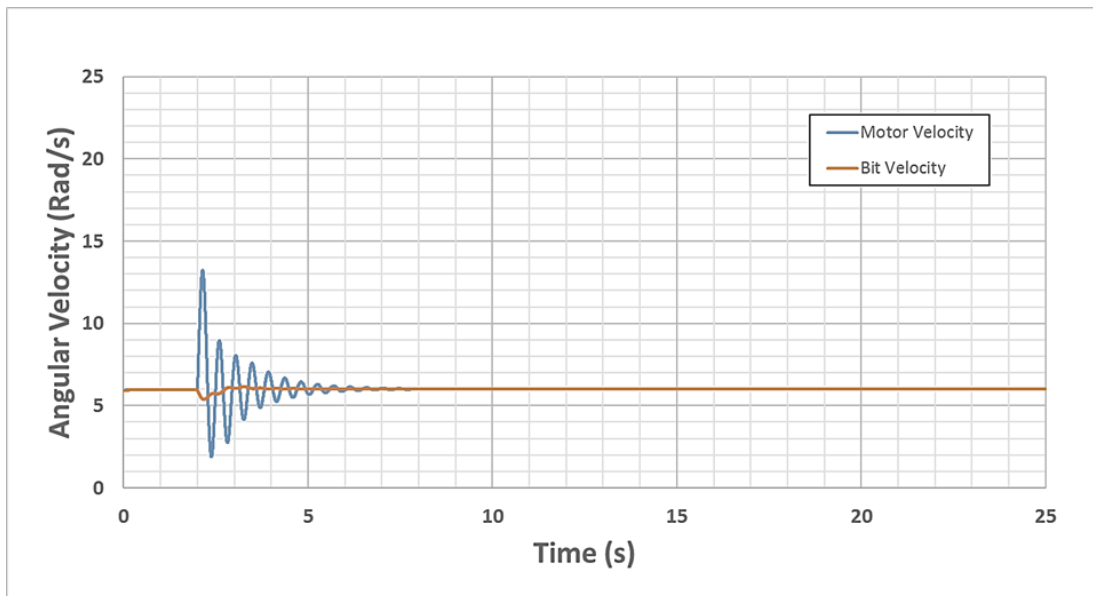
Figure 3.14: Angular velocity verses time for closed-loop load disturbance (Bit Rock Interaction)

Figure 3.15 below, shows the system response to the torque feedback controllers; torsion experienced in the string for open and closed loop systems, observe that, under this modelling approach, open loop control method performs by completely eliminate the torsional vibrations and to ensure an optimal torsion, it is necessary to maintain certain amount of the weight on the cutting device. The differences of the torsion values in the string during the stick slip event reaches nearly 5 times that required to maintain velocity at the speed required.
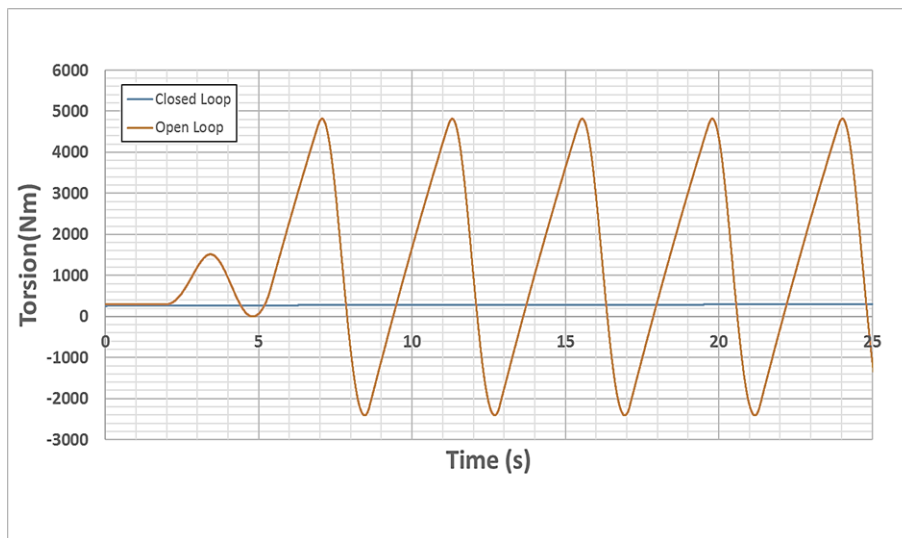
Figure 3.15: String Torsion model verses time for both open and closed loop load disturbance (Bit Rock Interaction)

The result below from field data and simulations of the drilling model Figure 3.16, it shows the weight on bit regulation, the purpose is to prevent torque on bit exceed the maximum torque require at the motor, as we know varying rock lithology will result either increase or decrease the required cutting force so we can conclude here that, where this achieve the maximum motor torque the weight on bit is reduced. Refer to the result obtain, the varying weight on bit as the friction force exceeds maximum motor torque. At 2 seconds the weight on bit is applied and the first friction coefficient represent the bit rock interaction is applied, since the motor torque did not exceed the maximum torque required therefore no reduction was observed. However due to large oscillations and high motor torque, the filtered feedback torque does not respond, when the load is applied, it will not affect the velocity regulation. It is concluded that the maximum motor torque only limits to the torque required to maintain a constant velocity at a constant load therefore this is significantly below than the motor

competences. This regulation still tolerates at higher torque to be applied while rotational speed is increased and decrease at the motor to dampen the vibrations. Some variations were observed when weight was decreased and increased suddenly; this is happen because of a small variation experienced particularly close to maximum torque boundary or maximum motor torque. As a result, it shows consequently for motor and velocity oscillations. This can be done through further tuning to prevent the controller strategy from responding to small variations close to the maximum.
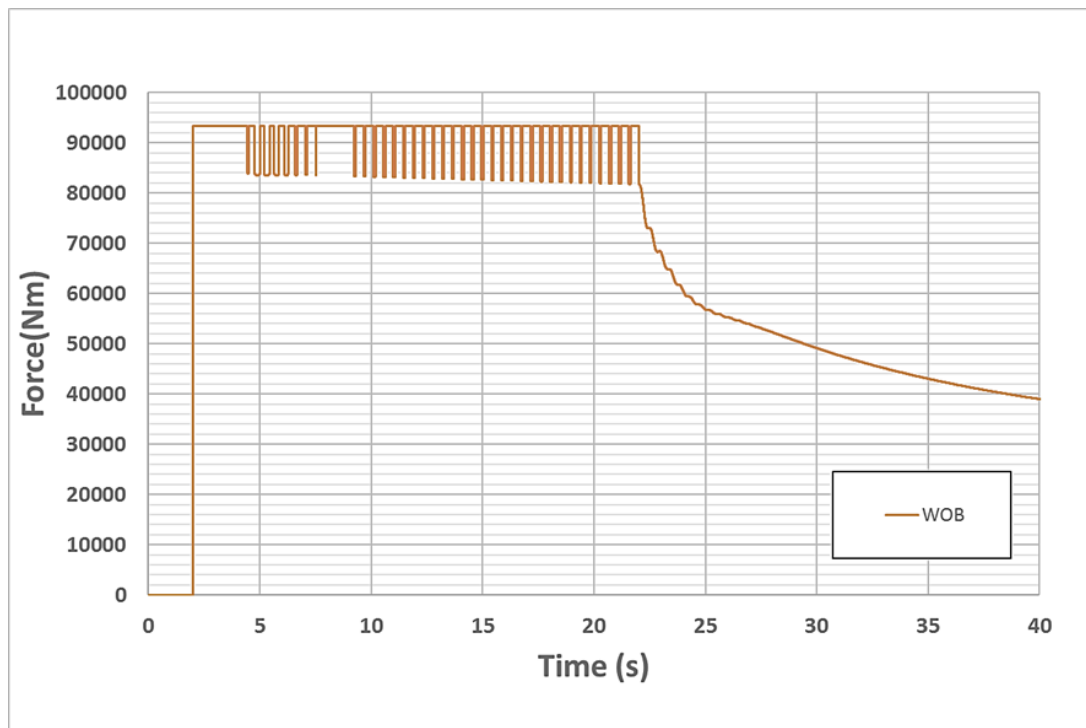
Figure 3.16: Effective Weight On Bit verses time for varying load disturbance (Bit Rock Interaction)

The Weight On Bit, is an efficient strategy to counteract torsional oscillations as the effective torque on bit increased which damped by the velocity regulation control in Figure 3.19, therefore it still showing a significant improvement compared to the open loop response. In Figure 3.17 and Figure 3.18, for motor torque and motor velocity indicate significant variations which could be potentially to drill string failure therefore further improvement of the WOB regulation would be purposed.
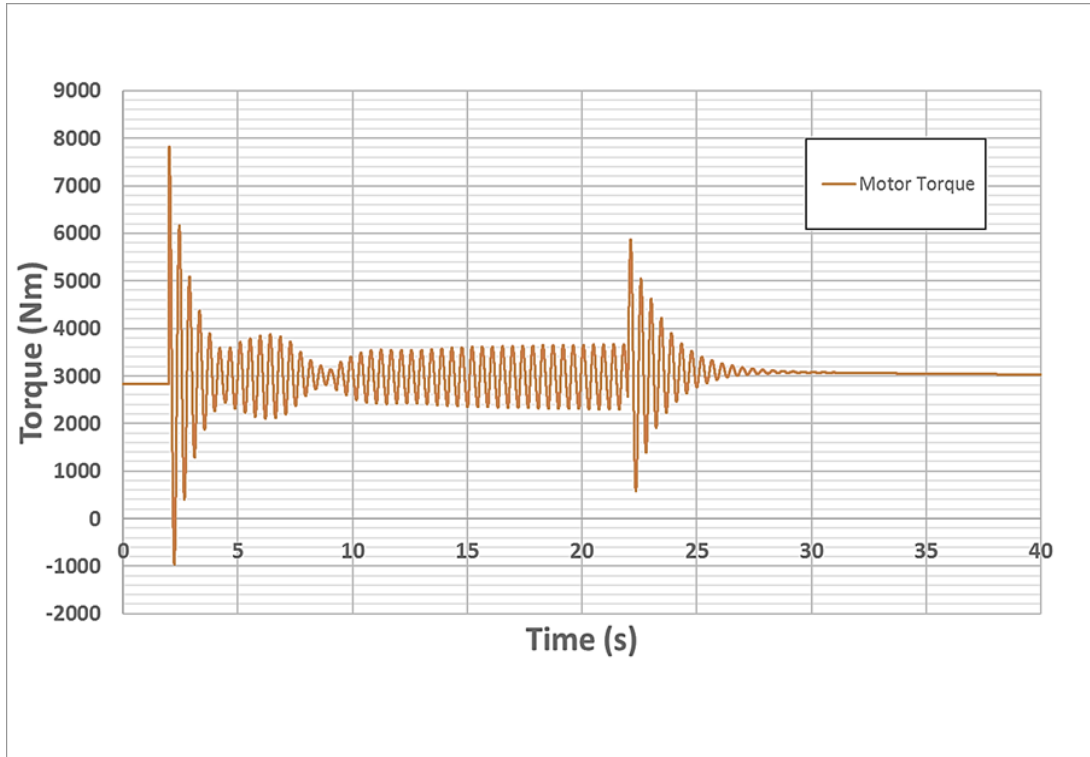
Figure 3.17: Motor torque verses time for varying load disturbance (Bit Rock interaction)
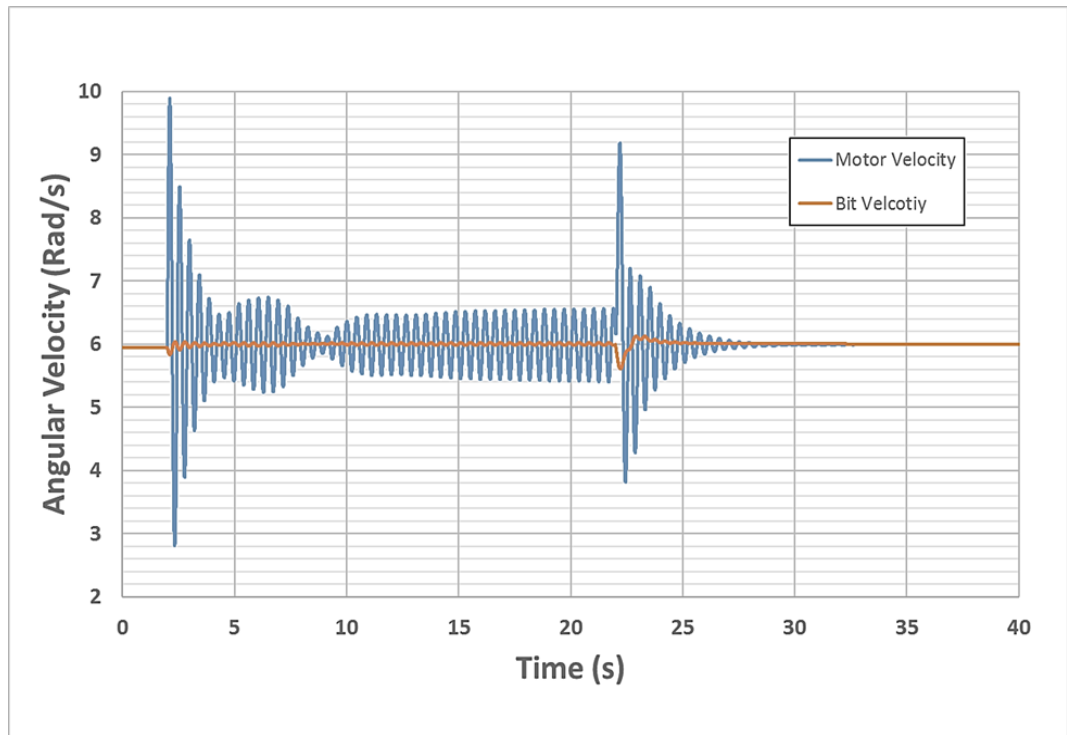
Figure 3.18: Angular velocity verses time for varying load disturbance (Bit rock interaction)
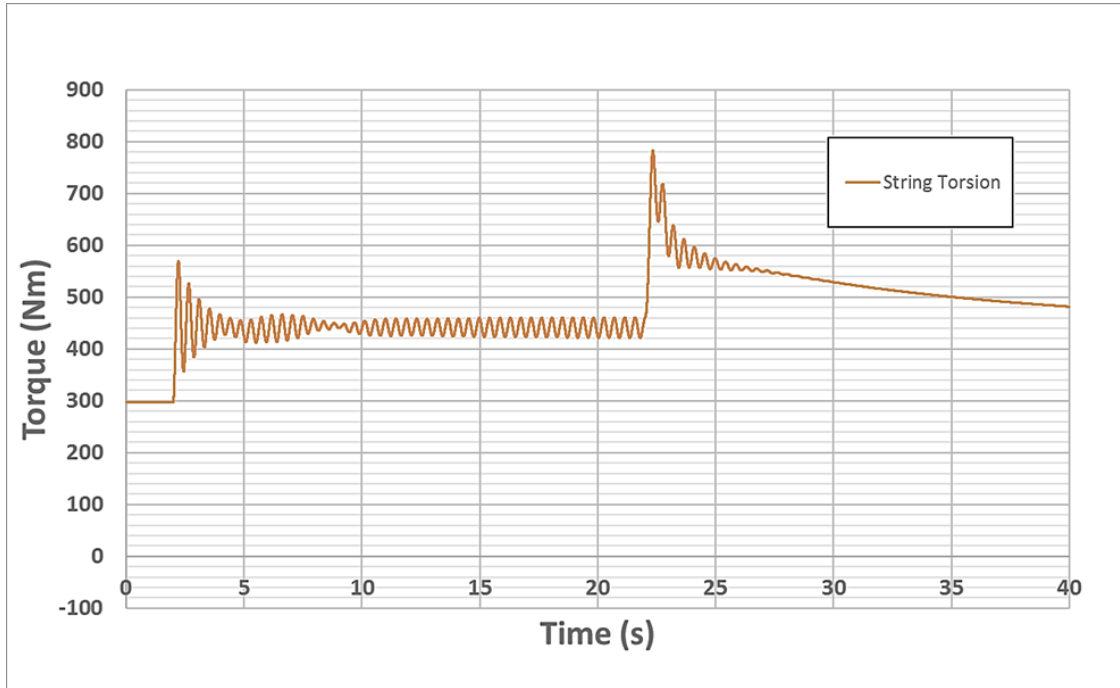
Figure 3.19: String torque verses time for varying load disturbance (Bit rock interaction)

3.7 Simulation Results for controller design by SIMULINK

For the final simulation result, it shows that the controller design strategy successfully reduced the torsional vibrations, so when it comes into a realistic drill-string model application in drilling field scenarios, the angular velocity controller developed was incapable to do so. In this section, the controllers designed are applied to the drill string model. Thus, this result in transient oscillations with larger amplitude in the angular velocity as can find in Figure 3.20, Figure 3.21 and Figure 3.22 for bit velocity, the amplitude of the oscillations decays faster for controller compared to uncontrolled.
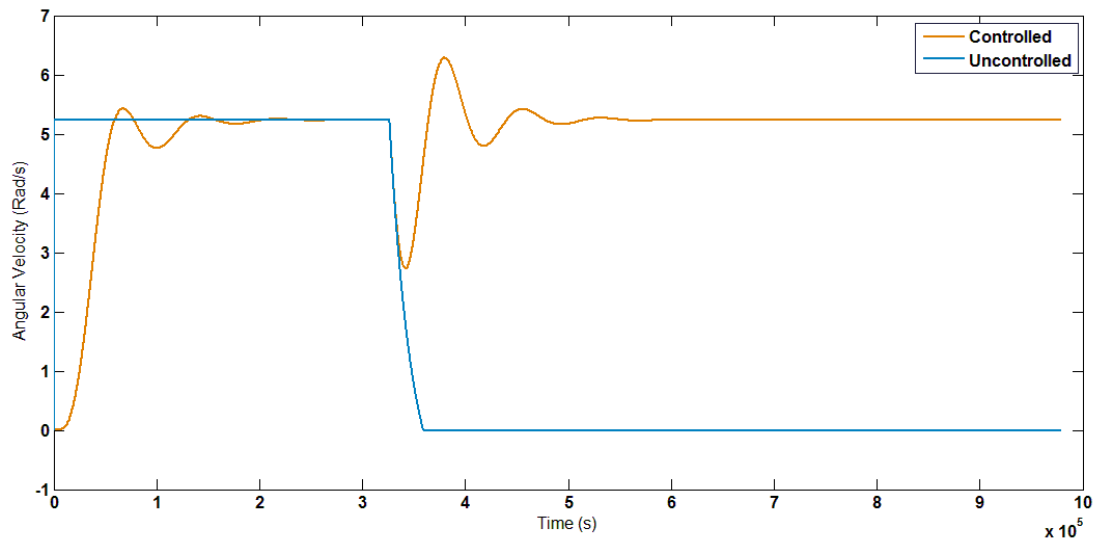
Figure 3.20: Angular velocity verses time at 5.236 rad/s (50 rpm) and 1N load disturbance
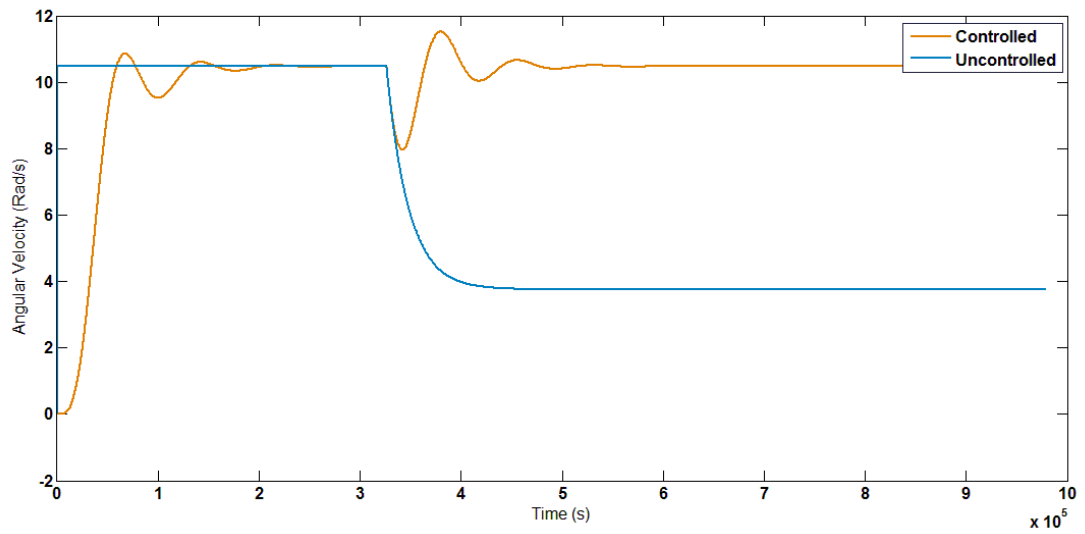
Figure 3.21: Angular velocity verses time at 10.472 rad/s (100 rpm) and 1N load disturbance
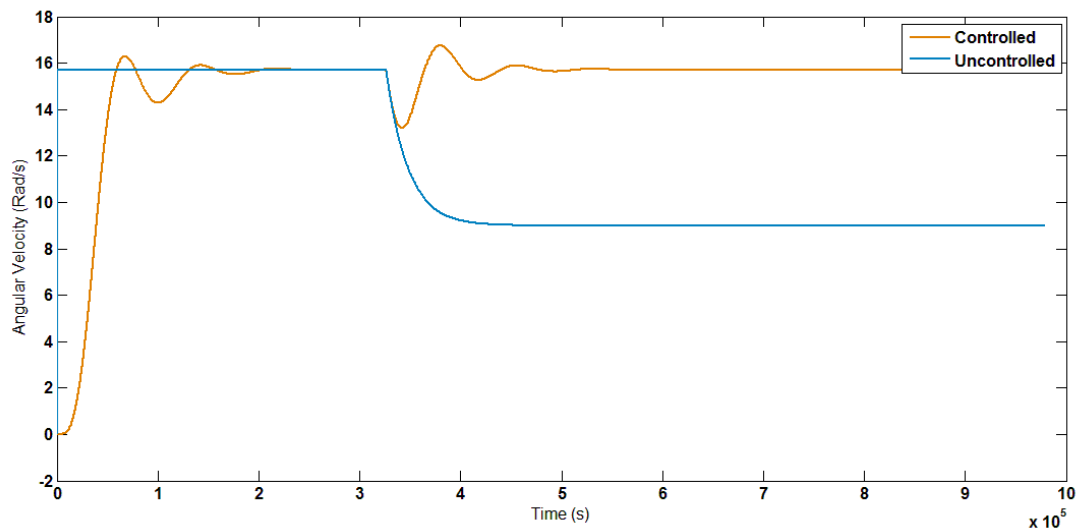
Figure 3.22: Angular velocity verses time at 15.708 rad/s (150 rpm) and 1N load disturbance
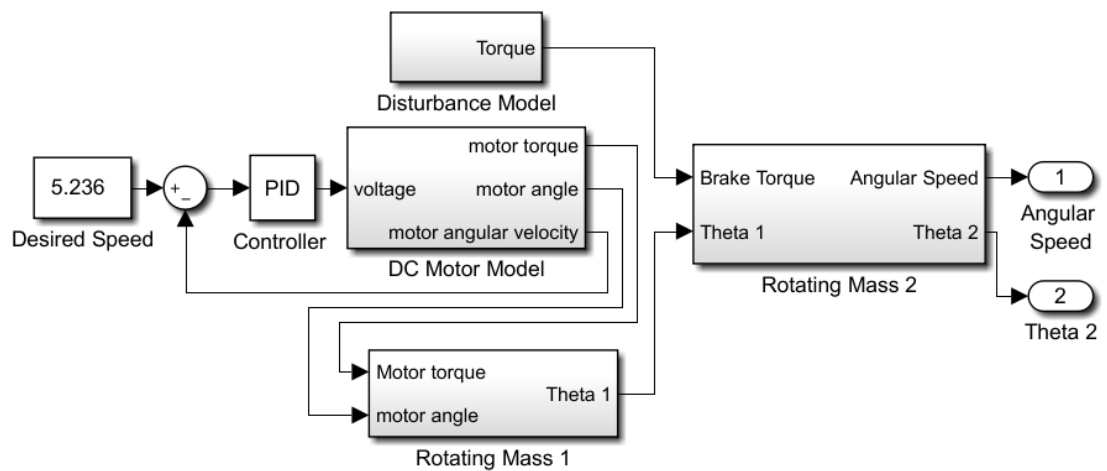
Figure 3.23: Controlled angular velocity

Figure 3.23 above show the overall Simulink design where the desired speed was set to 5.236 rad/sec (50 rpm), 10.472 rad/sec (100 rpm), 15.708 rad/sec (150 rpm), it consist of four sub function of DC Motor model, rotating mass 1, disturbance model and rotating mass. The outputs of the controlled angular velocity are the value of angular speed and also theta 2
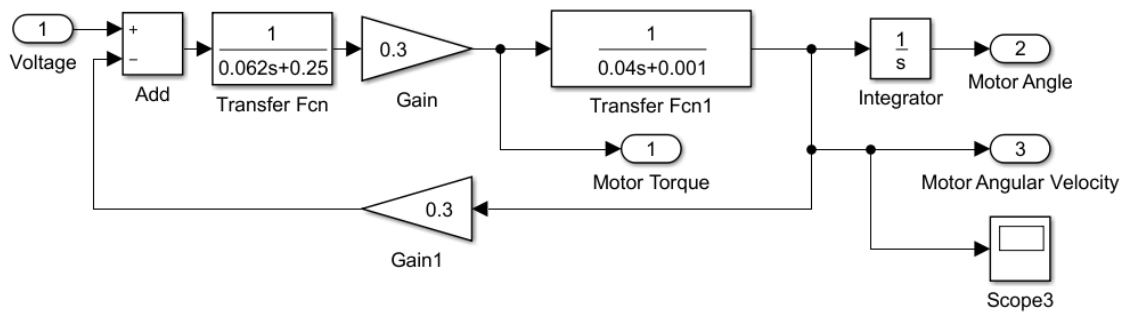
Figure 3.24: DC Motor Model

The DC motor model in Figure 3.24 above requires voltage input and provide three outputs which are motor angle, motor angular velocity and motor torque.
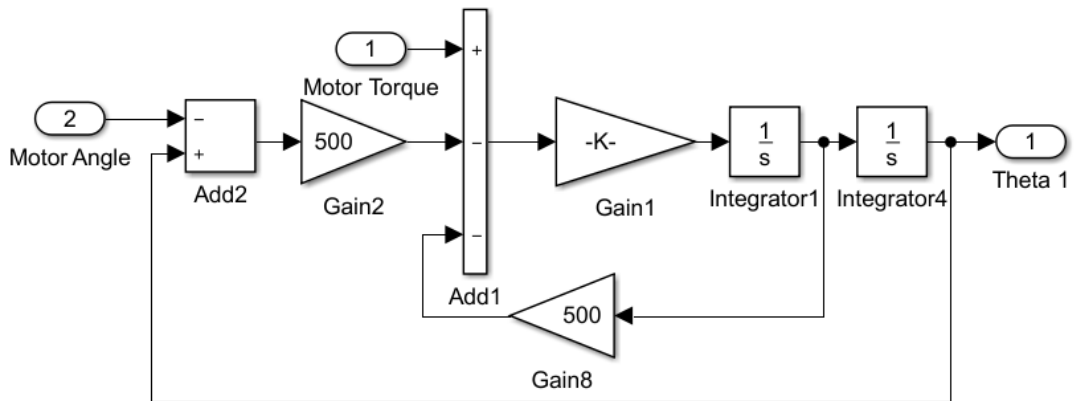
Figure 3.25: Rotating Mass 1

Figure 3.25 above shows that the input of this rotating mass 1 subsystem used the motor angle and motor torque output from DC motor model to generate theta 1.
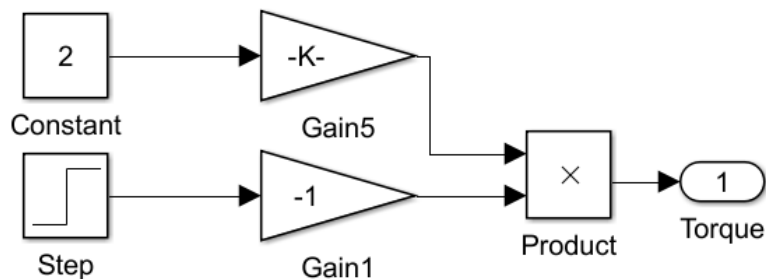
Figure 3.26: Disturbance Model

Figure 3.26 above shows the disturabance model function that generates brake torque output for rotating mass 2 input.
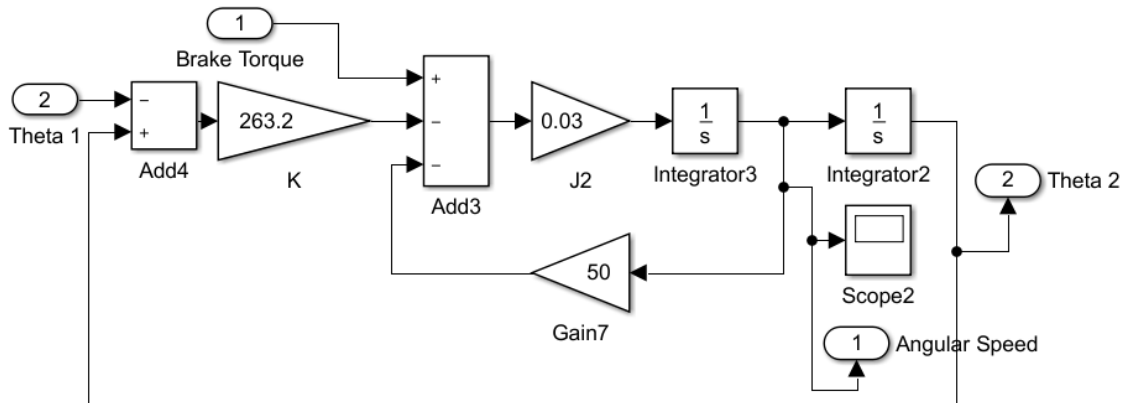
Figure 3.27: Rotating Mass 2

Figure 3.27 shows the sub function of rotating mass 2 also known as lower disc, this sub function provides the output of controlled angular speed and the value of theta 2

3.8 Comparison of Results: Simulation vs. Experiment

The results obtained from both experiment and simulations across three different speed conditions as depicted in previous sections were gathered in Table 3.3 for reference purpose. The explanations for each result were already discussed in section 4.12 and sections 3.7

Table 3.3: Comparison of results

Angular velocity (rad/s)*	Simulation *(see section 3.7)*	Experiment *(see section 4.12)*
5.236		

10.472		
15.708		
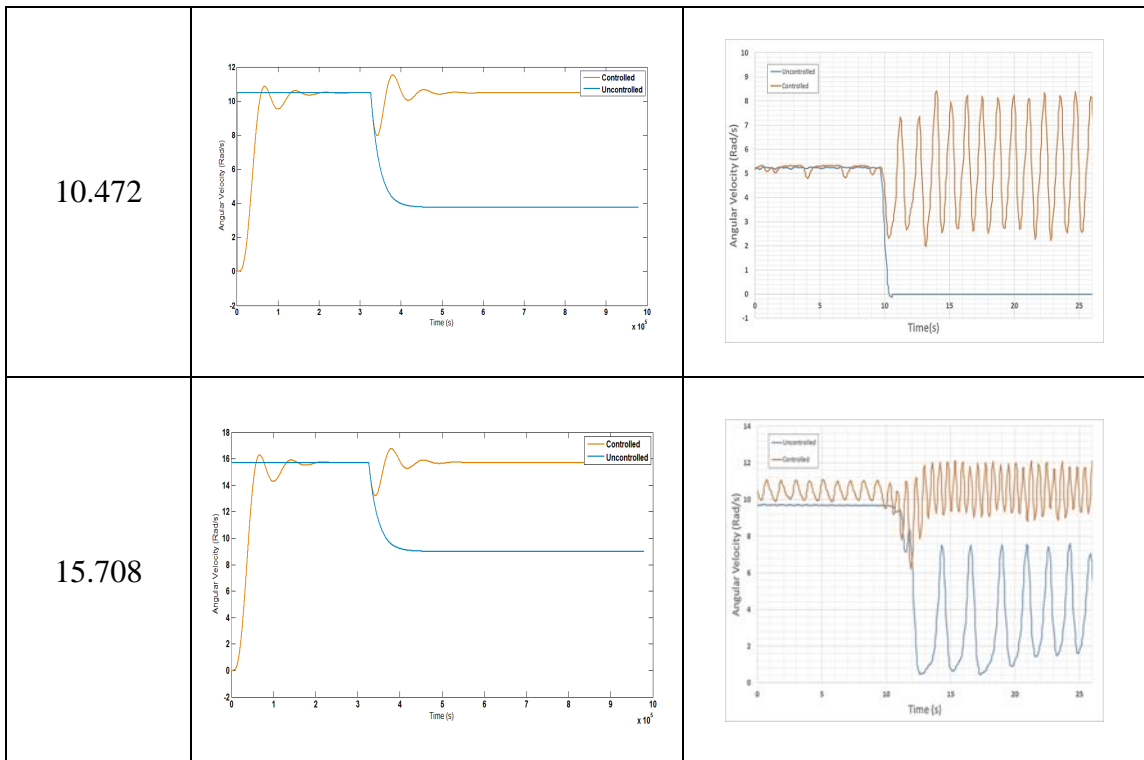
Note: 1N load disturbance was applied to all speed

3.9 MSC ADAMS Simulation Control System: Natural Frequency or Resonant

The main purpose of simulation is to improve the product and enhance safety. MSc ADAMS software was capable to model the real model in this case the model will design as similar as experiment in dynamic laboratory. ADAMS software is capable to simulate complex problem in any disciplines. In real operation environments a few challenges will be faced and the effective tools are more important to solve the problem task. The significant is that, it was a cost effective solution for example to get ready and testing of real test rig might longer period of time due to design time constraint, increased the cost of production based on incomplete data. In additional, simulation gives ability to examine of system responses in hard to measure regions and control the failure without any cost wasted due to failure on physical testing. MSc Adams software, capable of covering multiple categories such as in this research are nonlinear static and dynamic simulation, frequency domain analysis, time domain transient analysis, rotary dynamic and also system control.

Control systems in ADAM simulation have a critical goal in reducing the safety purpose and efficiency, it also support the operation of various mechanical and power

system and process equipment, for example, a model system can be used to adjust the impact, rotational speed to match the model through the bit rock interaction conditions. A braking control system is used to control the friction of bit rock interaction; one of the tools in MSc Adams, it can be used as to model the various mechanisms to simulate complete control system (digital/analogue) normally in electrical and electronic part. By join apply MSc Adams, mechanical, electrical, hydraulic and pneumatic systems can be modelled accurately by optimizing the operational efficiency.

3.9.1 Lower part - Bottom Hole Assembly (BHA)

As discussed in chapter 1 varieties of equipment used stages of drilling, including drills, coupling, and joints subs that comes with design issues. In this case, drill string design has to address the vibrations to support MSc Adams to enabling users to do simulation by controlling the speed limits of the rotational speed, in order to reduce the resonant up to the known resonant, which could deform the drill string, while CATIA, in static simulation perform as finite element analysis FEA for stress analysis of each components contact interaction and deformation of the drill string can be perform accurately. The model designed was imported to generate structural analysis where tools for frequency analysis are feasible. Dynamic Simulation Procedure

3.9.1.1 Without Brake System

There are several speed test based on the experimental research Table 3.4 shown the detail of the unit function of the ADAMS simulation. The coding of the function will be attach in Figure 3.28 and Figure 3.29, from the data script time to run will take about 45 minutes to reach the desired individual speed. The control system for rotational speeds were described in the script which required a conversion into degree/second before starting to simulate the drill string model.

Table 3.4: Function in MSc ADAMS simulation

Speed (rad/sec)	Speed (RPM)	ADAMS Function	Unit (degree/sec)
4.922	47	282d	deg/sec
10.472	100	600d	deg/sec
17.802	170	1020d	deg/sec
22.620	216	1290d	deg/sec
27.227	260	1560d	deg/sec
35.605	340	2040d	deg/sec
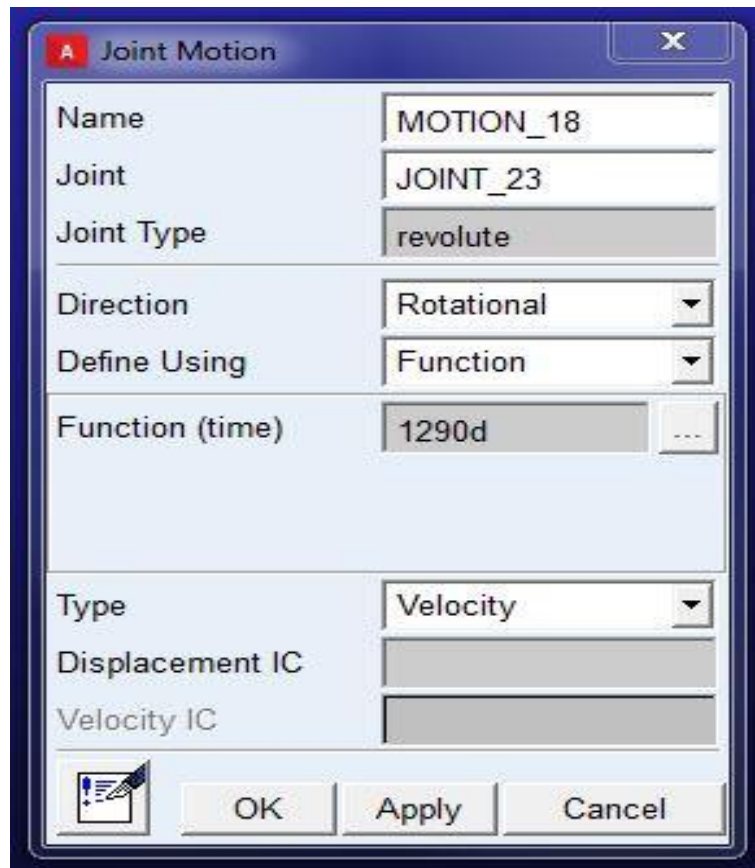
Figure 3.28: Script configuration of rotational motion for speed control by MSc ADAMS
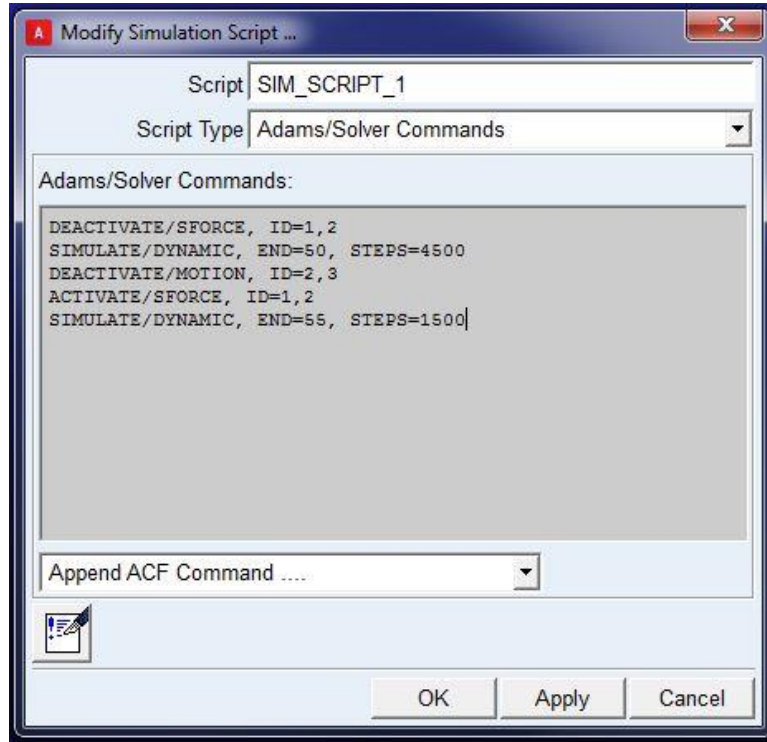
Figure 3.29: Script configuration of simulation for increasing brake and sudden brake system in MSc ADAMS

3.9.1.2 Sudden and Linear Brake Actuator

At the BHA bottom hole assembly that is the lower part of the model, the brake disk and brake pad was attached together as Figure 3.29, in order to represent the bit rock iteration hence to induce the friction force of the drill string operation. Simulation for applying brake and without brake, the function for motion is the same as the difference are the brake that will applied force to induced friction force to the function.

Table 3.5: Brake system and function

Brake mechanism	Upper brake pad	Lower brake pad
Sudden brake force	Step (time,0.0,0,1,10)	Step (time,0.0,0,1,10)
Brake force-increasing	Step (time,0.0,0,7,10)	Step (time,0.0,0,7,10)

There are two different braking system apply into model design which is sudden hard brake force and linear actuator brake by increasing brake force, Table 3.5 shown the system of brake apply and function used to set brake force system, both of the system

need different configuration to be set on the script, the configurations for both braking system are illustrated in Figure 3.28, Figure 3.29 and Table 3.5. For sudden brake, 70 N is apply at a time 35 seconds and 3 seconds meanwhile for linear actuator braking system (increasing brake force) is about around 7 to 10 seconds, for brake released to default position, it was actually exactly where were apply at experiment setup at laboratory as illustrated in Figure 3.30.
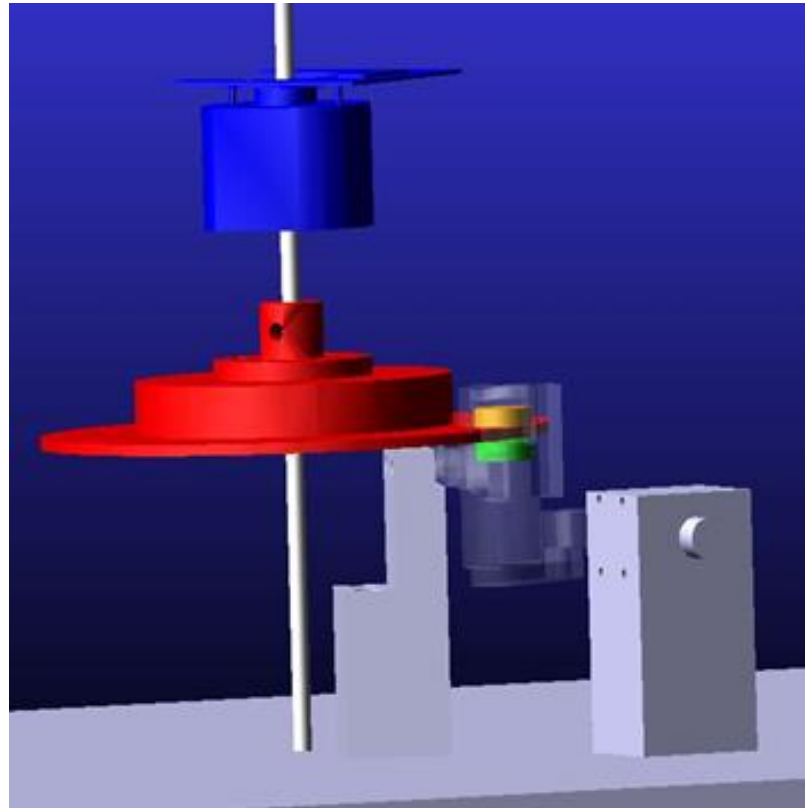
Figure 3.30: Detail of the BHA of the brake model by MSc ADAMS simulation

Step time function was used to define the force needed as shown in Figure 3.31 and Figure 3.32. The STEP function also plays, to estimate the step function with a cubical polynomial. The sample for STEP function written as; STEP (x, begin at, initial function value, end at, final function value).

After all the script done, model design by simulation started to rotate with the required rotational speed motion, at 35 seconds, the motion of simulation was neutralised and leaves the inertia in order to animated the rotational speed of the drill string. however, for the braking system, the forces was activated and in the motion the string were stopped from rotating and all the raw result of that direction were collected and stored.
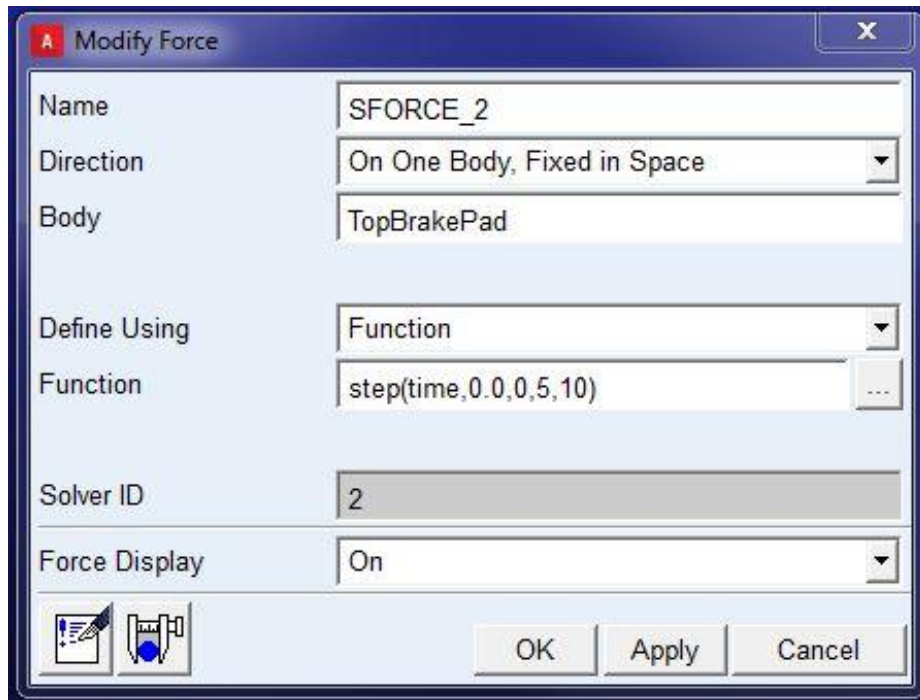
Figure 3.31: Script for configuration of force applied to the system in MSc ADAMS - increasing braking system
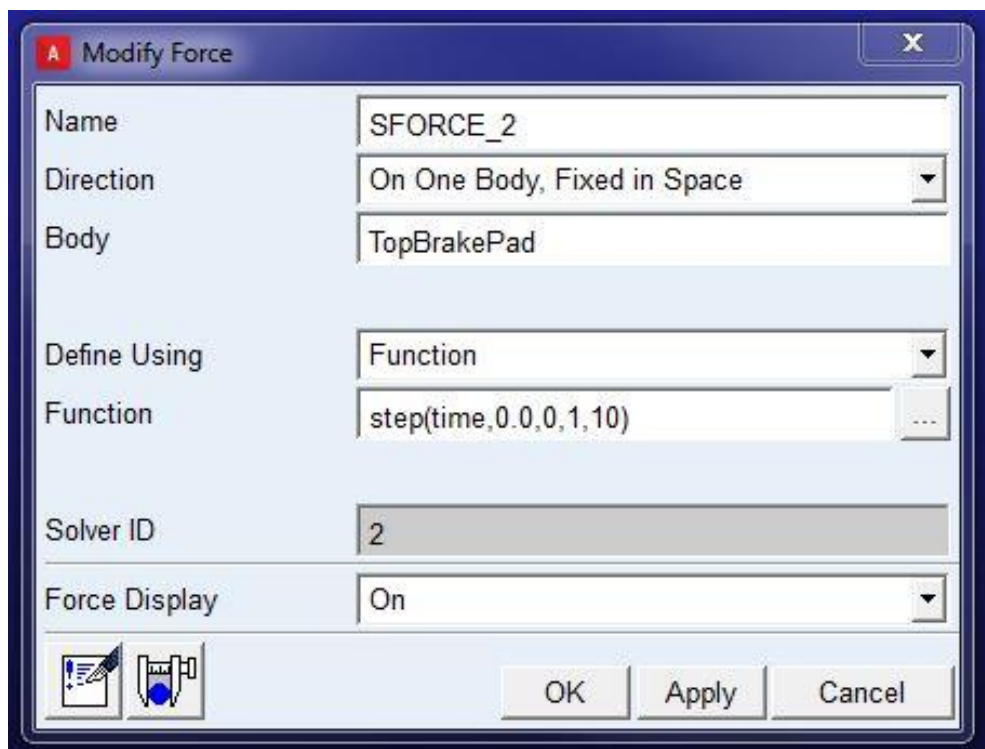
Figure 3.32: Script for configuration of force applied to the system in MSc ADAMS - sudden braking system

3.9.1.3 Dynamic Simulation Result for Natural Frequency or Resonant by MSc ADAMS

Torsional vibration analysis was conducted in this research by creating a stick slip condition on the model designed, by applying a high inertia at the top disc of the drill string and also by applying braking at the lower disk to induced friction force to the drill string system, then torsional vibration can be created. The upper disk and brake at the lower extreme create the difference in rotary speed which the difference resulting torsional vibration as stated by (Mohammed Fayez Al Dushaishi, 2012).

Based on the data obtained from the simulation analysis, graphs were plotted to investigate. The natural frequency of the drill string model system for each rotational speed, which is Figure 3.33 to Figure 3.38 respectively that illustrate the torsional vibration frequency occur on the model. All the graph were plotted based on the solenoid and sudden brake, while without brake, the torsional vibration did not occur because there is no external force applied to the lower part of the drill string to create the differences in rotational speed between the upper and lower part of the drill string system.
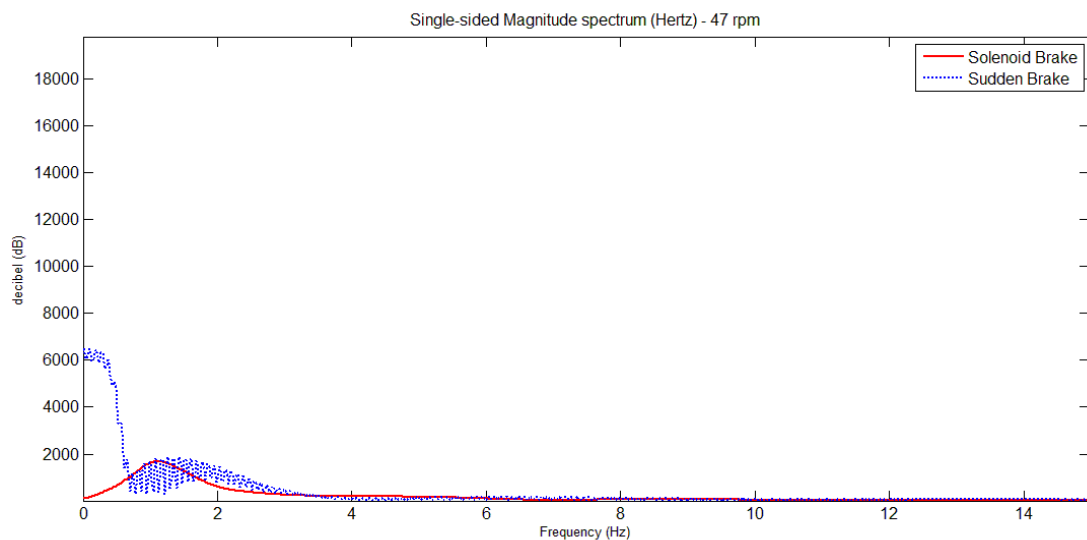
Figure 3.33: Single-sided magnitude spectrum at 47 rpm
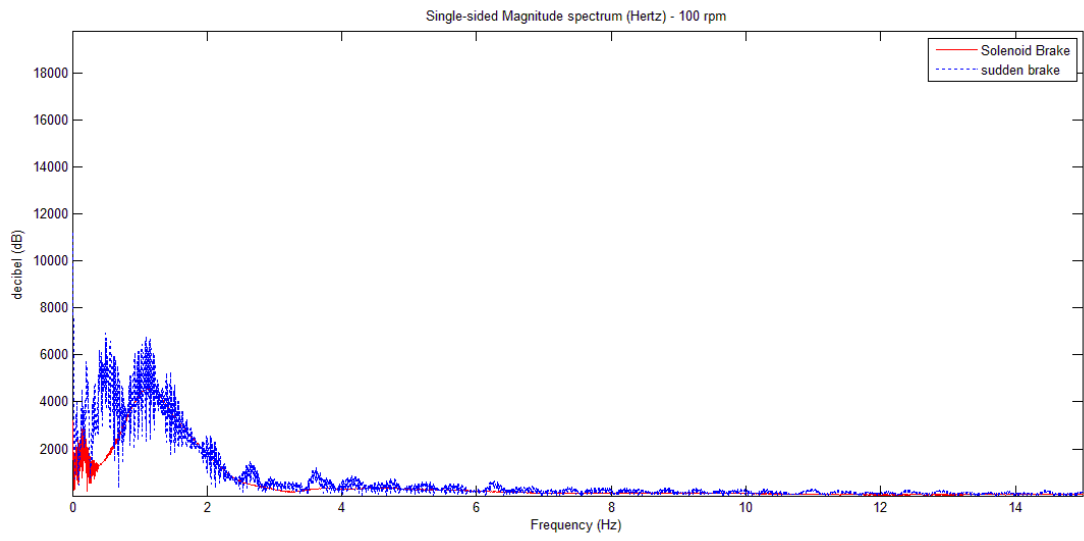
Figure 3.34: Single-sided magnitude spectrum at 100 rpm
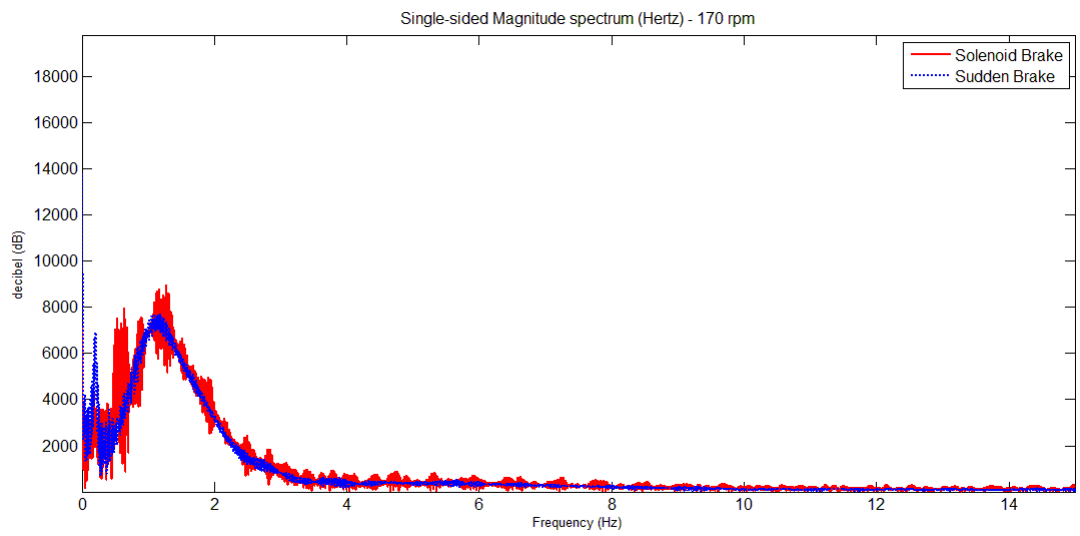
Figure 3.35: Single-sided magnitude spectrum at 170 rpm
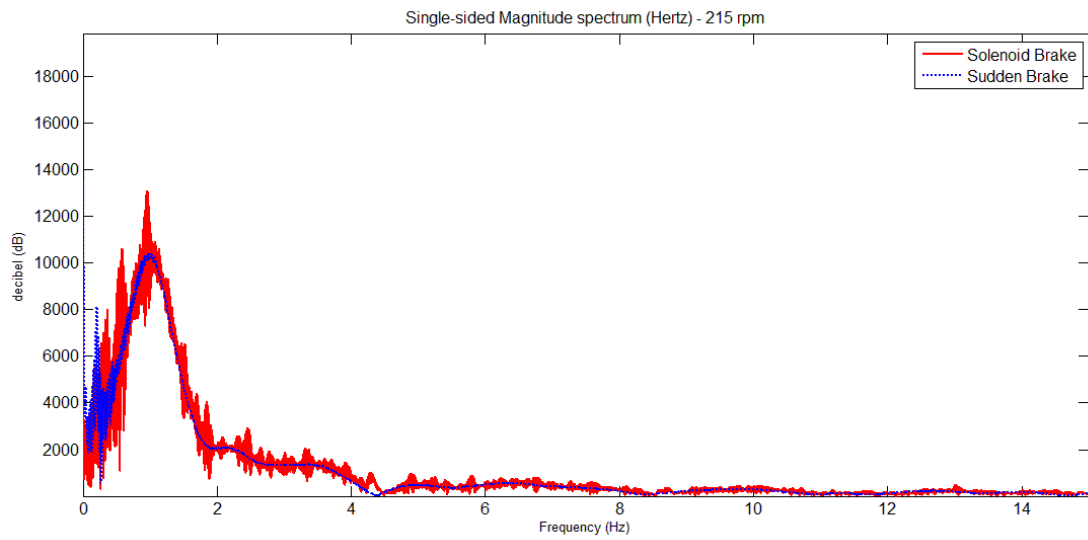
Figure 3.36: Single sided magnitude spectrum at 215 rpm
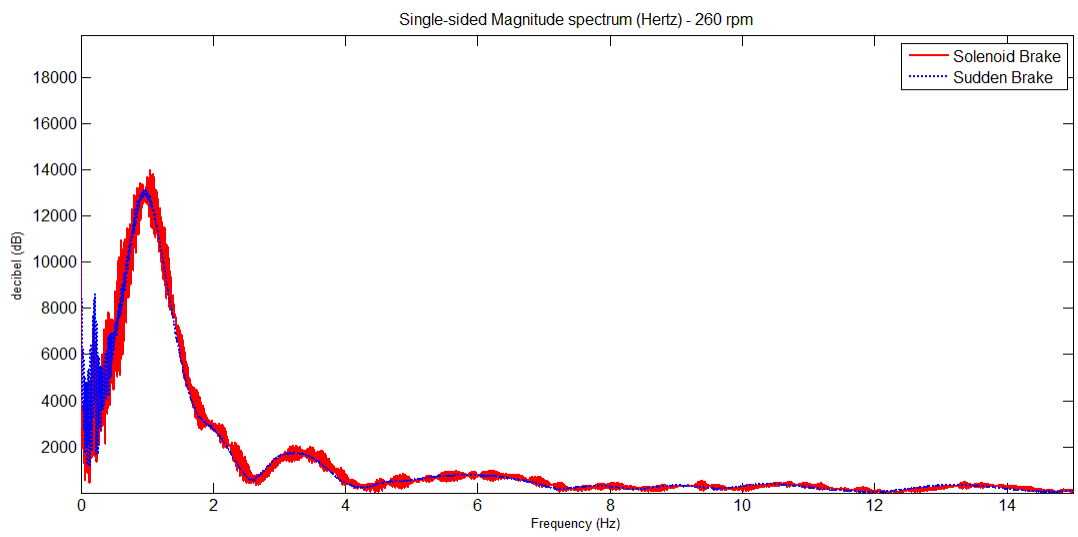
Figure 3.37: Single-sided magnitude spectrum at 260 rpm
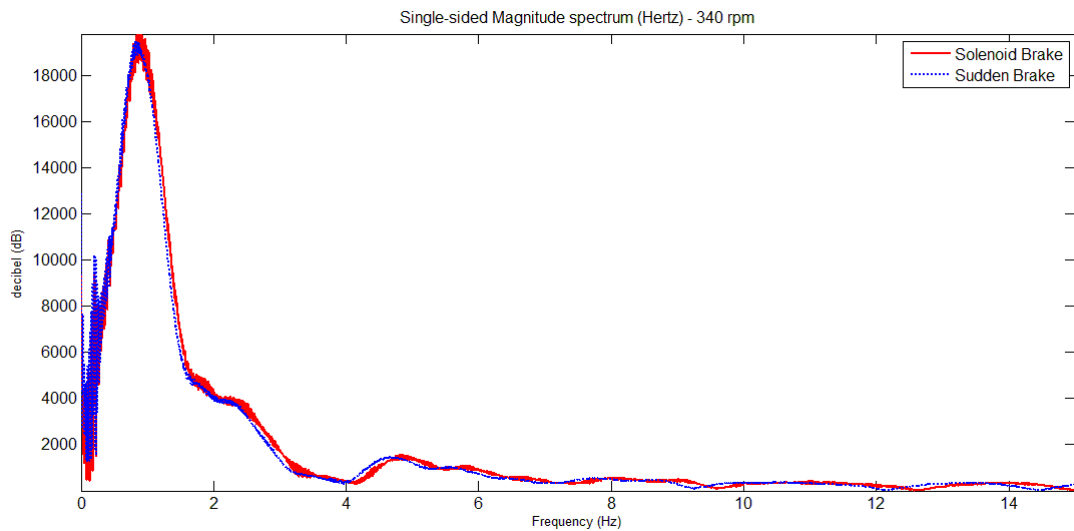
Figure 3.38: Single-sided magnitude spectrum at 340 rpm

Based on the graph obtained on each speed using solenoid and sudden braking force, the natural frequency for each graph was tabulated in Table 3.6 for the highest frequency magnitude that present the natural frequency of the drill string system.

Table 3.6: Natural frequency of torsional vibration for simulation of the drill string

	Natural Frequency of Drill String Model					
Rotational speed, (rev/min)	47	100	170	216	260	340
Solenoid brake force, (Hz)	2.11	2.49	2.82	3.71	3.96	4.72
Sudden Brake, (Hz)	2.91	3.48	3.95	4.34	4.75	4.93

Referring to Table 3.6, it can be seen that torsional vibration frequency takes place easily within the range of natural frequency that can cause fatalities and previous discussed at section 2.4 From this data allocation, it is also proved that the drill string model designed has been made successful in creating the torsional vibration and simulating stick slip condition on the drill string system.

From the Figure 3.33 to Figure 3.38, it can be seen clearly that the natural frequency magnitudes excite if the torsional vibration are increasing rapidly with the increment of the rotational speed of the drill string. This situation happened because of when the rotational speed of the drill string is high, it produced more kinetic energy that being

stored and then released during stick slip phenomenon happen. This situation also caused the torsional vibration to happen frequently during drilling operation.

The comparison between the solenoid brake force and the sudden brake force, shows that the sudden brake force frequency intensity are decreasing for the frequency above 5 Hz. This situation happen because of the rotational speed leading to dangerous torsional frequency to occur, which the frequency 5 Hz is a reliable natural frequency for the system to avoid stick slip but approaching to another consequences as stated in Table 2.2.

Meanwhile for the solenoid brake force, the intensity of frequency above 5 Hz is increasing from rotational speed of 47 rpm (4.922 rad/sec) to 100 rpm (10.472 rad/sec) and then decreasing from rotational speed of 100 rpm (10.472 rad/sec) to 340 rpm (35.605 rad/sec). This shows that when the external force is applied and increasing in a long duration occurs. However for the low rotational speed of 47 rpm (4.922 rad/sec) and 100 rpm (10.472 rad/sec) , it cannot overcome the increasing force, thus forcing the rotation to totally stop, hence the torsional vibration occurs more often on the frequency of below 5 Hz.

3.9.2 Static Simulation Result for Natural Frequency or Resonant by CATIA

Static frequency deformation by using CATIA conducted according to manipulated speed which is to perform the natural frequency of the model design and then will control the speed limit using dynamic simulation. Deformation of the system Natural Frequency is initially examined through static simulation CATIA using frequency deformation, then conducted throughout all level of operation speed from low to high speed 340 rpm (35.605 rad/sec). (Dareing 1984) State the fundamental calculation mode of the critical natural frequency on this case equation 3.22 used to calculate the critical frequency by the operational speed. Result obtained, tabulated in Table 3.8 is a static simulation to categorize the fundamental of natural frequency and noticed here the result is a close value with critical rotational speed of the drill string. Table 3.7 are the mechanical properties, boundary condition included and also the inertia of the drill string, meanwhile the critical rotary frequency are only established on the theoretical equation, the details of the result by using CATIA simulation is attach appendix for reference.

$$60f_{cr} = RPM_{cr} \quad [rev/min]$$

Table 3.7: Material properties of the experiment drill string

Drill string – Stainless Steel Grade - 303		
Mechanical properties	Measurement	SI unit
Diameter	6	mm
Length	1500	mm
Modulus of Elasticity	193	Mpa
Tensile strength, ultimate	620	Mpa
Tensile strength, yield	240	Mpa
Shear Modulus	77.2	Gpa
Poisson's ratio	0.25	

Table 3.8 shows static critical natural frequency response in relation to the speed domain were fundamentally categorized and we noticed here that the result is at a close approximation value with critical rotational speed of the drill string. Table 3.7 shows the mechanical properties, boundary condition included and also the inertia of the drill string, meanwhile the critical rotary frequency are only established on the theoretical equation, the details of the result by using CATIA simulation is attach at appendix for reference.

Table 3.8: Static simulation (CATIA) - Natural frequency

	Speed					
Rotational speed, (rev/min)	47	100	170	216	260	340
Critical rotary frequency, (Hz)	0.783	1.667	2.833	3.600	4.333	5.667
Simulation critical frequency, (Hz)	0.718	1.788	2.978	3.573	4.466	5.657

Drill String Laboratory Setup

4.1 Design and Arrangement

This section describes the experimental arrangements. The drill string 1.5 meter has been used with 6mm diameter meanwhile the two disks on upper and lower end are attached together to the string. The key testing mechanism device is built on rectangular frame with 2ft (length) x 2ft (width) as shown in Figure 4.2. The cross-section size of each column and beam is 2in x 2in and the structure is made from aluminium 40 x 40 profile, meanwhile the total height of the main frame structure is about six feet. The two plates are mounted on top and bottom of the frame structure. The experimental system, is adapted from Min Liao (2011) respectively stated that the experimental system is scaled down of the actual the drill string system in term of drill string diameter between 25:1. A turn table speed motor is used to derive the system at the top. In order to maintain a constant rotating speed, the motor is connected to a upper disc using aluminium bridge and eight inches disc diameter. The disc on the top as described in Figure 4.2, represents stabilizer and also represent the large rotary table at the surface of rotary drilling. Two absolute encoders are built in on top and bottom of the disc which use 11 bits of signal to represent 2048 revolutions and the detail of the absolute encoder is describes in tuning and testing LabVIEW section the main function is to record the rotations of the top and the bottom discs, whereas in the lower disc attached with the disc brake represents the rotating mass of the BHA (Bottom Hole Assembly). In order to study on effects of friction and its influence on the system, different type of combination are apply through the rotor or brake mechanism, the different contact surface combinations such as aluminium-aluminium (Al-Al) combination, rubber-aluminium (R-AL) combination, and rubber-rubber (R-R) combination, these arrangement correspond to low to moderate and low to high

levels of friction, on this experiment setup, is using the rubber-aluminium (R-Al) due to get a higher friction level.

Each part is modelled and assembled as shown in Figure 4.1 using CATIA V5 software, before being fabricated in metal workshop – followed by the electric / electronics works. The mechanism for rotary drilling begins at the electric generator which delivers the driving energy for whole entire drilling operation. When the energy is full and stored they transmitted to the drill string and along the BHA area. The drill bit is the part which actually comes in contact with the surface.

Many researchers allow experimental setup to get a better understanding of the parameter and downhole dynamics, and better support to verify their findings and result. For an example they used similar experimental setup, such as (Mihajlovic et al. 2004b) used vertical drilling rig comes with mechanical braking system at lower part of the BHA in order to simulate the effects of the friction between wall of borehole and drill bit. According to (F.A. Majeed 2013) and (Mihajlovic et al. 2006) drill string instrument design, the mechanism for inducing friction are only acting at one point vertically and rubber to rubber as the contact material of the brake, (Hernandez-Suarez et al. 2009) applied friction induced limit cycling in flexible rotor system, as a result this is helped with inducing torsional vibrations in their study. (Hanson & Hansen 1995), one of the early investigations on experimental drill string dynamic, (Warren 1997) do a very similar to actual drilling field, reported on large scale laboratory rig,with account to drill-bit diameter under WOB, rotary speed and hydraullic conditions. Meanwhile (Patil & Teodoriu 2013), said that large scale rigs normally owned by companies, most of the institutions consider rigs as a cylinders tube string driven at top by an electric motor. BHA also are usually represented as cylinder tube. Bit rock interaction simulated through shaker or brakes and also this is applied for an axial mode vibration and torque profiles meanwhile for torsional vibration phenomena they simulated through a special gear-pulley-spring system (Wiercigroch et al. 2015). M.Wiercigroch also state their rig is very comprehensive experimental setup because allow the researcher study all important effect in drill string dynamics, drill-bit and also bit rock interacrtions, this design complete with two configurations, rigid and flexible shafts. The purposed for rigid shafts is to determine mechanical characteristics of the drill bit, especially relationship between Rate Of Penetration (ROP), and

Weight On Bit (WOB). A flexible shaft is used to simulate all the dynamic phenomenom such as stick-slip, bit bounce and whirling. Most of experiment setup the drill string are drive by an electric motor and have been ran 0.5 to 1370 rpm which is angular velocity ranges, the angular velocity is measured by two encoders by locating on top and bottom of the drill string, Thus all the data acquisition signal are controlled by LabVIEW graphical interface monitor real-time responses of the system.
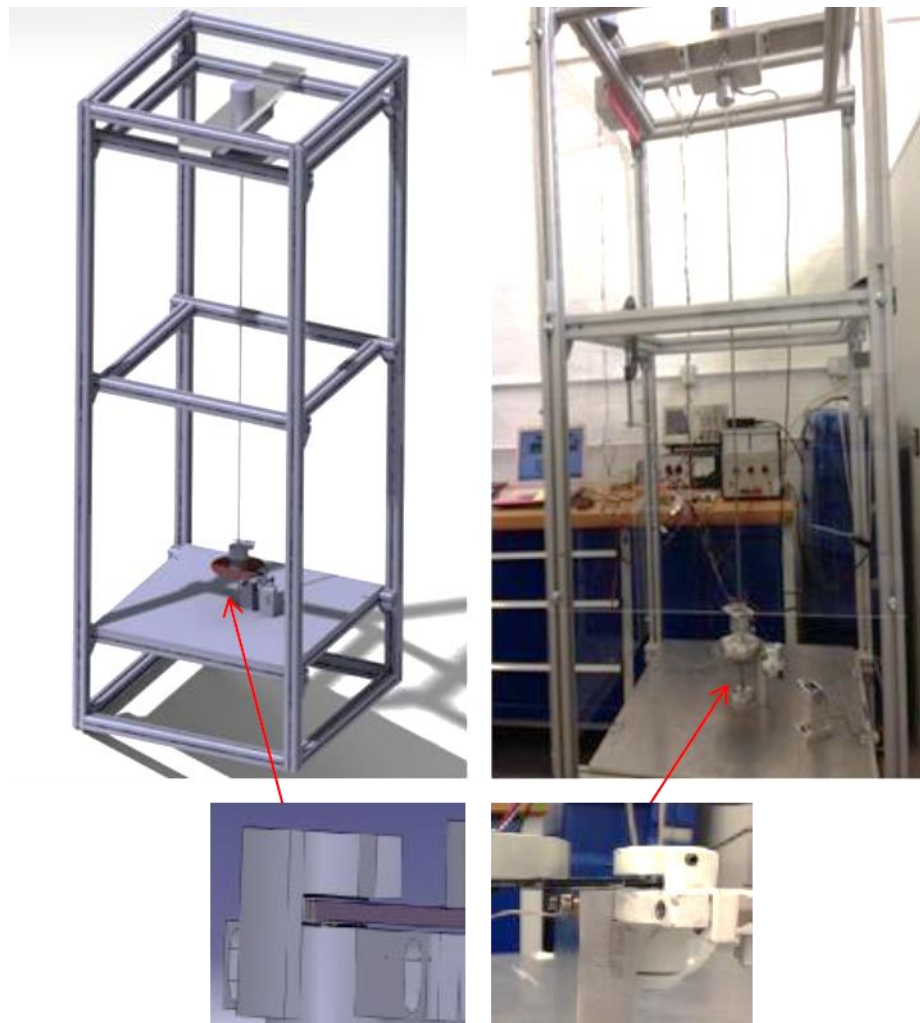
Figure 4.1: Laboratory experiment test setup

Table 4.1: Part of laboratory experiment setup

No	Description
1	BL58EB Brushless DC motor – rated up to 3000 rpm.
2	Bridge – stainless steel for encoder holder
3	960 Single turn absolute rotary encoders – attached upper and lower part of the string, to measure the angular velocity of the upper rotary and drill bit.
4	Upper disk – represents stabelizer and also represent the large rotary table at the surface of rotary drilling.
5	1.5 meter long string – represent the drill string as in rotary drill rig, (made of mild steels is attached to DC motor and connected with upper rotary table).
6	40 x 40 aluminium profile – the entire frame .
7	Accelerometer ADXL 335 - to sense vibration force in respect to X, Y, and Z direction of the string.
8	The lower disk – attached with the disk brake represents the rotating mass of the BHA (Bottom Hole Assembly).
9	A disk brake with a disk pad – as represent as bit rock interaction and the mechanism to induce brake.
10	Bottom plate 600mm x 600mm with 10mm thickness – base support
11	Brake mechanism – two contact points.
12	Linear actuator – to create a brake which is representing a rock formation.
13	Desktop – monitor and generate result
14	Load cell – to measure the force required.
15	Power supply – to run motor that connected to the drill string.
16	Microcontroller Chipkit UNO32 – used as data acquisition
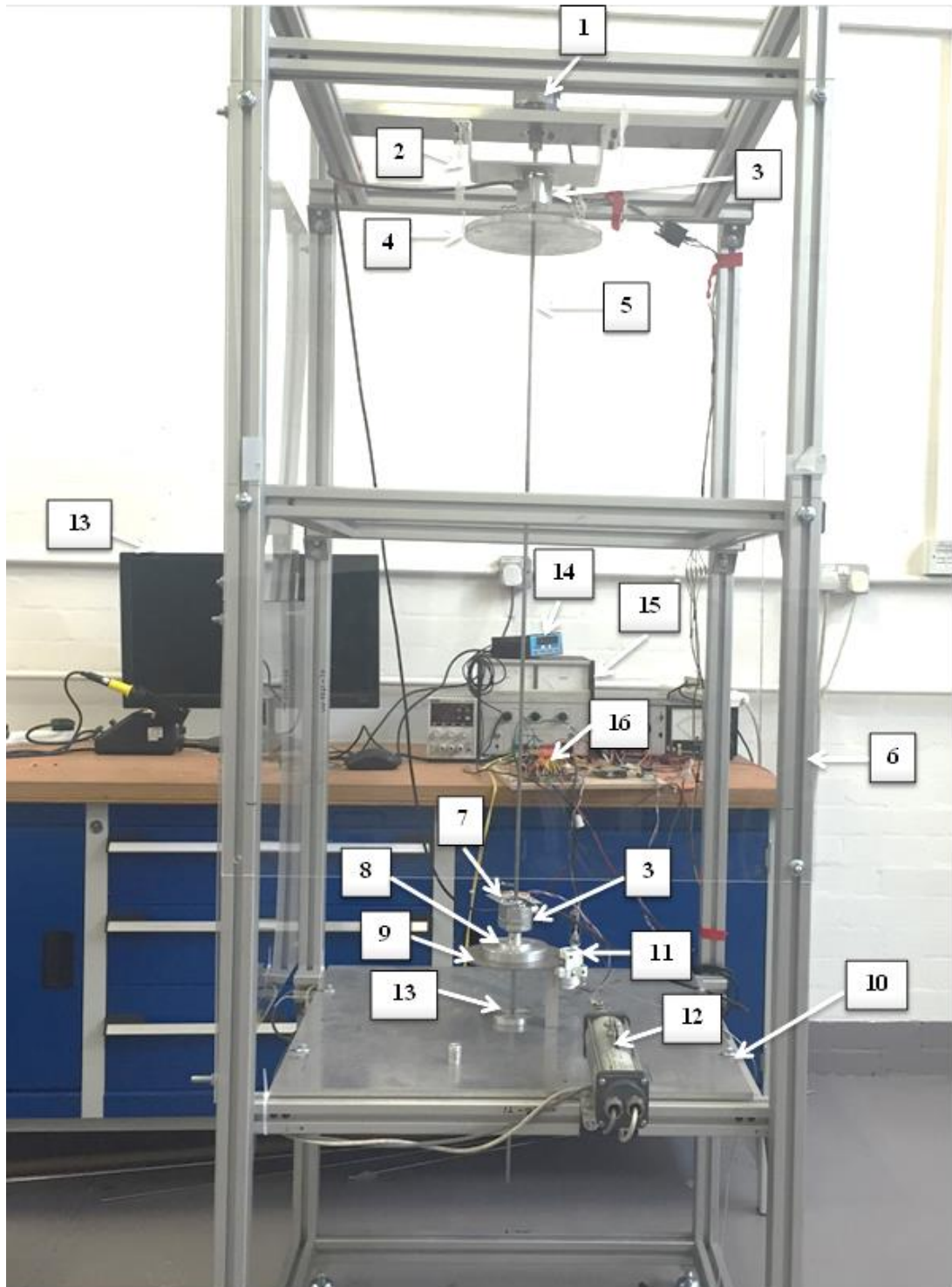
Figure 4.2: Detail experiment setup

4.1.1 Brake Mechanism System

The prototype was developed and used in this study was based on a design that was adopted in the previous studies (i.e. Min Liao 2011, Majeed 2013 and Mihajlovic et al.

2004). In those studies, Majeed (2013) and Mihajlovic, Van de Wouw, et al. (2006) have applied one vertical contact point as mechanism to induce friction (as depicted in Figure 4.3 and Figure 4.4 respectively), while Min Liao's (2011) brake approach is induced as drill bit bumping each other or in contact with borehole wall which resemblance (see Figure 4.5).

Nevertheless, a minor change was made to the design to improve and simplify the rotary turn table and the drill bit representation i.e. the mechanism to induced friction force or bit rock interaction at the BHA area, as depicted in Figure 4.6. The change refers to the two-contact point with vertical force is applied at the top and bottom of the lower disk, as illustrated in Figure 4.6(b) in order to obtain a sudden brake and to represent the bit rock interaction at the bore hole surface especially at very high speed up to 300 rpm (31.416 rad/sec).
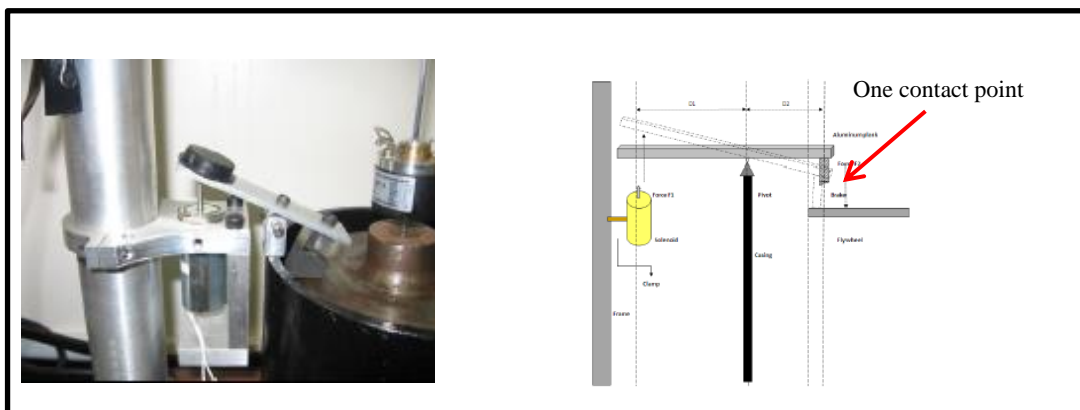
Figure 4.3: Hard brake for inducing friction force (Majeed, 2013)
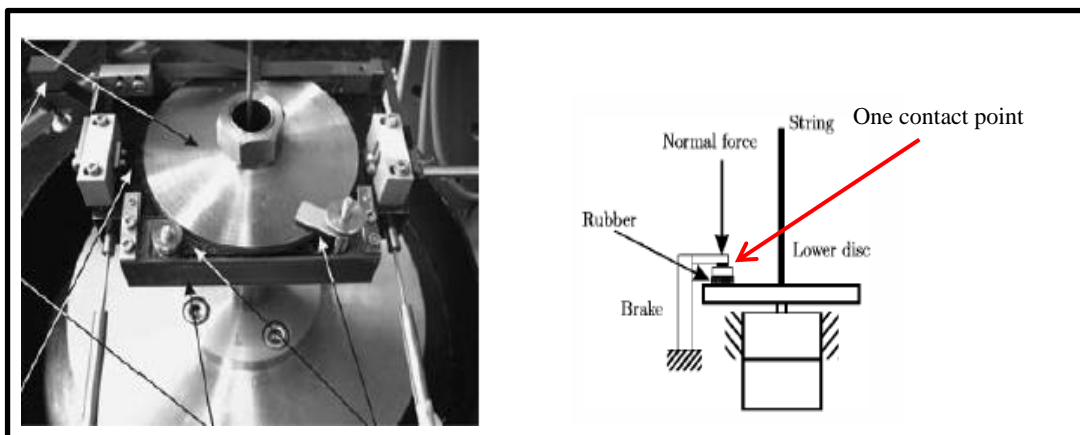
Figure 4.4: Hard brake for inducing friction (Mihajlovic, Van de Wouw, et al. , 2006)
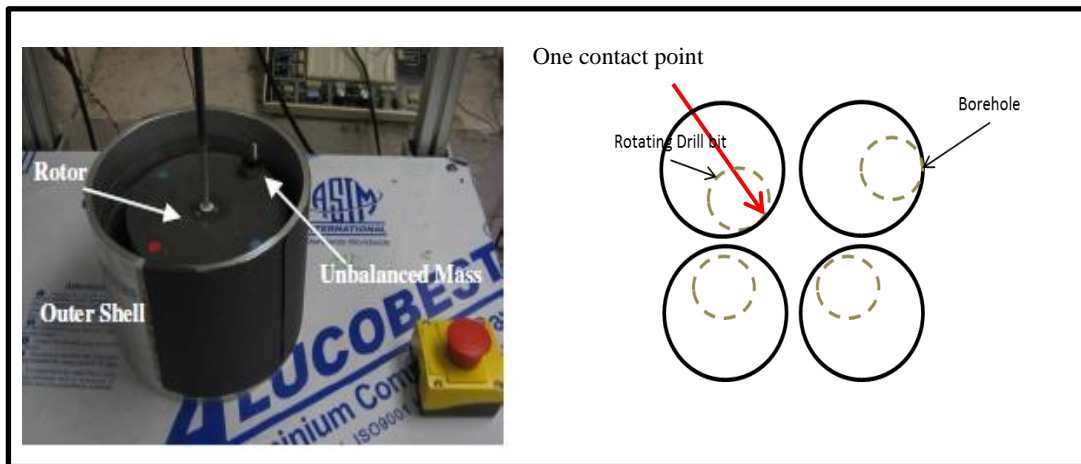
Figure 4.5: Illustration of rotating drill bit (Min Liao's, 2011)

In the hard brake mechanism, a wired cable is connected the to the solenoid actuator and the weight force load for this hard brake is up to 1 kg, shown in Figure 4.6(c), and brake clamp illustrated in Figure 4.6(b). As the solenoid actuator obtains voltage and signal from the power source, as the function is pull and release pull the wire and automatically brake pad of lower and upper disk pad closer to the disk brake and eventually the mechanism will stop and brake from rotating disk. In mechanical view, the solenoid actuator does not receive any current voltage, so the elastic potential energy inside will finally pulling back the wires cable into an original position. A steel cable is attached to the solenoid actuator with capacity up to 1kg and the brake clamp as shown in Figure 4.6(c). As the solenoid actuator receives voltage and signal from the power source, it will eventually pull the string and drives the top and bottom disk pad closer to the disk brake to gives a very hard brake stop. However when it stops getting voltage from power source, the elastic potential energy inside the brake will eventually pull back the steel cable into its original position. As for the circuit connection, relay module is used as a H-Bridge to pass through current voltage to the solenoid actuator mechanism. The brake positioning is coordinated between 2.8 and 4.74 displacement from the dril bit. The solenoid braking system produced immediate hard brake, especially when run at very high speed. Next, the solenoid brake was upgraded to the linear actuator brake system as depicted in Figure 4.6(a) to enable the incremental break, mimicking actual oil-drilling situation. The linear actuator is connected to H-Bridge circuit, together with Arduino Mega and 1 ampere power supply. The application of the brake is working when the power supply up to the 1 ampere, when the amount current below than 1 ampere the brake is not working

because the current is needed to produce sufficient force in order to apply the brake into the drill bit. Hence, the maximum weight force of the linear actuator is about 3 kg to 5 kg Figure 4.6(a). The brake was running while the motor run and represented to the real wellbore friction as bit rock interaction.
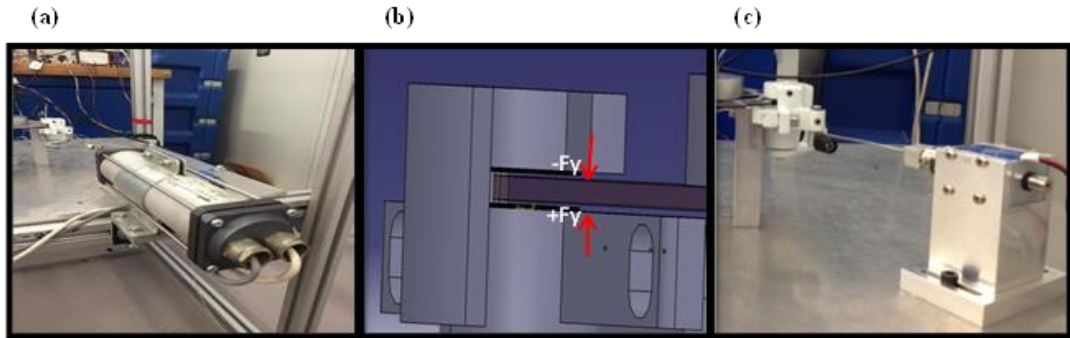
Figure 4.6: (a) Linear actuator   (b) brake clamp   (c) Solenoid braking system

4.2   Drill String Instrument Configuration
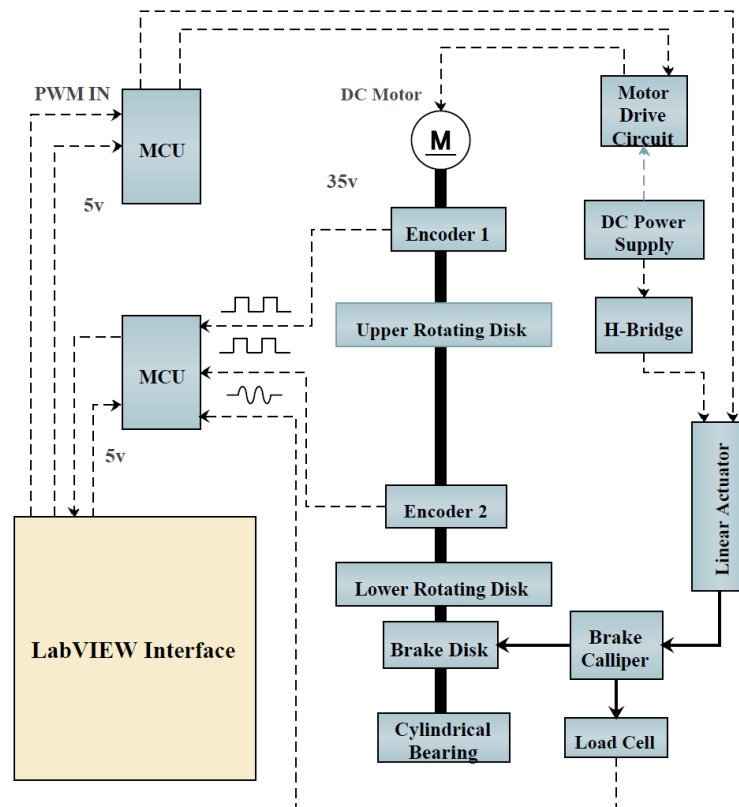
Figure 4.7: Overall system of drill string experiment - I

The braking application was discussed before but for the brake force introduced by means of a linear actuator and the resultant force was measured using load cell connected through spring. The load cell voltage change was measured using a transducer and the data recorded by Chipkit MCU. The linear actuator is supplied by a power H-bridge circuit which is connected to a power amplifier; the reason is to allowed control of the higher voltage using the lower voltage supply on the MCU. A 50W Brushless DC motor was choose, motor power is supply directly by amplifier, and the motor speed is controlling using a MCU (Arduino Mega) which differs the speed using a pulse width modulation (PWM) signal. This allowed the application of analogue signal using a variation of ON and OFF digital in square wave. The signal was 948 Hz is about the equivalent for voltage output supplied to the motor. Motor control speed is controlled by adjusting the pulse width, in Figure 4.7.
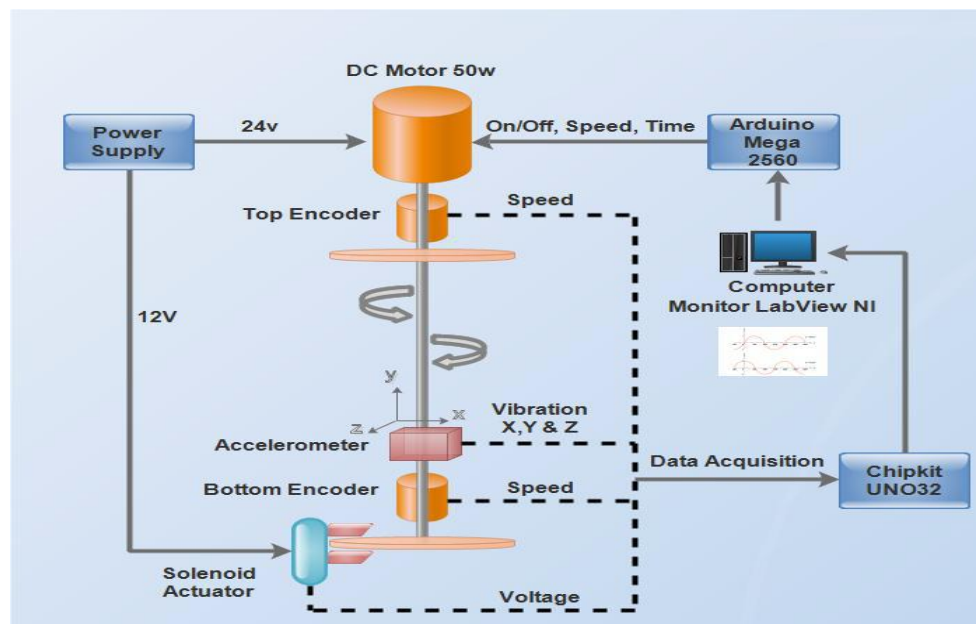
Figure 4.8: Overall system drilling string instrument - II

In this experiment the data communication was using one way communication in order to run the motor and acquired data feedback from both sensors. The computer is based point to translate the data and act as a communicating agent for microcontroller between Arduino Mega and Chipkit Uno 32. Two different microcontrollers was used since the speed of Chipkit Uno32 is higher than Arduino Mega. The data transfer is up to 80 MHz compared to Arduino Mega 16 Mhz. Figure 4.8 show the Arduino Mega is use to run the DC motor and being defined and control into LabVIEW NI environment. In this experiment, pre-setting also includes three aspects which are

speed required, time setting and braking time. This is because to analyse and investigate the result more efficiently by using the time frame. As mentioned earlier Arduino Mega function is to run the rotary DC motor in order to rotate the drill string, meanwhile Solenoid actuator used to acquire braking system. Computer is used to monitor and gain result during the operation for rotational speed in term of revolution per minute for both top and bottom encoder. LabVIEW environment software again used as function as monitors all sensors activities in terms of time domain. In LabVIEW also all the raw data obtained and recorded and export to excel for further analysis and study.

In order to run and test the experiment, all the allocated instruments went to calibrate and test in terms of mechanical funcionality and electronic device proficiency. All the device and instrument were tested regularly and separtely before assembled into a single unit system. DC motor model BL58 EB required 50W as rotating operation speed can be up to 400 revolution per minute, Figure 4.8 shows that the connection with circuit schematic. 24 Volt power capacity is capable to run the motor itself. External power suppy is installed as a DC power source to provided the DC motor to run as ideal.The minimum speed of motor capable to run is 40 revolution per minute or 0.04 volt. Motor performance is attached at apendix, from the performance of motor itself show the minimum current allow to operate is about at 0.02 ampere at 4% of the current rated 0.5 ampere at 1000 revolution per minute (rpm).

This method is implementing into this project as a one of a method on controlling process and output. As for this project, rotary DC motor account as a process control while its rotary speed represent as response or feedback. The illustration is shown as Figure 4.9.
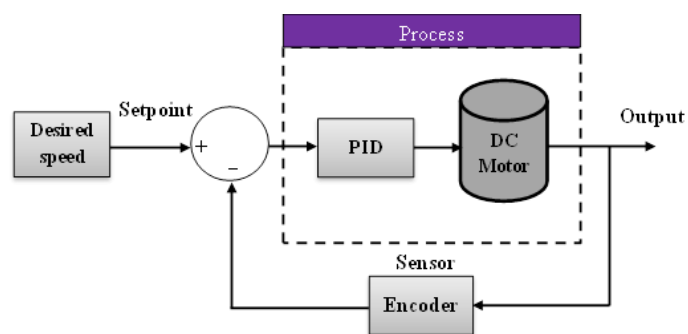
Figure 4.9 Proportional Integrated Derivation (PID)

The investigation itself presented as PID controlled system, therefore a review of this controls method was performed to investigate and justify the tuning ability.

4.3 Test Rig Gain Tuning

The parameters determined obtained in previous were used into the system open-loop stability. The overall system was stable and open loop response will find below. Velocity at the lower part at BHA was take into account as design a feedback parameter with PID control, the motor controlled using PWM signal, the primary PID gains were found using the tuner the input signal for PWM resulted in non-linear relationship. As a result the auto tuning function could not be developed. Once the initial gain were obtained the PWM signal generator was include and the gain consequently adjusted to improve the response. Estimation value of the saturation 0-20 was applied to the PID output control.
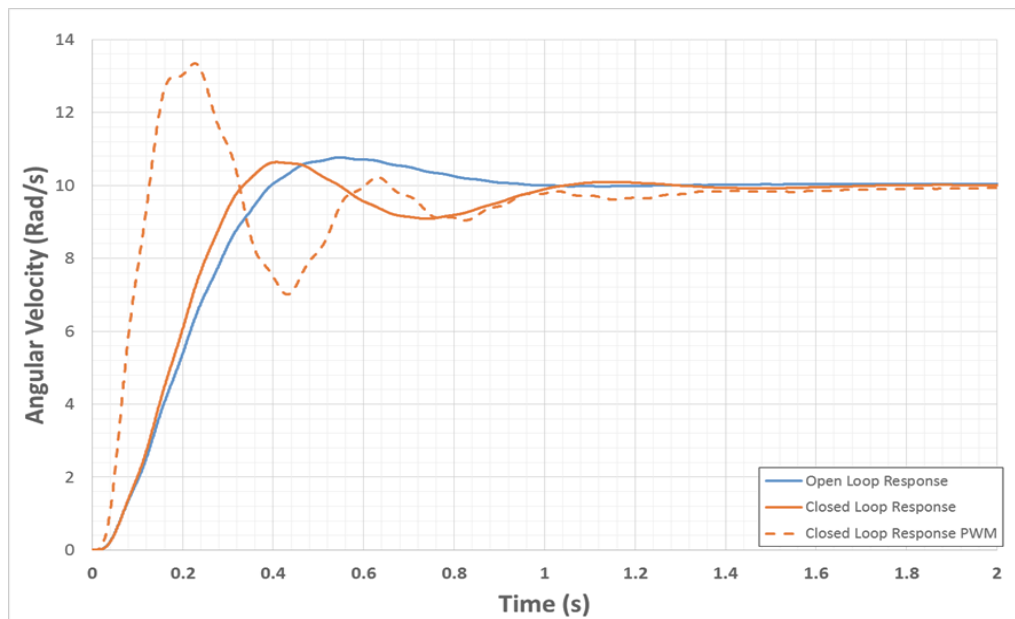
Figure 4.10: Angular velocity response for model representing the experimental setup

Figure 4.10 above describes the Simulink model used to determine the preliminary gain for the PID controller then the controller will apply to the test rig in Table 4.2. Meanwhile the open loop response shown the best result according to settling and over shot, but here faster response was required when load was applied, but it was later optimised on the test rig. The huge overshoot for the closed loop because of

braking mechanism is not appear or active reduction in speed in the system, which reduce the velocity if the set point was exceeded. When it comes to the experimental test rig, it will depend on limitations of the hardware itself.

The transfer function equation 4.1 is already derived before to describe the relationship between voltages and position which dividing by *s* and the system parameters gives the relationship between voltage and angular velocity. The Figure 4.11 below describes the Simulink model used when selecting the gain values.

$$\frac{\theta_2(s)}{v_a(s)} = \frac{0.3164}{4.962 \times 10^{-8}s^4 + 7.319 \times 10^{-7}s^3 + 0.0003273s^2 + 0.003086s + 0.0176} \qquad \textbf{4.1}$$

The signal generator can found at **Figure 4.12** below as describe, creating a square wave signal at the voltage, desired frequency and also duty cycle. The voltage and frequency is set by the user and determined by the motor voltage and MCU signal frequency.
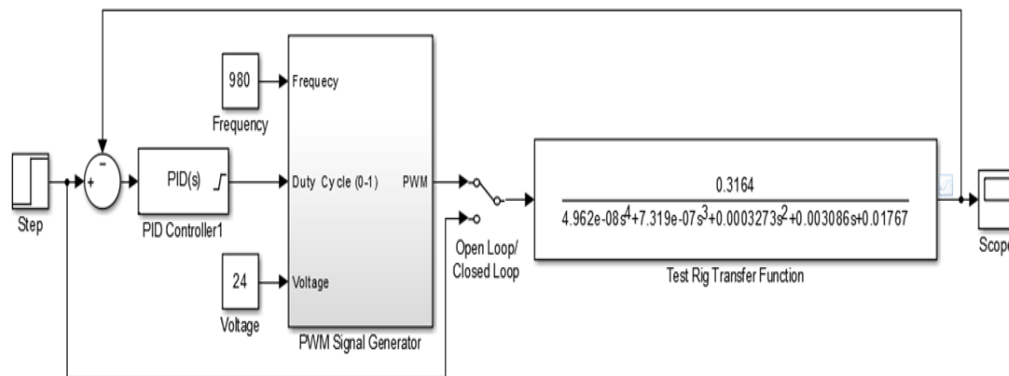
Figure 4.11: Overall Simulink model representing the experimental set-up
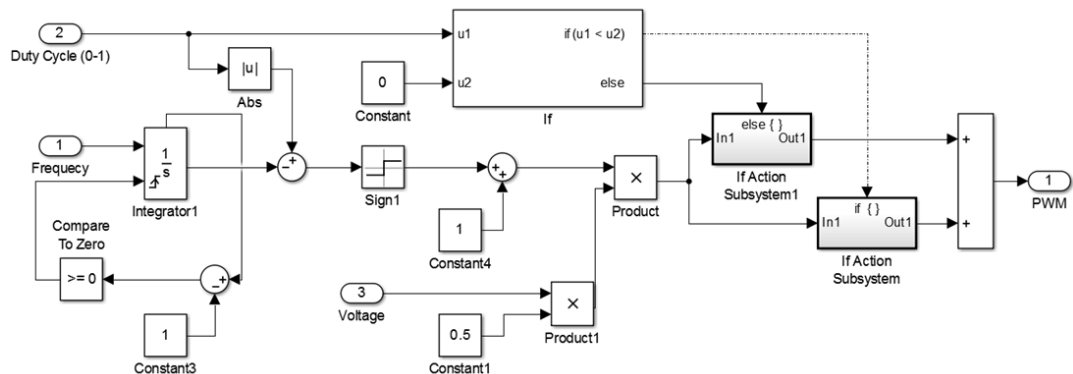
Figure 4.12: Simulink model for pulse-width modulation signal generator

Table 4.2: PID gain

	Closed Loop	Closed Loop with PWM
P	0.145561728669621	0.01
I	0.353561995849398	0.02
D	0.0120380590116512	0.0001
N	23.5995317513462	-

4.4 Testing and Optimisation

After designing the Simulink model and implemented to the simulation, the model was then transferred into national instruments LabVIEW, for final result on experimental test rig which uses graphical programming syntax. The angular velocities for each part, upper and lower extremities, and force were applied by brake mechanism and torsion in the string as illustrated graphically, in LabVIEW. All of the data was captured and exported to excel for data analysis. The system controls and monitor panel were displayed on the main user interface. Figure 4.13 below shows the displayed in visualisation window.
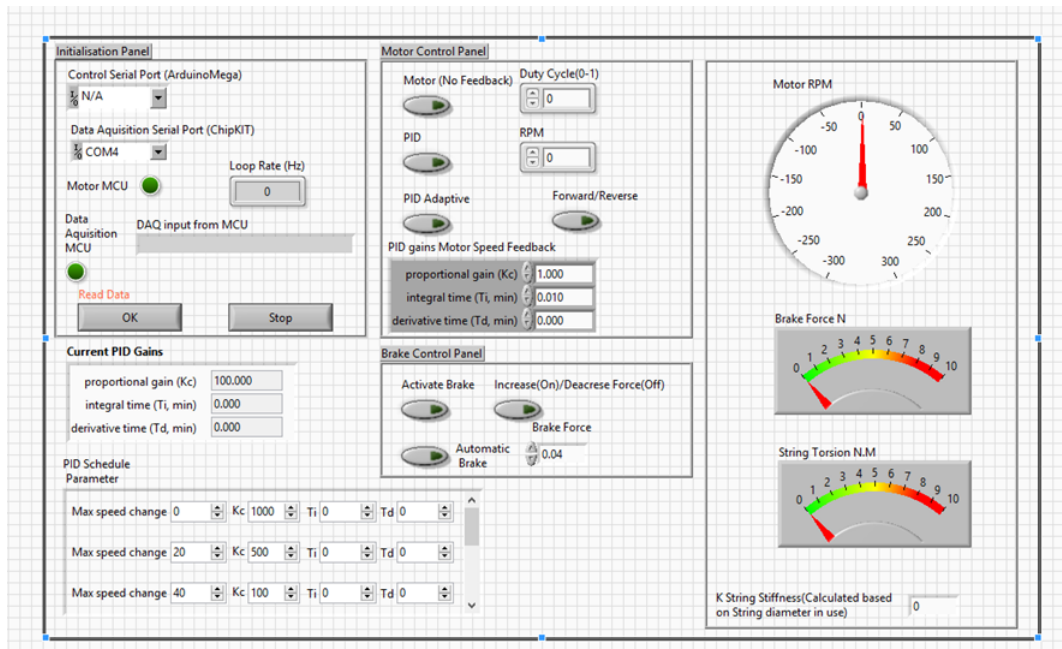
Figure 4.13: Visualisation window for the LabVIEW setup

For the final stage some differences between the control systems proposed before compared to the implemented, on the experimental setup, it is because of the shortage of the hardware as stated before, the motor had no active braking mechanism limited to the controllability of the system and implemented to the control suggested scheme. The program system were included open-loop, closed loop PID and closed loop PWM with gain scheduling for the motor control. In open-loop, the cycle was attuned to directly vary the effectiveness voltage that supplied to the motor. For the closed loop PID motor velocity set as feedback parameter and after that were adjust velocity in revolutions per minute (rpm). In the meantime the PID adaptive (gain scheduling) employs bit velocity as feedback parameter and finally the gain scheduling parameter was the bit velocity since the motor current are not recorded.

Since the WOB regulation only for reduce the effective brake force. In this system program also included manual modification of the breaking force position. The serial ports were selected on the desktop and the signal input was verified. The system setting only activated once the signal was received by the computer. The LabVIEW software was chosen to simulate the functions because it allows the interaction of coding between the systems.

The Figure 4.14 illustrates the main part of coding system used to process the input signals and control the outputs. The coding is divided into three main sections which are data acquisition, brake force and motor control, each of them open up another visualisation window where the relevant code is performed.

The signal is sent to the MCU's board from circuit sensors, and experienced signal noise from circuit will filtered using PID control input filter, the filter applies a fifth-order pass finite impulse response filter to measure values and process variables. This filter built applied at upper and the lower encoder signal which mean the transducer signal used to record the load cell voltage.
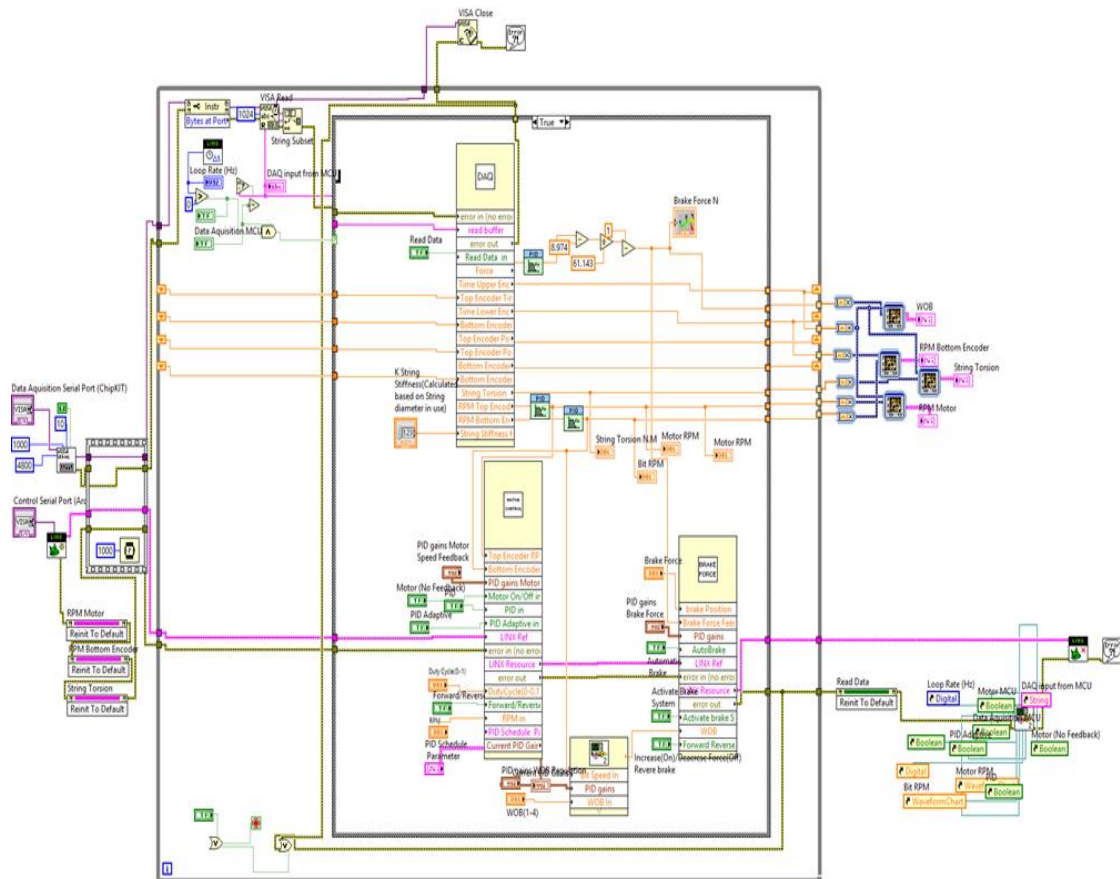
Figure 4.14: LabVIEW - Block diagram

4.5 Tuning and Testing (LabVIEW)

This section discuss about the experimental setup, LabVIEW programs and data acquisition sensors, as the laboratory procedure and setup for the experiment has already been decribed in section 4.1 previously explained, the experiment was performed to analyse rotary drilling dynamics under various external influences, in Figure 4.7 and Figure 4.8 shows the connection of the drill string to the upper rotary disk. The laboratory set up is similar in dynamics and degrees of freedom to the actual drilling operation.

On the data acquisition section, normally all the data are from sensors, encoder and accelerometer recorded in a real time and it's monitored and control through LabVIEW NI environment.

Figure 4.15 shows all the circuit connections, the amount of digital pins which is in I/O and they are required to read the changes in phases for 11 bit encoder. In order for

the individual encoder to function accordingly the 12 digital pins are needed. The data read for all the pins are binary code, where each pin will read in phase changes from high to low, hence, it is necessary to covert the Gray code into binary and decimal that gives a number from 0 to 2048 for one cycle of rotation as shown in Table 4.3 each degree of rotation will result in cumulative of number until it reaches 2048 and repeat again from 0, indicating one cycle has been counted. The ADXL 335 accelerometer is used to measured instantaneous acceleration response in x, y, and z direction. The circuit illustration diagram is presented in operation.as a circuit connection. In this research, for acceleration, the measurement value is presented in gravitational acceleration (G) with S.I unit ms^{-2}. One of the benefits using this type of accelerometer that it's provides flexibility to user to change sampling rate from as low as 1 Hz to 500 Hz depending on application used. The maximum sampling rate captured in this research is ranging to 10 Hz due to the limitations of hardware and software integration. The accelerometer ADXL 335, in Figure 4.16 and its specification can be found in the appendix as reference.

Table 4.3: Conversion of grey code to decimal for a rotation - 360°

Wire cable	Gray code	Gray code conversion to decimal	Decimal
Cyan	1 or 0	x 1	1
Yellow-red	1 or 0	x 2	2
Green-red	1 or 0	x 4	4
Pink	1 or 0	x 8	8
Grey	1 or 0	x 16	16
Purple	1 or 0	x 32	32
Blue	1 or 0	x 64	64
Orange	1 or 0	x 128	128
Green	1 or 0	x 256	256
White	1 or 0	x 512	512
Brown	1 or 0	x 1024	1024
Total		**2048**	
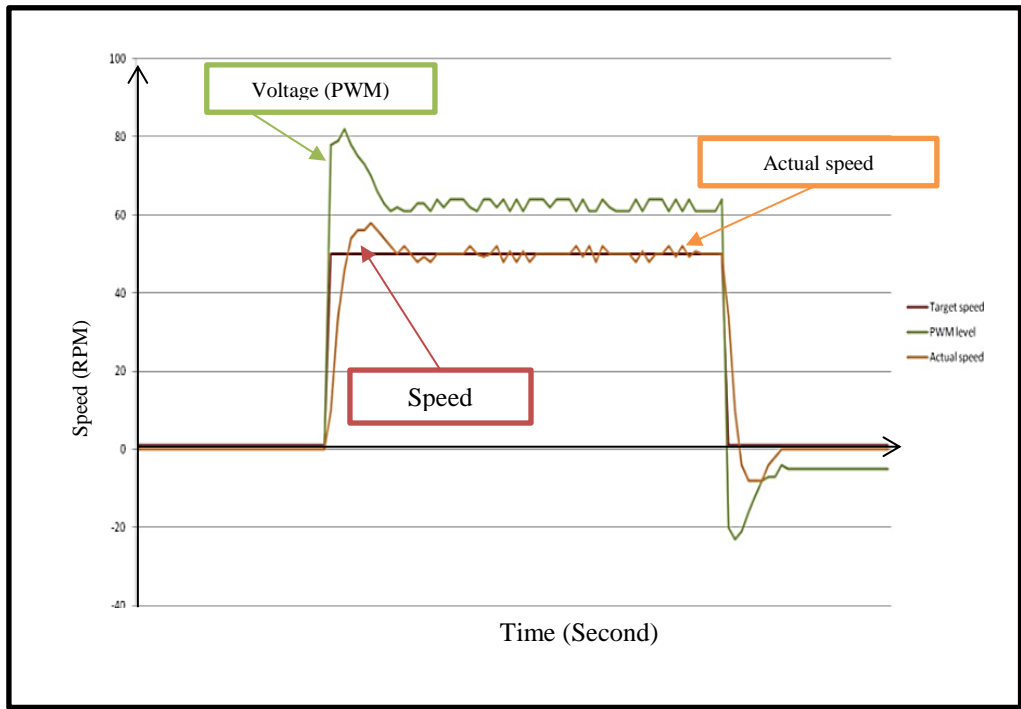
Figure 4.15: Example of speed response PID
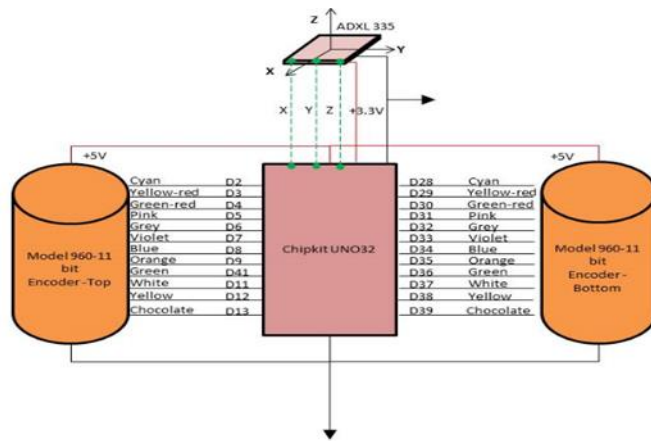
Figure 4.16: Sensor connection for accelerometer ADXL 335 and encoder 960
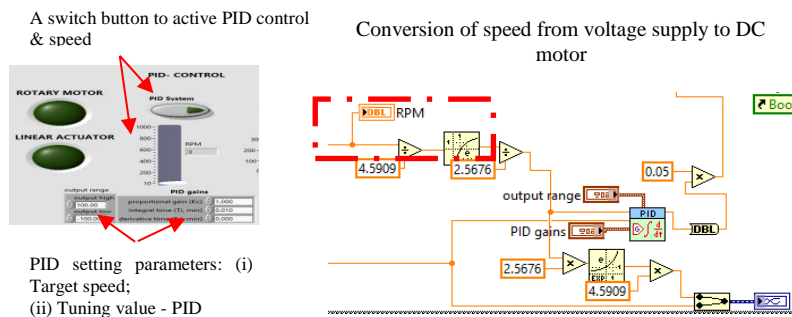
Figure 4.17: Example LabVIEW program for PID control

System operation user interface (UI)
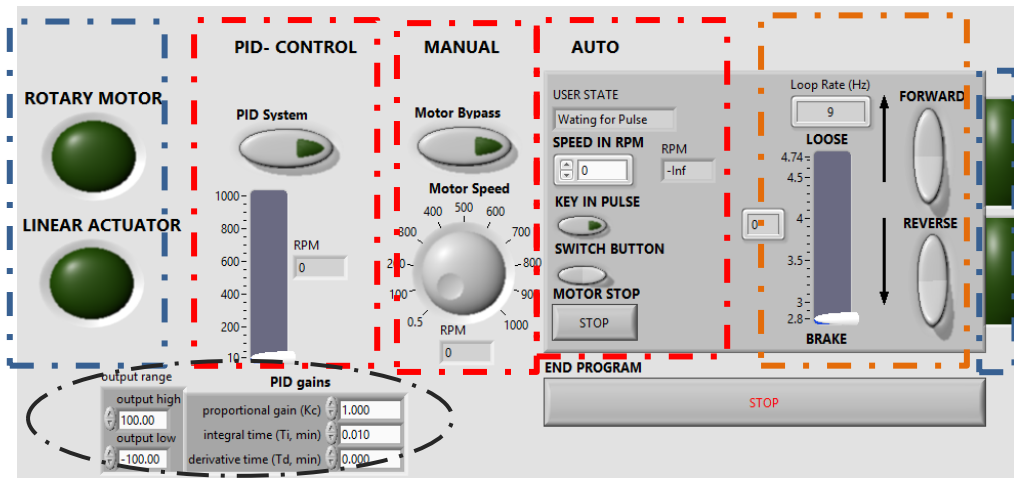
Figure 4.18: Interface window for Drill String System

Indication;

3 systems (Manual, PID, Auto)
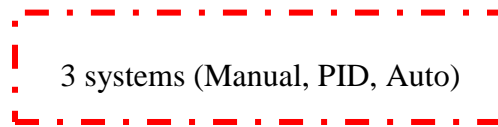
Figure 4.19: Modes of operating system

4.5.1 Manual

Users are able to set speed and run the motor as in manual mode, in Figure 4.19. Speed of motor varied as user tune up or down the knob speed.

4.5.2 Auto

Users will be asked to pre-set configuration for the motor speed. The motor shall run as the user switch ON "button". In this mode, in Figure 4.19, user is restricted to vary the speed.

4.5.3 PID

User is able to set the system as process control with manually setting configuration. Tuning for the rotary motor is required in order to acquire best response, in Figure 4.17 and Figure 4.18 Shows user indicator, this prompt user on the system behaviour and shall notify user when rotary and linear motor is working. Near operation for braking, forward and reverse switch button will operate as releasing and braking operation apply to the rotary disk. This operation is fed by load cell attached to the brake via steel cable. Readings in "Force" are measured through amplifier and converted from mV desired unit.

4.6 Operation for H-bridge

H-bridge circuit, in Figure 4.20: rotary motor operation reverse/forward (Tantos 2011)
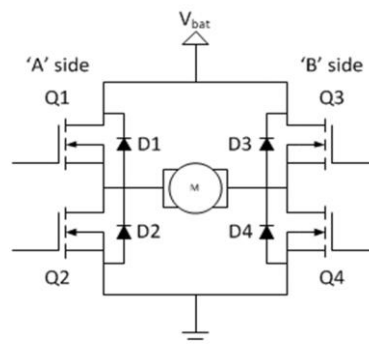
Figure 4.20: Schematic H-bridge

4.6.1 Static Operation

Electrical component in Figure 4.21, from (Q1 to Q4) are commonly bi-polar or FET transistor, meanwhile D1 to D4 as a diode. The top end of the bridge is connected to power supply and the bottom is grounded.
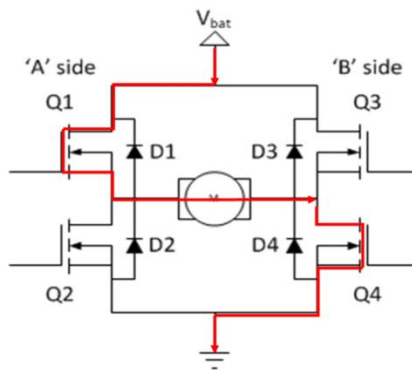
Figure 4.21: H-bridge static operation flow circuit

When (Q1 and Q4) is switch "ON" the left side motor will be connected to the power supply, while the right wiring is connected to the ground. Current will start flowing through the motor which energizes the motor in the forward direction and the motor shaft starts spinning

4.6.2 Dynamic Operation

Meanwhile if (Q2 and Q3) are turned on vice versa Figure 4.22, the reverse will happen whereby motor gets energised in counter direction and the shaft will start spinning backwards. In this simple circuit diagram, it is suggested that (Q1 and Q2) or (Q3 and Q4) closed at the same time. This will create a really low-resistance path between power and ground; effectively short-circuiting your power supply. This phenomenon is called "shoot-through". As for the counter measure for such condition, a relay is introduced at side A and B for triggering power one at a time.
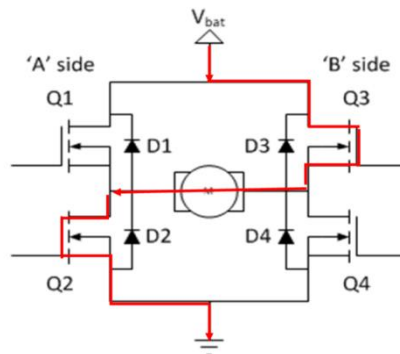
Figure 4.22: H-bridge dynamic operation flow circuit

4.7 Load Cell
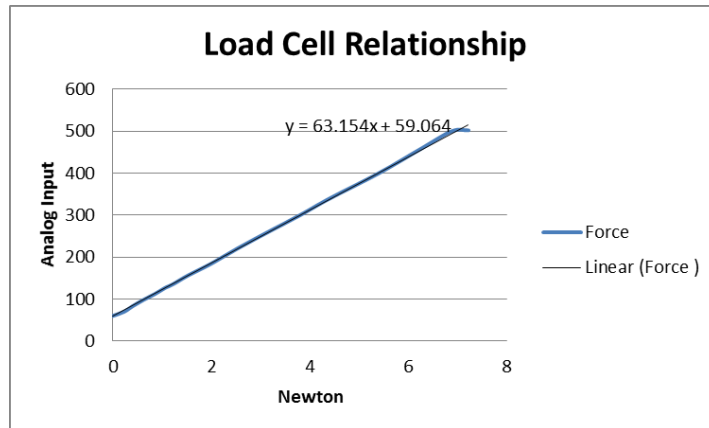
Figure 4.23: Load cell calibration and voltage relationship

The force equation is gained from the amplification of load cell connected directly. The force produce and analogue input signal are directly produce and analogue input signal are directly proportional to each other. As shown in the Figure 4.23, the relationship 4.2 between analogue signal and force from load cell.

$$y = 63.154x + 59.064 \qquad\qquad\qquad \textbf{4.2}$$
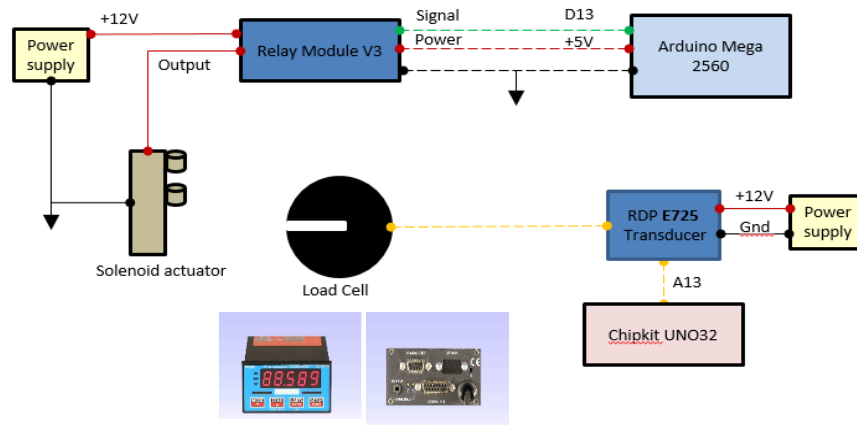
Figure 4.24: Analog signal to load cell for braking mechanism

The load cell is attached to the cable and directly attached to the braking motor, in

Figure 4.24. This is to measure the force required to decelerate the lower disk and put it on hold, Figure 4.25 and Figure 4.26 illustrated force unit into LabVIEW program. The maximum forces in kg measured to put the disk on decelerate and into static is at 3 kg.
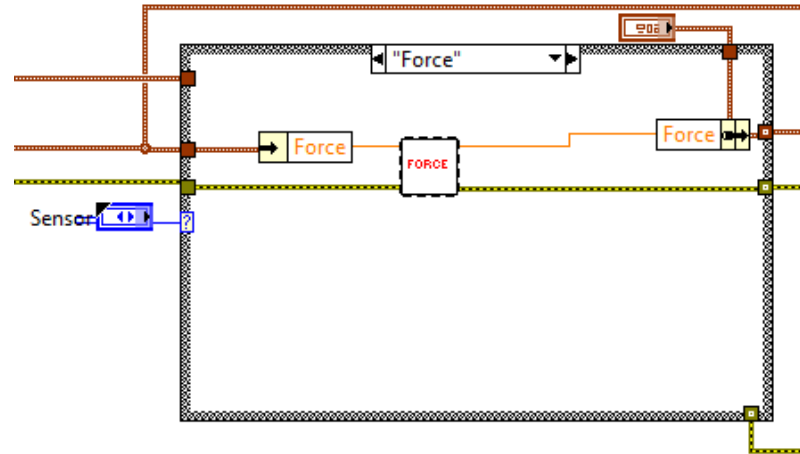
Figure 4.25: LabVIEW program for translating raw voltage to force unit
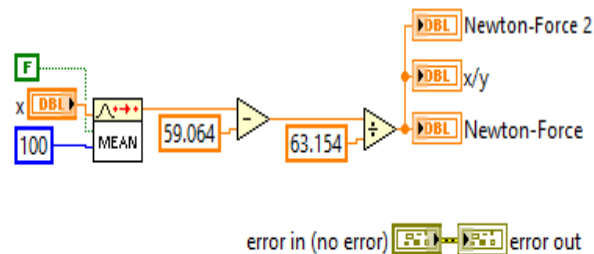
Figure 4.26: Program inside force diagram

Experimental results are obtained at different rotating speed in RPM as listed out in Table 4.4, Different levels of rotation speed are used to drive the DC motor based on the voltage required which responds in a linear relationship to the rotational speed. The minimum speed able for the motor to start is approximate 40 revolutions per minute. This is the initial and the lowest speed tested for this research. The corresponding relationship is shown in Figure 4.27. The relationship is polynomial curve fit with obtained in equation 4.3 with lowest linear least regression of 0.9933.

$$\text{RPM} = -71.278(\text{Voltage})^2 + 1003.6(\text{Voltage}) - 9.136 \qquad \textbf{4.3}$$
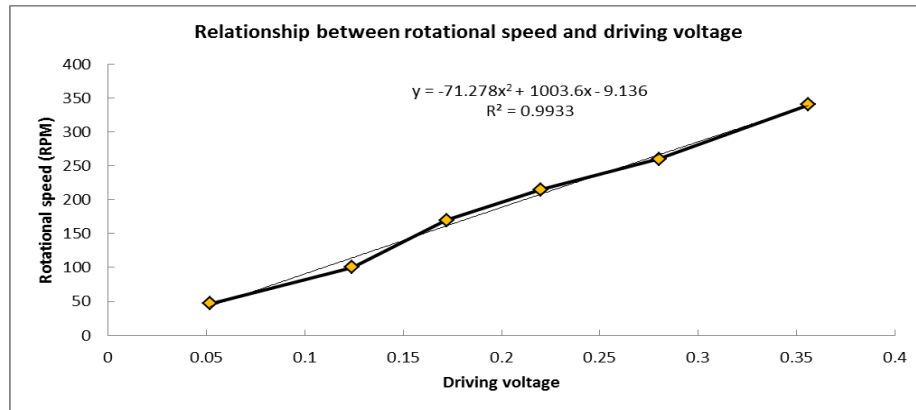
Figure 4.27: Motor driving voltage to rotational speed relationship

The experiment conducted initially covered 3 level of speed comprised from low, medium and high. It is then focus between two level of speed in order to zooming the investigation at that particular range. It is noted that the actual rotational speed and the Table 4.4 may be varied due to limitation of hardware and experimental complications.

Table 4.4: Range of rotational speed for investigation in drill string vibration

No	Voltage	Unit (RPM)	Speed (rad/sec)
1	0.052	47	4.922
2	0.124	100	10.472
3	0.172	170	17.802
4	0.280	215	22.620
5	0.356	260	27.227
6	0.600	340	35.605

4.8   Experimental Test Rig Model Approach

In order to simulate the drilling rig model, the experiment test rig model was build and on this case was aimed at reproducing the torsional vibrations which exist during the drilling process and dampening the vibrations by varying the upper disk rotational speed. Other vibrational modes were not consider due to implement the control system, although the test rig some limitations in the design resulted in unrealistic conditions for the presence of other vibration modes as example borehole for the drill string itself which is will creating whirl phenomena. Therefore the experiment model

was present; this is according to certain conditions to designing the control system which is in real drilling would result to other damaging modes. The experiment setup is illustrated in section 4.1 and Figure 4.1: Laboratory experiment test setup. The setup consisted of electrical input to change to mechanical output. The drive motor of the experiment rig was represented by brushless DC motor and fixed at the upper part of the model system and connected directly to the string (flexible shaft coupling) and gear box is not included. As discussed in literature review in section 2.12.1 torsional vibrations or stick slip phenomena were include upper and at the lower extremities rotating at varies speeds; this will produce shear stresses within the string. The equations below equation 4.4 elaborate how to determine the minimum torque, because motor provide such a different speed so that the motor must capable to produce such a sufficient torque.

$$J = \frac{\pi}{2}r^4$$
<div align="right">**4.4**</div>

$$T_{Min} = \frac{\emptyset GJ}{L}$$
<div align="right">**4.5**</div>

Where T_{min} is the minimum torque (N.m) and theta is a minimum angle, which can find by the encoder, meanwhile G is the shear modulus of the string, J is the second moment of the area of the string r in meter represent string radius, L also in meter as the length of the string.

The minimum torque requirement was based on the resolution of the absolute encoder used to measure the rotational position of the string. Two absolute 11-bit rotary encoders count the rotational position, the 11-bit equivalent to a 2048 pulse resolution and therefore a minimum angle gives a 0.018 radians. This is resulted in a 0.01 Nm is a minimum motor torque requirement for 6mm diameter string. All the data recorded using micro control unit or ChipKit Uno required 80 Mhz operating speed. The maximum operating speed limited to the string torsion detection, the MCU had to be able to detect for each pulse and also calculate the position following positions were reached. At 20.9 rad/s (200 rpm) and resolution of 0.018 radians, means 1161.1 Hz is minimum value required to read each position. ChickKit multi-platform IDE was used, the development platform allowed the acquisition and processing of the digital

signals received by the encoders. Some tests were performed in order to determine the time taken to obtain the data from each encoder and were calculate the position. 0.1 Mhz acquisition yielded and speed calculation is more sufficient for encoder resolution. Once calculated, the data was transfer through serial port thus amount rate of transfer (baud rate) was adjusted to minimise the delay between the actual measurements that was provided as feedback to the controller.
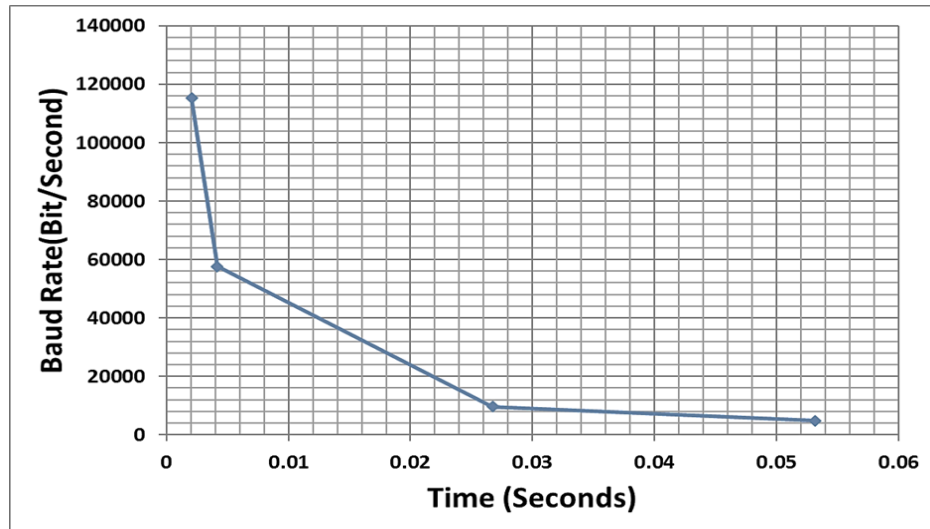
Figure 4.28: Data transfer rates

The maximum baud rate of the MCU is about 115200, at this rate an average time delay is about 0.00186 was calculated and show in Figure 4.28. Therefore a baud rate suggest for this system is about 57600 for corresponding delay.

4.8.1 Control Design-tracking problem

The proposed control design was based on the preliminary result obtained from drilling field. The effectiveness of the proposed control approach is highlighted through simulation results. The parameters values of physical parameters used in the following are given through actual oil well drilling platform field data. The dynamic equations represent the model system applied to the experimental test rig Figure 4.28 in order to develop preliminary gains and access the system controllability for the hardware used.

4.8.2 Drilling System Analysis

The drilling system analysis was divided into two dimensions i.e. frequency and transfer functions. The details of each dimension are discussed in the following subsections.

4.8.2.1 Stability of Neutral System- frequency domain approach

This analysis framework, frequently refer to as Laplace domain approach, is powerful tool to investigate the stability of the solution, frequency domain approach will show the relationship between the input voltage and rotational position of the lower part of BHA, this is used approximate the non-linear system before proceed to optimisation on the experimental test rig.

4.8.2.2 Transfer Functions

Laplace Transformation:

$$J_1\theta_1 S^2(s) + k\theta_1(s) - k\theta_2(s) + c_1\theta_1 S(s) = k_t i(s) \tag{4.6}$$

$$J_2\theta_2 S^2(s) + k\theta_2(s) - k\theta_1(s) + c_2\theta_2 S(s) + T_f(\dot{\theta}_2) = 0 \tag{4.7}$$

$$v_a(s) = Ri(s) + LiS(s) + k_e\dot{\theta}_1(s) \tag{4.8}$$

To simplified derivation the following notations were used;

$$E_2 = (J_2 S^2 + k + c_2 S) \tag{4.9}$$

$$E_1 = (J_1 S^2 + k + c_1 S) \tag{4.10}$$

$$E_1\theta_1(s) - k\theta_2(s) - k_t i(s) = 0$$

$$E_2\theta_2(s) - k\theta_1(s) = 0$$

<div align="right">**4.11**</div>

Rearranging equation **4.8** for current, gives;

$$i(s) = \frac{1}{R + LS}v_a(s) - \frac{k_e S}{R + LS}\dot{\theta}_1(s)$$

<div align="right">**4.12**</div>

Substituting into equation 4.6 and then equating equation 4.6 and equation 4.7 gives;

$$E_1\theta_1(s) - k\theta_2(s) - \frac{k_t}{R + LS}v_a(s) + \frac{k_t k_e S}{R + LS}\dot{\theta}_1(s)$$
$$= E_2\theta_2(s) - k\theta_1(s)$$

<div align="right">**4.13**</div>

Eliminating θ_1

$$\theta_1(s) = \frac{E_2\theta_2(s)}{k}$$

<div align="right">**4.14**</div>

$$\frac{E_2 E_1}{k}\theta_2(s) - k\theta_2(s) - \frac{k_t}{R + LS}v_a(s) + \frac{k_t k_e S E_2}{(R + LS)k}\theta_2(s)$$
$$= E_2\theta_2(s) - k\frac{E_2\theta_2(s)}{k}$$

<div align="right">**4.15**</div>

$$\left(\frac{E_2 E_1}{k} - k + \frac{k_t k_e S E_2}{(R + LS)k}\right)\theta_2(s) = \frac{k_t}{R + LS}v_a(s)$$

<div align="right">**4.16**</div>

$$\frac{\theta_2(s)}{v_a(s)} = \frac{\dfrac{k_t}{R + S}}{\left(\dfrac{E_2 E_1}{k} - k + \dfrac{k_t k_e S E_2}{(2R + LS)k}\right)}$$

<div align="right">**4.17**</div>

The following transfer function established the formal stability of the drilling model represents the entire system:

$$\frac{\theta_2(s)}{v_a(s)} = \frac{kk_t}{(E_2E_1(R+LS) - k^2(R+LS) + k_tk_eSE_2)}$$ **4.18**

4.9 Parameter Experimental Test Rig Estimation

Designing the controller and simulating the system response will required a number of parameter before substitute into experimental test rig. The parameter of some specific components was provided by the suppliers such as, string stiffness, viscous damping coefficient and motor constants were valued by experimental data. Table 4.5 below describes the values used in the simulation.

Table 4.5: **Experimental data parameters**

Symbol	Description	Values	Unit
J_1	Moment of inertia	0.004615	Kg m^2/rad
J_2	Moment of inertia	0.00192148	Kg m^2/rad
C_1	Viscous Damping ($\theta<70$)	0.000543	Ns/m
C_1	Viscous Damping ($\theta>70$)	0.005427	Ns/m
C_2	Viscous Damping ($\theta<70$)	0.000149	Ns/m
C_2	Viscous Damping ($\theta>70$)	0.001547	Ns/m
K	Drill string stiffness	26.32	Nm/rad
k_e	Electromotive Force Constant	0.367	V/rad/sec
k_t	Motor Torque Constant	0.367	Nm/Amp

4.10 Upper Drilling Dynamic for Motor Constant

Main characteristics which define the electrical motor were required. K_v was stated by supplier which is constant as rpm per volt, which as can stated in volt seconds per radian known as electromotive constant equation 4.19. The motor torque constant describes the torque per unit armature current and this is also equally to the electromotive Force constant equation 4.20. These are important to required motor speed and output torque to electrical power supply.

$$\left(\frac{1}{k_v \times \frac{2\pi}{60}}\right) = k_e \qquad \textbf{4.19}$$

$$k_t = k_e \qquad \textbf{4.20}$$

4.11 Viscous Damping for C

The viscous friction damping of the system can be recognised to the fluid lubrication in the bearings at the motor and the lower part of the BHA, the damping effect of the upper and lower masses/disk is not negligible. C_1 is represent of the damping of the motor and upper mass meanwhile C_2 described for damping of the lower bearing and mass. This viscous friction damping results in energy losses in the system. In this experiments were carried out for two variables constant which is the input voltage and rotational speed. There are three experimental setups in this research that were investigated:

- Motor, string and lower bearing

- Motor, string, upper disk and lower bearing

- Motor, string, upper disk, lower disk and bearing

Equation 4.21 was applied to determine the results, by using equation of motion for each instance and Kirchhoff's voltage law each value is estimated and three velocities are ran for each case 30 rpm (3.142 rad/sec) , 70 rpm (7.330 rad/sec), and 340 rpm (35.605 rad/sec).

The motor's electrical equation is then;

$$v_a = Ri + L\frac{di}{dt} + v_b \qquad \textbf{4.21}$$

The electromotive force V_b equation 4.22 is defined by the product of e.m.f constant and angular velocity will be applied in equation 4.24. In the same way for motor

torque is related to the current supply and the relationship is shown in as a product of the torque constant and current.

$$v_b = k_e \dot{\theta}_m \tag{4.22}$$

$$T_m = k_t i \tag{4.23}$$

Rearranging for i

$$i = \frac{v_a - k_e \dot{\theta}_m - 2L}{2R} \tag{4.24}$$

Angular velocities between the motor, rotational masses and bearing are assume equal and also rotational difference between upper and lower parts is too small for instrumentation to detect; therefore the following assumption is used in equation 4.25

$$\dot{\theta}_1 \approx \dot{\theta}_2 \tag{4.25}$$

$$c_n = \frac{k_t \left(\frac{v_a - k_e \dot{\theta} - 2L}{2R} \right)}{\dot{\theta}} \tag{4.26}$$

The two second order differential equations described the system for each case can be rearranged to estimate each viscous damping coefficient equation 4.26. The results gather is suggested viscous damping at lower speeds was estimated, thus more torque were be able to initiate rotation.

Figure 4.29 shows the result where the initial friction was higher due to the initial static friction, stribeck friction model described by (Saldivar et al. 2015) indicate full fluid lubrication occurs where the surface are completely separated by a fluid film. In order to simplify the model but still account for the initial higher torque required two damping coefficient were used C_1 and C_2 speed below 70 rpm (7.330 rad/sec), and above 70 rpm (7.330 rad/sec), . It was showed that the varying damping had minimal effects on the system response.
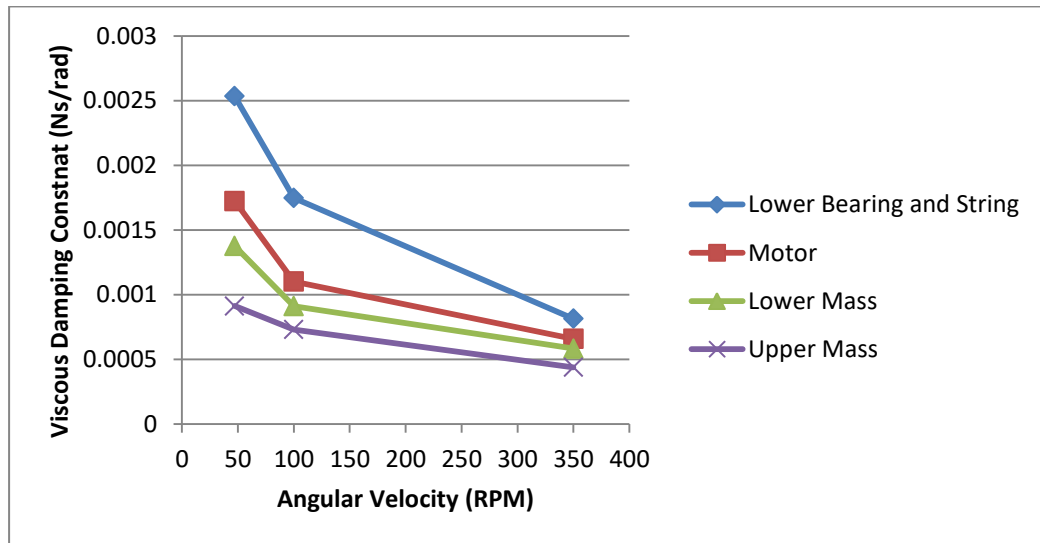
Figure 4.29: Viscous Damping Constant

4.12 Experimental Result for angular velocity variation at the bit and string torsion

In this section will discuss the experimental test rig results. The test experiment was carried out with three angular velocities as previously mentioned. Those results presented the effect of the increased friction force applied at the lower part of the BHA provided by the torsional rectification controller feedback. The angular velocity variation at the bit and string torsion were obtain and the result showed for controlled and without control action strategy (uncontrolled). The Figure 4.30 describe the angular velocity at the lower part of the string, at 5.236 rad/s (50 rpm) the uncontrolled test remain with continuous constant velocity and at 10 seconds force 1Nm was introduced by the brake mechanism and so that increase in the friction affected the lower mass to slow quickly. The torque supplied by the motor was not sufficient to sustain the rotation. When the rotation totally stopped the motor could not overcome the higher static friction that requires initiating rotation so that the system model completely standstill. Meanwhile effective controlled action also started with constant velocity, some variation were detected which is small decreases in speed, the measurement and feedback of certain variables at the bit level are required. When the load was applied at 10 seconds one more time the velocity dropped however the velocity increase at 2.1 rad/s (20.054 rpm) and the controller adjusted the pulse width while motor power maintain the set velocity. The controller is not sufficient to

maintain a constant velocity. The frictional resistance between point contact of the rubber and the disk was higher at lower velocities. Therefore effective control motor will purpose, as the velocity increased and decreased oscillation at the set point.
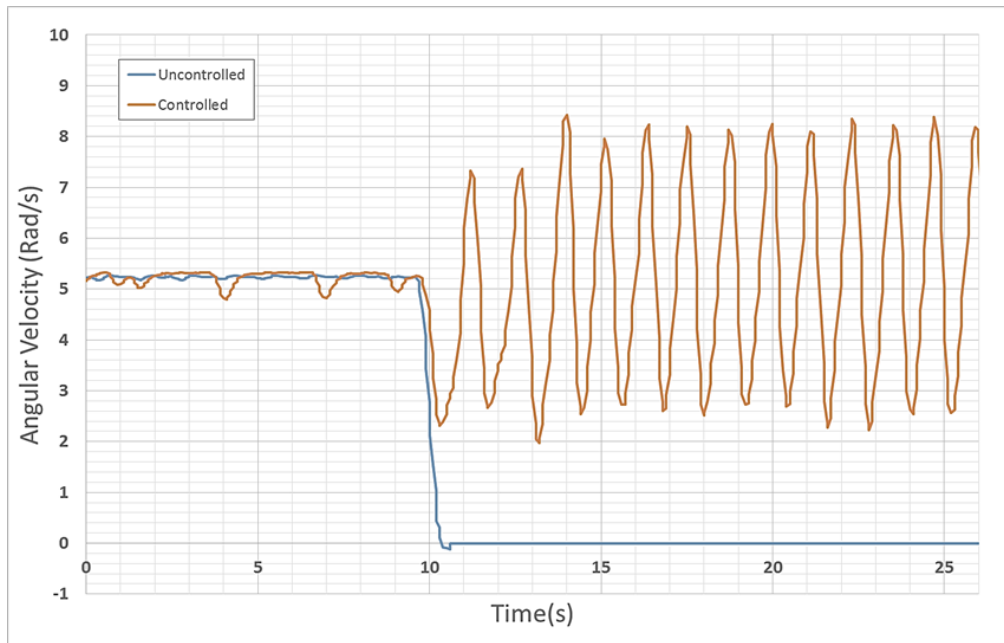
Figure 4.30: Angular velocity verses time at 5.236 rad/s (50 rpm) and 1N load disturbance
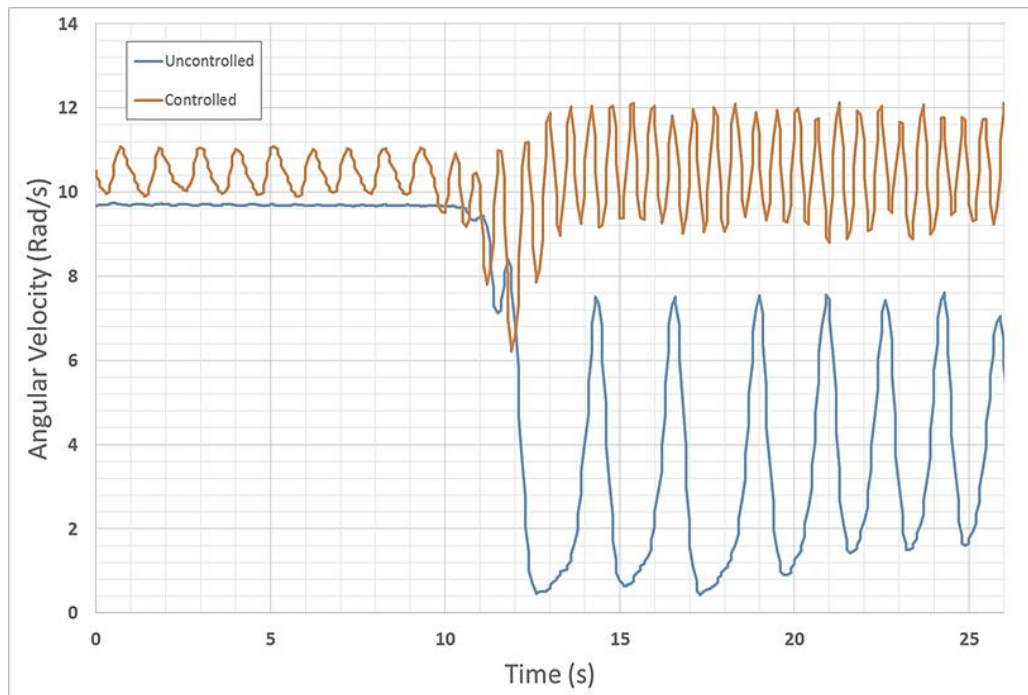
Figure 4.31: Angular velocity verses time at 10.472 rad/s (100 rpm) and 1N Load disturbance
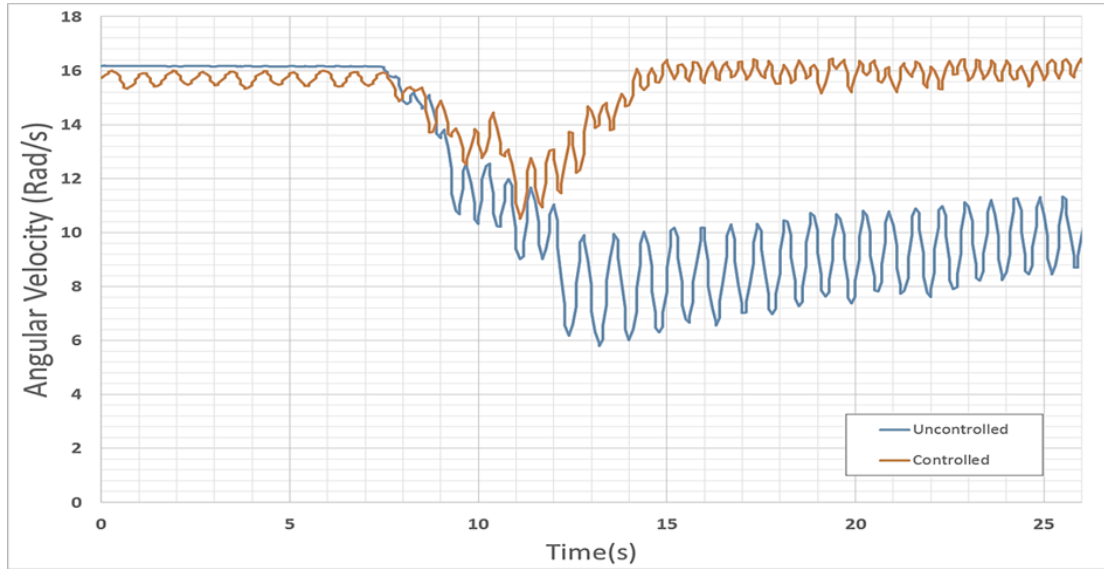
Figure 4.32: Angular velocity verses time at 15.708 rad/s (150 rpm) and 1N load disturbance

The Figure 4.31 shows the control performance for 10.472 rad/s (100 rpm). respectively regulate the angular velocity at the bottom end, after brake applied, the uncontrolled action decrease at rotational speed and the velocity oscillate below the set point 0.212 Hz with an amplitude of 6.58 rad/s (62.834 rpm). meanwhile when controlled action was active the velocity were maintained at the set velocity only slightly deviation after load was applied but it is not completely eliminated the oscillation were reduced yielding a 40 and 58 percentage change for frequency and amplitude respectively. Figure 4.32 Its similar observe at velocity 15.708 rad/s (150 rpm) yielding a 41 and 71 percentage also change for frequency and amplitude, however the controller response was slower and the velocity did not back to the desired point until 15 seconds. The torsional vibration significantly reduced at higher speeds and the proposed controlled strategy was established was increased with only a 7.8% variation between amplitudes before and after the load is applied. At the same time the string torsion increases with velocity, the motor velocity increases and decrease to compete with the frictional resistance.
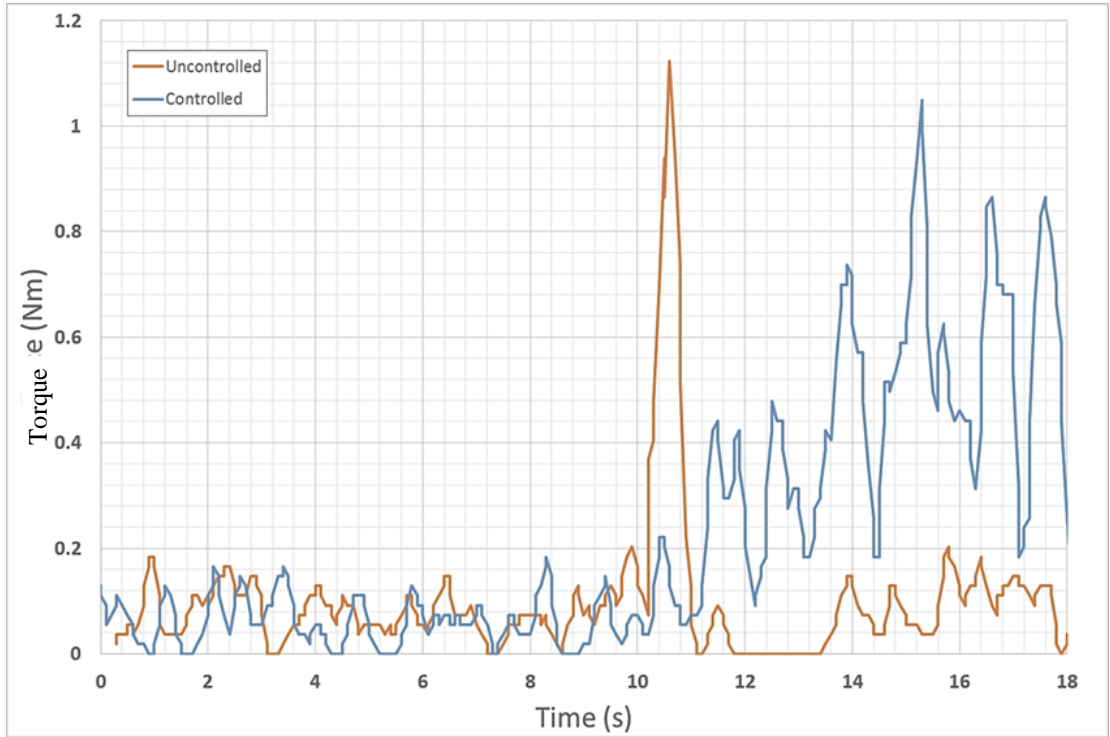
Figure 4.33: String Torsion verses time at 5.236 rad/s (50 rpm) and 1N load disturbance
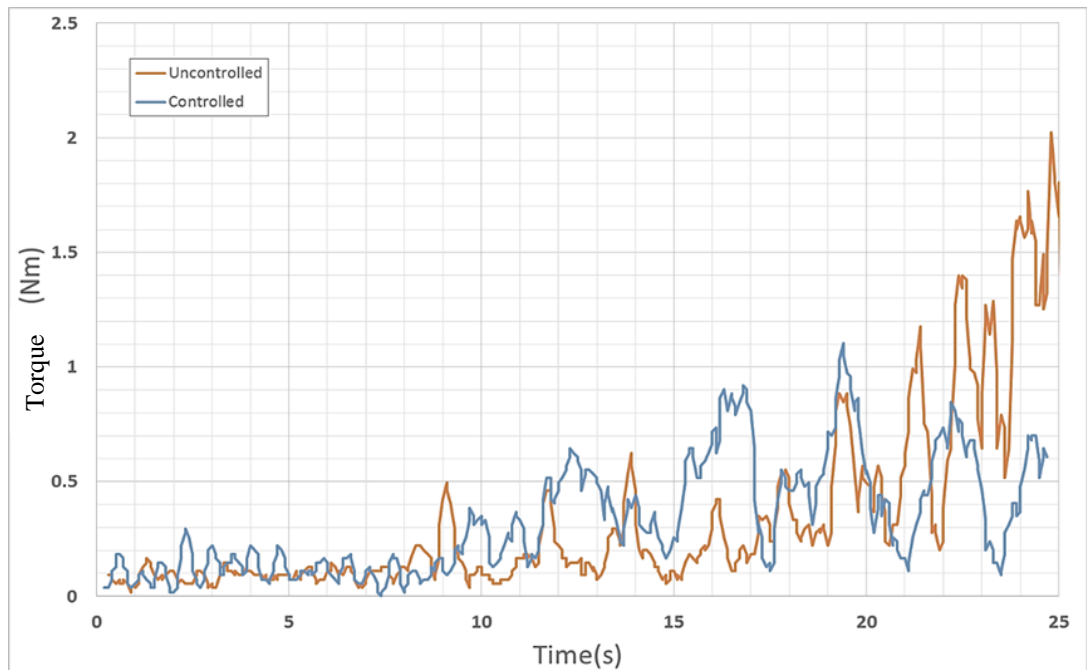
Figure 4.34: String torsion verses time at 10.472 rad/s (100 rpm) and 1N load disturbance
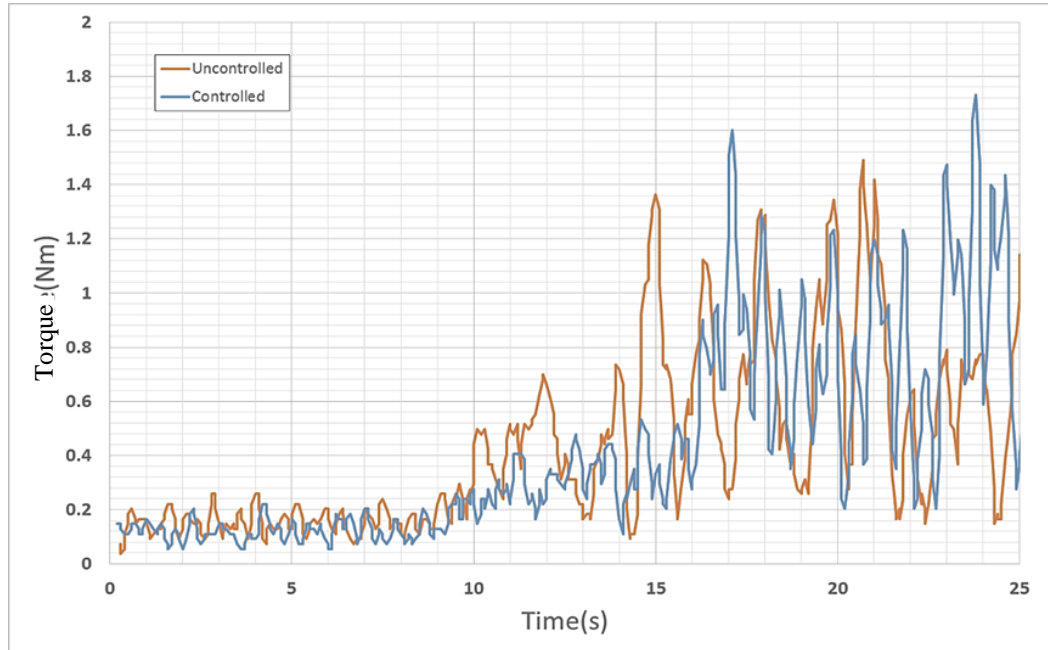
Figure 4.35: String torsion verses time at 15.708 rad/s (150 rpm) and 1N load disturbance

The result at Figure 4.33, Figure 4.34 and Figure 4.35 describes the torsional force and the difference in rotational speed between upper part (motor) and lower mass. Based on a five point moving average, signal noise reduce were calculate. At constant velocity small variation and low fluctuate were observed, when force was applied a force reaches large spike occurred and torsional energy stored in the drill string is released that causing very large torsional vibrations. When rotational speed had stopped, the motor power was disconnected, in order to prevent failure on the motor. However if the motor had sufficient power and the static friction was to overcome this energy stored in the string, it would have resulted a sudden higher speed at downhole lower part.

4.13 Natural Frequency on the Drill String Experiment

Discussing Figure 4.36 to Figure 4.41, the investigation of resonance are shown and appear during the operation with and without any braking system apply, which represent the bit rock interaction at the bottom disk. By investigating the result plots, it was observed that the speed level have individual resonance. Table 4.6 shows all the individual resonance frequencies for each of operation speed.
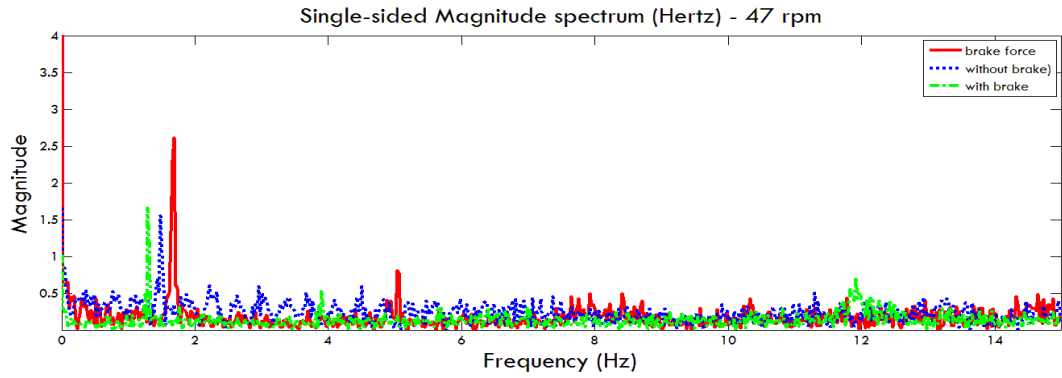
Figure 4.36: Single sided magnitude spectrum for 47 rpm (4.922 rad/sec) with and without applying brake
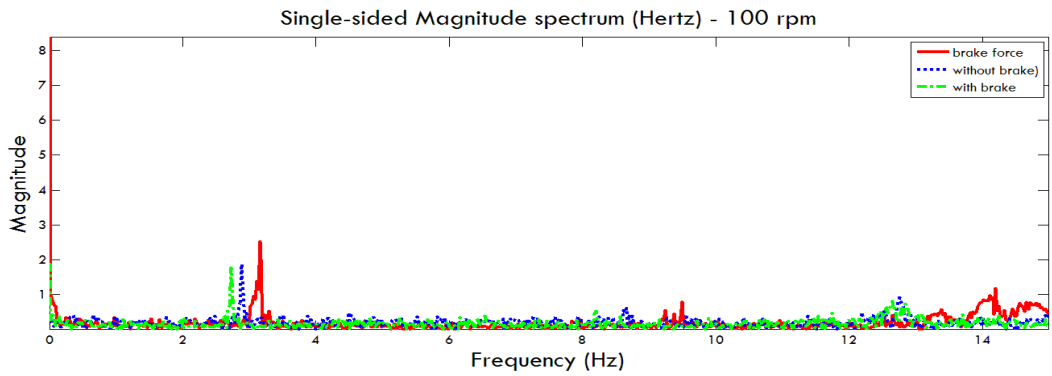
Figure 4.37: Single sided magnitude spectrum for 100 rpm (10.472 rad/sec) with and without applying brake
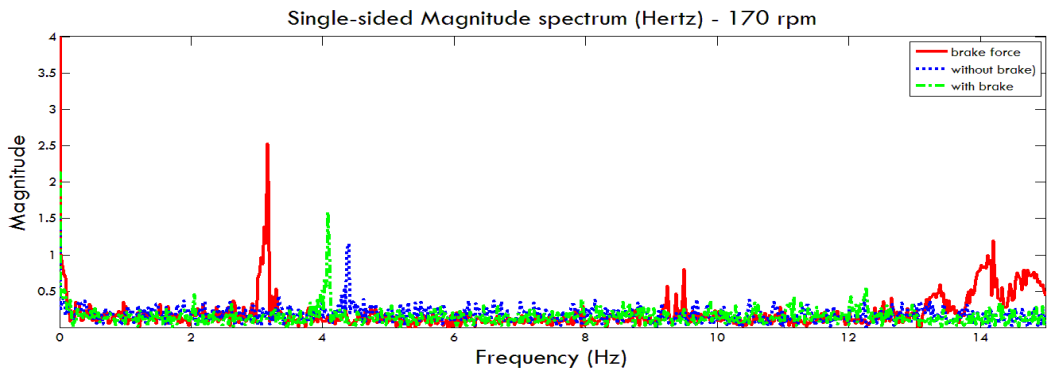
Figure 4.38: Single sided magnitude spectrum for 170 rpm (17.802 rad/sec) with and without applying brake
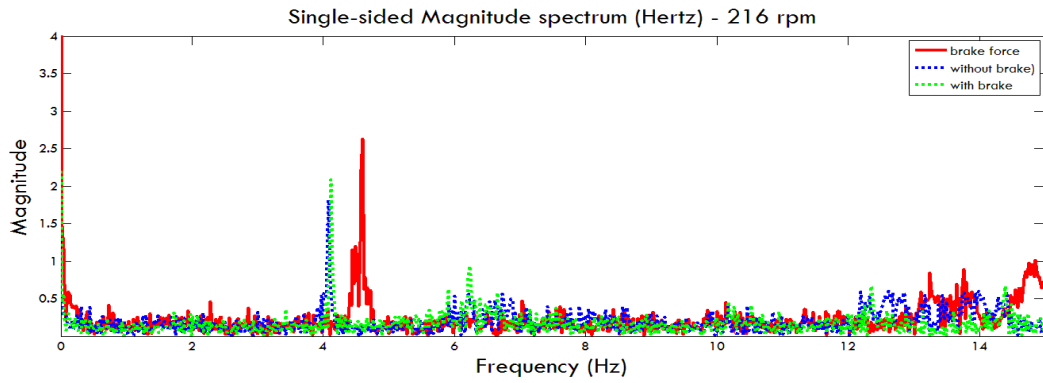
Figure 4.39: Single sided magnitude spectrum for 216 rpm (22.620 rad/sec) with and without applying brake
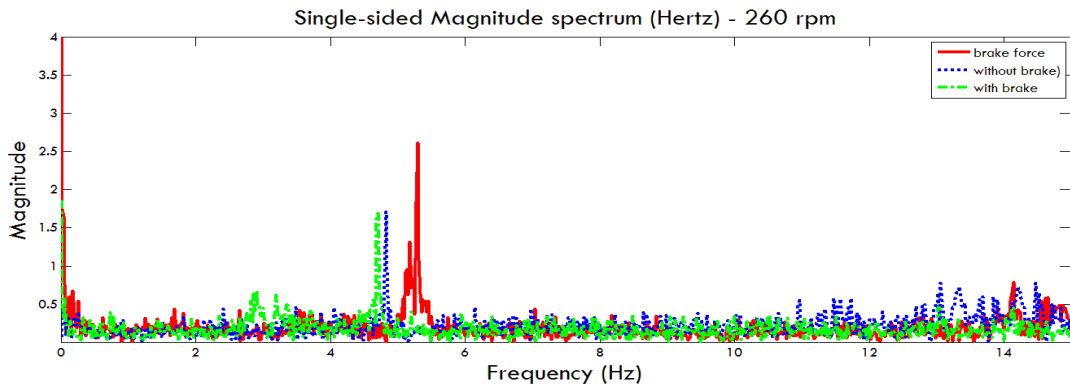
Figure 4.40: Single sided magnitude spectrum for 260 rpm (27.227 rad/sec) with and without applying brake
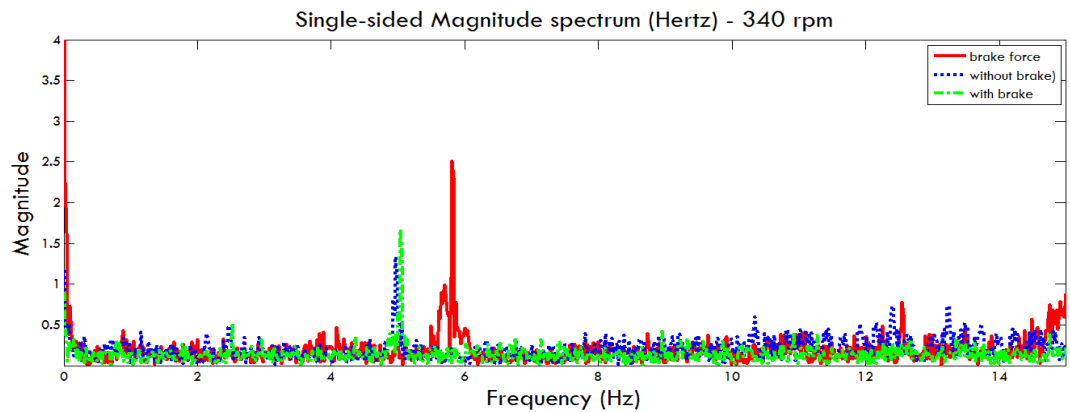
Figure 4.41: Single sided magnitude spectrum for 340 rpm (35.605 rad/sec) with and without applying brake

4.13.1 Speed without Brake

Figure 4.36 to Figure 4.41 shows the resonance without brake with dotted blue line, it is also show that, operations analysing the plots for each individual speed.

4.13.2 Speed with Hard Brake System

Referring to Figure 4.36 to Figure 4.41, dashed green line shows, an external friction is applied to the experiment, which is to signify the behaviour of the rotary drill string and the ground formation. The external friction is induced by a sudden hard brake by clamped at the bottom disk, or in real drilling we called hard bit rock interaction in this experiment.

4.13.3 Speed with Force Brake System

According also from Figure 4.36 to Figure 4.41, with the straight red line shows, an external friction has also been applied but this external friction is induced by linear actuator brake system and force also applied onto brake disk.

Table 4.6: Natural frequency of the system - without brake, sudden brake and force brake

Speed (rad/sec)	Speed (RPM)	Natural Frequency of the drill string Experiment			
		Natural Frequency (Hz)	Without brake Frequency (Hz)	With brake Frequency (Hz)	With force brake Frequency (Hz)
4.922	47	0.783	1.32	1.37	1.72
10.472	100	1.667	2.74	3.88	3.97
17.802	170	2.883	3.88	3.96	4.21
22.620	216	3.600	4.60	4.62	4.38
27.227	260	4.333	5.20	5.25	5.46
35.605	340	5.667	5.81	5.81	5.96

4.14 Finding the Existence of Natural Frequency for Experimental Result

Overall study, has been focusing on analysing the natural frequency of the system at each individual rotational speed and shown here external vibration is appear on the operation with their own phenomena. It was observed on each rotational speed there is large peak in magnitude of frequency which can be found at Table 4.3 for each operational speed. Here, the FFT of the drill bit angular velocity was analysed and plot

using MATLAB®. The part of the MATLAB® program used to find the natural frequency can be found in the appendix. The frequency response plot based on FFT with each configuration verified that the vibration presented by the drilling operation were made worse in the presence of the brake system, and noticed the resonant frequencies of the system did change with operational speed. By comparing the result based on FFT plot analysis Figure 4.36 shows here that the magnitude of the resonance peak excited and the peak occurs at a lower frequency which stated at Table 4.6, meanwhile Figure 4.37, Figure 4.38, Figure 4.39, Figure 4.40, and Figure 4.41 the resonant comes very excited and more significant especially when applying linear actuator brake on the rotational operations. Drill string with 3 configurations (without, hard brake, linear/ force brake) applied, resonant region zone is where vibration is a high/ amplified and automatically comes to the deformation and fatigue problem will happen at the drill string. and from the result shows at speed 100 rpm (10.472 rad/sec) to 260 rpm (27.227 rad/sec) with brake apply, the resonance frequencies are diverged further of the natural critical frequency of the system operation, hence as we noticed at highest and lowest speed 47 rpm (4.922 rad/sec) and 340 rpm (35.605 rad/sec) , the resonant of this rotational speed is near or closed to the value of critical natural frequency, therefore chances of the excitation vibration may vigorously arise at this range of speed.

Thus experimentally, the lateral and torsional vibrations demonstrated by the system were prominently more extreme under the friction effect. In the other hand, the natural frequencies are depending on the model for the drilling prototype setup into laboratory. In this experiment, the model is using two degrees of freedom. By using the data in the frequency response plots, the critical speeds for the several excitation mode and calculated using equation 3.22, that was developed by (Dareing 1984). So if the system was operated at rotational speeds close to critical resonant frequencies that obtained shown at Table 4.6, its means that higher vibration is exist. Hence experimental test conducted can conclude the existing of resonant vibrations was reflected in angular velocities critical speeds of this test and subsequent high vibrations were notice at speed 216 rpm (22.620 rad/sec).

Chapter 5

Conclusion

5.1 Overview

Many studies have been conducted to understand the drill string behaviour. Nevertheless, the optimum control strategies that can be implemented to reduce stick slip event remain scarce. Therefore, this research was conducted to find and propose an optimum control strategy. The major significance of this research laid in the methodological approach i.e. the application of classical numerical equation in the advanced computer software. The following sub-sections summarise the overall strategies – highlighting the novel technique to reduce the stick slip, its challenges, limitations and avenue for future research. This chapter was concluded by outlining the attempts made by the researcher to communicate the research.
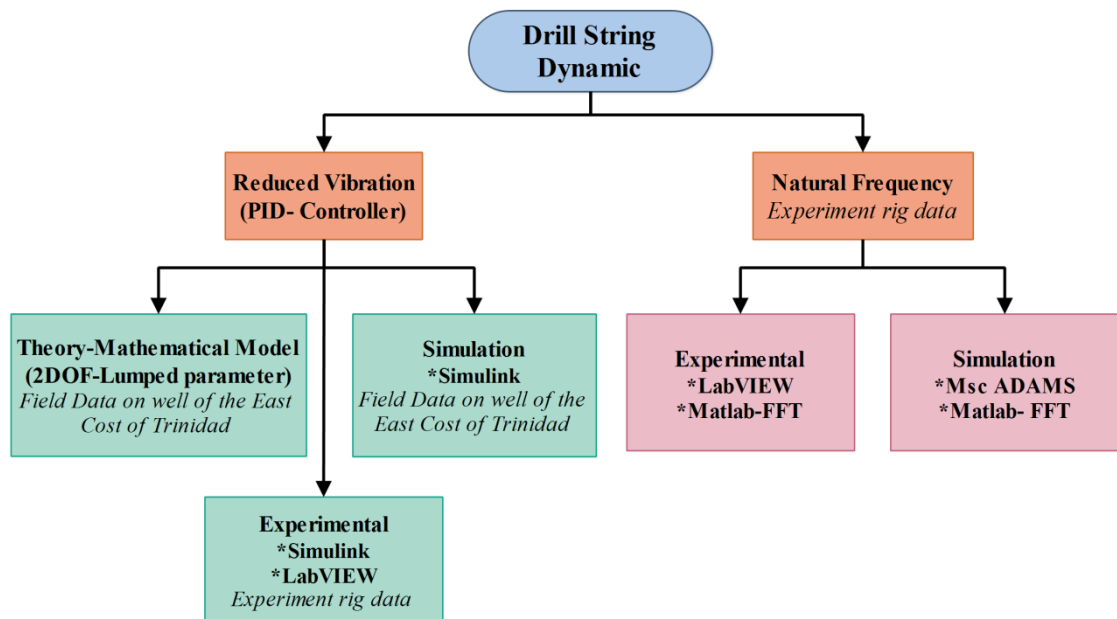
Figure 5.1: Research summary chart

5.2   Research Summary

Performance of drilling operation is a very critical issue in the oil and gas drilling industry. However, most frequently it was threatened by the drilling vibration (e.g. bit wear, mass imbalance, friction, pipes disconnections, and borehole disruption) – an issue that can be tackled by utilising controlling software that enables automation of the drilling process. Research on the dynamic behaviour of the drilling equipment i.e. drills string and control technology, focusing on the control approaches that can reduce the torsional vibration; it is an avenue that can facilitate the development of such solution. This factor has been disregard in the existing simple mathematical model to calculate the optimum strategy of controlling the vibration behaviour. Against such backdrop, this research proposes the optimum control strategy by applying system theory.

To obtain the findings, Figure 5.1, series of approaches involving mathematical model, followed by experiment and simulation were applied. In both - the experiment and simulation, external friction is applied to lower extremity of drill string by inducing the load disturbance. This was done to analyze the stick slip and lateral vibrations. After getting the analysis results, LabVIEW NI and microcontroller were used to investigate vibration amplitude and occurrence of resonance, based on real-time monitoring. PID control was introduced in the LabVIEW to mitigate the responds, yielding to the proposed optimum control strategy as the results. Increased velocity produced less vibration magnitude, where the velocity feedback was able to monitor the velocity of the bit – resulted in a considerably faster response, besides minimizing vibration oscillations.

Decades of laboratory experiments were unable to produce precise results to control the drill string vibrations. It was discovered that to produce the desired results, the BHA laboratory condition (stabilizer, cylinder tube pipe) has to be replicated, and other component part of the drill string should be accounted for. As the environment closely resembles the actual conditions, more precise results will be obtained. Consideration of all possible factors should be done in the future.

Meanwhile, the simulation approach facilitates understandings on vibration behavior i.e. vibration and natural frequency that can be used to estimate the critical rotational

speed. MSc. Adams enables the mechanical system simulation, by utilizing the force obtained from the motion simulation. Unlike experiment, the simulation model enables the simulation of lateral and torsional vibration. The lateral vibration emerges due to the application of WOB on the breaking system (load disturbance) i.e. bit rock interaction. In this analysis the model created not related to borehole because it assume the condition of the borehole is already bigger than the diameter of the drill pipe. Therefore, critical rotation speed is needed to avoid drill string bending (i.e. failure). Meanwhile, the torsional vibration emerges due to the application of friction on the breaking system. Simulation dynamic analysis is a reliable platform to conduct analysis and simulate the model designed.

To summarize, the optimum control strategy proposed in this research offers practical insights and novel contributions in both practical and academia fields. The three significant features highlighted are:

1. The torsional vibration was discovered through a non-linear friction model that was applied in simulation and test rig. In the absence of active control, the vibration continued to oscillate without any presence of damp. This proves the usefulness of the control application in the PID control system.

2. The gain scheduling in the active control of the PID control system allows varying control both load and non-load conditions, inducing a smooth start-up and faster response to variations in bit velocity. This event reduces the stick slip phenomena, as bit velocity is maintained within 2% of the preferred value.

3. At the maximum threshold, the WOB regulates the torque, which potentially causes oscillations at the motor and bit. The tuning of PID will help to offset this problem, resulting into smoother response.

5.3   Challenges

As mentioned in chapter 1 and the previous sections, the drill string failure is the biggest challenge that motivates this research. Studies proved that such failure has reduced the industry's profit, due to high maintenance cost and suspended operations. It is posited that those risks can be minimized by exercising the optimum control strategy as proposed by this research.

This research has evidently proved that the application of classical regulators law to tackle the research problem can bring some improvements on the real drilling operations, lowering the risk of the drill string failure and subsequently optimizing the operational costs. Such regulators have been applied in the numerical simulation of the torsional drilling model through the 'torsional lumped parameter equations'. Although this is a common method, the introduction of the PID gain tuning in this approach has provides a different and practical way to eliminate the stick slip events. It is hope that this perspective will be widely adopted in the future, as it has been validated against the actual environment, where the simulation results closely resemble the field observation.

Control strategy has been derived in order to eliminate stick-slip vibrations. The main advantages of control performance with a fast response time with velocity feedback were able shown by the performed simulations, which come out with satisfactory results.

Chapter 6

Future Work

6.1   Overview

This research has encountered a few limitations, which can provide avenue for future research. Such limitations are as follow:

1. In the subsection 4.4, it was explained that PID was as used as a control algorithm in the LabVIEW to mitigate the respond function. In future, it is suggested for the PID to be combined with Fuzzy Logic control functions in presence toolkit, to enhance the program development in obtaining the optimal gains.

2. It is vital for the future analysis to consider other vibration-causing factors, such as effects of vibration coupling, parameter non-linearity, and fluid flow of drilling string to measure the vibration effect. To be more precise, the drill bit contact with the borehole should also be observed.

3. The test rig that was used in this research was composed of encoders and a microcontroller. The performance of these tools can further be enhanced through upgrading it with more advance physical hardware that will improve the data recording process. Among the potentials tools are high speed camera such as CCD or CMOS, and sensor, which enable the capture of image that can provide more accurate data. Besides this, it is also proposed for the future research to consider different parts in the rig experiment to gauge other outcome possibilities, such as AC motor or Induction Motor. Currently, the vibration was produced by the DC motor torque (i.e. measured against time response vs. torque), which restrain the data acquisition rate generated by the computer.

It was believed that by overcoming these constraints, the accuracy of the results will be improved. Subsequently, it will provide better understanding on the research problem. Considering that the proposed enhancements will entail additional costs, the implementation of them are highly depends on the allocated research budget.

6.2   Communicating the Research

The paradigm of the design science has its roots in engineering (Simon 1996). Fundamentally, design science is a problem solving process that results into innovations of ideas, practices, technical capabilities, or products. The process outlines seven principles, i.e. design as an artifact; problem relevance; design evaluation; research contributions; research rigor; design as a search process; and communication of research (Hevner Von Alan et al., 2004). Communicating research is important to ensure that it can be applied in both practical filed, as well as knowledge domain. In terms of practicality, a known research potentially support the management decision–making process, and increase the implementation possibility. Hence to enable such applications, this research has been constantly communicated to the technical and managerial audience as well as other researchers in several events as follow:

1. International Conference on Mechanical and Aerospace-ICMAE, London, U.K., 18-22 July 2016.

2. Research Poster Conference, Brunel University London, U.K., 25 June 2016.

3. Offshore Technology Conference Asia, Kuala Lumpur, Malaysia, 23-25 March 2016.

4. International Conference on Mechanical Engineering-IJAER, Bandung, Indonesia, 17-19 March 2015.

5. Drill String Failure Prevention Training, Aberdeen, U.K., 27-29 April 2015.

Besides providing platforms to communicate the research, such occasions enabled the researcher to build professional networks with other researchers, as well as practitioners and industry experts, which is essential and crucial component for a successful career as a researcher.

References

Aadnoy, B.S., 1986. Transversal Vibrations in Stabilized Drilling Assemblies. *Energy Sources*, 8(4), pp.305–329.

Aarrestad, T.V. & Kyllingstad, A., 1988. An experimental and theoretical study of a coupling mechanism between longitudinal and torsional drillstring vibrations at the bit. *SPE drilling engineering*, 3(1), pp.12–18.

Abdulgalil, F. & Siguerdidjane, H., 2005. Backstepping Design for Controlling Rotary Drilling System. In IEEE, ed. *control application, IEEE conference*. Toronto, Canada, pp. 120–124.

Adejo, A.O. et al., 2013. Oil and Gas process monitoring through wireless sensor networks: A survey. Ozean Journal of Applied Sciences. *Ozean Journal of Applied Science*, 6(2), pp.39–43.

Ahmadian, H., Nazari, S. & Jalali, H., 2007. Drill String Vibration Modelling Including Coupling Effects. *IUST International Journal of Engineering Science, Industrial & Mechanical Engineering Special Issue*, 18(3–4), pp.59–66.

Al-Hiddabi, S.A., Samanta, B. & Seibi, A., 2003. Non-linear control of torsional and bending vibrations of oilwell drillstrings. *Journal of Sound and Vibration*, 265(2), pp.401–415.

Von Alan, R.H. et al., 2004. Design research in information systems research. *MIS quarterly*, 28(1), pp.75–105.

Azar, J.J. & Samuel, G.R., 2007. *Drilling engineering*, PennWell.

Bailey, J. & Finnie, I., 1960. An Experimental Study of Drill-String Vibration. *Journal of Engineering for Industry*, 82(2), pp.129–135.

Bailey, J.R. et al., 2008. Drilling vibrations modeling and field validation. In *IADC/SPE Drilling Conference, Society of Petroleum Engineers*. Florida, USA: Society of Petroleum Engineers.

Balachandran, B., 2001. Nonlinear dynamics of milling processes. *Philosophical Transactions of the Royal Society of London A: Mathematical, Physical and Engineering Sciences*, 359(1781), pp.793–819.

Besaisow, A.A., Ng, F.W. & Close, D.A., 1990. Application of ADAMS (Advanced Drillstring Analysis and Measurement System) and Improved Drilling Performance. In *SPE/IADC Drilling conference Society of Petroleum Engineers*. Society of Petroleum Engineers.

Besselink, B., van de Wouw, N. & Nijmeijer, H., 2011. Model-based analysis and control of axial and torsional stick-slip oscillations in drilling systems. In *Proceedings of the IEEE International Conference on Control Applications*. pp. 495–500.

Bourgoyne, A.T. et al., 1986. *Applied Drilling Engineering*, Society of Petroleum Engineers.

Brett, J.F., 1992. The Genesis of Bit-Induced Torsional Drillstring Vibrations. *SPE Drilling Engineering, Society of Petroleum Engineers*, 7(3), pp.168–174.

Van Campen, D.H. & Keultjes, W.J.G., 2002. Stick-slip Whirl Interaction in Drillstring Dynamics. *Journal of Vibration and Acoustics*, 124(2), pp.209–220.

Canudas-de-Wit, C. et al., 2005. D-OSKIL: a New Mechanism for Suppressing Stick-Slip in Oil Well Drillstrings. In *Proceedings of the 44th IEEE Conference on Decision and Control, and the European Control Conference*. Seville, Spain: IEEE, pp. 8260–8265.

Canudas-de-Wit, C., Rubio, F.R. & Corchero, M.A., 2008. D-OSKIL: A new mechanism for controlling stick-slip oscillations in oil well drillstrings. *IEEE Transactions on Control Systems Technology*, 16(6), pp.1177–1191.

Challamel, N., 2000. Rock Destruction effect on the stability of a drilling structure. *Journal of Sound and Vibration*, 233(2), pp.235–254.

Che Kar, B.S. et al., 2017. Drill String Dynamic Improving the Drilling Performance by Optimizing the Speed Limit and Study the Resonance of the Experimental Drill String System. *Journal of Engineering and Applied Science*, 12(15).

Che Kar, B.S., Esat, I., Mohd Farid Woo, b M.E., et al., 2016. Improving the Drilling Performance by Optimizing the Speed Limit and Study the Resonance of the Experimental Drill String System. In *2nd International Conference on Mechanical and Control Engineering*. Bandung, Indonesia: Scopas.

Che Kar, B.S., Esat, I., Alkhamees, A.A.A., et al., 2016. Improving the Drilling Performance by Study the Resonance of the Experimental Drill String System Using 2 contact Points of Friction Force of Breaking system. In *7th International Conference on Mechanical and Aerospace Engineering*. London, England: IEEE, pp. 175–179.

Che kar Binti, S. & Esat, I., 2016. Drill String Dynamic. In *Brunel Research Student Conference*. London, United Kingdom.

Christoforou, A.P. & Yigit, A.S., 2003. Fully coupled vibrations of actively controlled drillstrings. *Journal of Sound and Vibration*, 267(5), pp.1029–1045.

Chunjie, H. & Tie, Y., 2009. The research on axial vibration of drill string with delphi. In *Computational Intelligence and Natural Computing, 2009. CINC'09. International Conference on. Vol. 1. IEEE*. IEEE, pp. 478–481.

Cobern, M.E. et al., 2007. Drilling Tests of an Active Vibration Damper. In *SPE/IADC Drilling Conference*. One Petro.

Cobern, M.E. & Wassell, M.E., 2005. Laboratory testing of an active drilling vibration monitoring & control system. In *AADE National Technical Conference & Exhibition, Houston*. Houston.

Dareing, D.W., 1984. Drill Collar Length is a Major Factor in Vibration Control. *Journal of Petroleum Technology*, 36(4).

Deily, F.H. et al., 1967. Downhole Measurements of Drill String Forces and Motions. *Journal of Engineering for Industry*, 89(11), p.78.

Draoui, E., 1996. Dynamic Behavior of a Drill-String: Experimental Investigation of Lateral Instabilities. *Journal of Vibration and Acoustics*, 118(3), pp.292–298.

Drumheller, D.S., 1992. An overview of acoustic telemetry. In *Geothermal energy program review*. Albuquerque, NM (United States).

Dubinsky, V.S.H., Henneuse, H.P. & Kirkman, M.A., 1992. Surface Monitoring of Downhole Vibrations: Russian, European, and American Approaches. *Society of Petroleum Engineers, European Petroleum Conference*, pp.16–18.

Dunayevsky, V.A., Abbassian, F. & Judzis, A., 1993a. Dynamic Stability of Drillstrings Under Fluctuating Weight on Bit. *SPE drilling & completion*, 8(2),

pp.84–92.

Dunayevsky, V.A., Abbassian, F. & Judzis, A., 1993b. Dynamic Stability of Drillstrings Under Fluctuating Weight on Bit. In *Society of Petroleum Engineers, SPE Drilling & Completion*. Society of Petroleum Engineers, pp. 84–92.

Al Dushaishi, M.F., 2012. *Investigation of drill string vibration reduction tools*. MISSOURI UNIVERSITY.

Dwars, S., 2015. Recent Advances in Soft Torque Rotary Systems. In *SPE/IADC Drilling Conference and Exhibition*. London: Society of Petroleum Engineers.

Fearnley, P.G., 2011. *Drill String Failure Prevention*, Scotland. Available at: http://www.fearnleyproctergroup.com.

Fubin, S. et al., 2010. Adaptive PID Control of Rotary Drilling System with Stick Slip Oscillation. In *2nd International Conference on Signal Processing Systems (ICSPS)*. IEEE.

Germay, C., Denoël, V. & Detournay, E., 2009. Multiple mode analysis of the self-excited vibrations of rotary drilling systems. *Journal of Sound and Vibration*, 325(1–2), pp.362–381. Available at: http://dx.doi.org/10.1016/j.jsv.2009.03.017.

Gonzalez-Garcia, S., Polyakov, A.E. & Poznyak, A.S., 2011. Using the method of invariant ellipsoids for linear robust output stabilization of spacecraft. *automation and remote control*, 72(3), pp.540–555.

Halin, A., 2017. *Model-based-design to develop sensorless fan*. University of Liège.

Halsey, G.W., Kyllingstad, A. & Kylling, A., 1988. Torque feedback used to cure slip-stick motion. In *SPE Annual Technical Conference and Exhibition*. Society of Petroleum Engineers.

Hanson, J.M. & Hansen, W.R., 1995. Dynamics Modeling of PDC Bits. In *Society of Petroleum Engineers, SPE/IADC Drilling Conference*. Society of Petroleum Engineers, pp. 589–604.

Hernandez-Suarez, R. et al., 2009. An Integral High-Order Sliding Mode Control Approach for Stick-Slip Suppression in Oil Drillstrings. *Petroleum Science and Technology*, 27(8), pp.788–800. Available at: http://dx.doi.org/10.1080/10916460802455483.

Horbeek, J.H. et al., 1995. Successful Reduction of North Sea Drillstring Failures. In *Society of Petroleum Engineers, Offshore Europe,*. Aberdeen, United Kingdom: Society of Petroleum Engineers.

Hutchings, I.M. & Shipway, P., Introduction to Tribology - Friction.

Isidori, A., 1989. *Nonlinear control theory*, International Federation of Automation Control.

J Bailey, J. & Finnie, I., 1960. An Analytical Study of Drill-String Vibration. *Journal of Engineering for Industry*, 82(2), pp.122–127.

Jansen, J.D., 1993. *Nonlinear dynamics of oilwell drillstrings*. TU Delft, Delft University of Technology.

Jansen, J.D. & Van den Steen, L., 1995. Active damping of self-excited torsional vibrations in oil well drill strings. *Journal of Sound and Vibration*, 179(4), pp.647–668.

Jeffryes, B.P. et al., 2001. Method and apparatus enhanced acoustic mud pulse telemetry.

K. Vandiver, J., W. Nicholson, J. & J. Shyu, R., 1990. Case studies of the bending vibration and whirling motion of drill collars. *SPE (Society of Petroleum Engineers) Drilling Engineering*, 5:4, pp.282–290.

Karnopp, D., 1985. Computer simulation of stick-slip friction in mechanical dynamic systems. *Journal of Dynamic Systems, Measurement, and Control*, 107(1), pp.100–103.

Khulief, Y.A. & Al-Sulaiman, F.A., 2009. Laboratory investigation of drillstring vibrations. In *Journal of Mechanical Engineering Science*. pp. 2249–2262.

Knüppel, T. et al., 2014. Flatness-based control for a non-linear spatially distributed model of a drilling system. In *Low-Complexity Controllers for Time-Delay Systems*. Springer International Publishing, pp. 205–216.

Lawrence, L. et al., 2009. Intelligent Wired Drill-Pipe System Provides Significant Improvements in Drilling Performance on Offshore Australia Development. In *Offshore Technology Conferenc*. Houston, Texas: Offshore Technology Conference.

Ledgerwood III, L.W. et al., 2013. Downhole measurement and monitoring lead to an enhanced understanding of drilling vibrations and polycrystalline diamond compact bit damage. *Society of Petroleum Engineers, SPE Drilling & Completion*, 28(3), pp.254–262. Available at: http://dx.doi.org/10.2118/134488-PA.

Leine, R.I. et al., 1998. Stick-slip vibrations induced by alternate friction models. *Nonlinear Dynamics*, 16(1), pp.41–54.

Li, B. & Zou, J., 2011. The design of oil drilling wireless data acquisition system. In *International Conference on Electrical and Control Engineering*. pp. 1810–1813.

Li, L., Zhang, Q. & Rasol, N., 2011. Time-Varying Sliding Mode Adaptive Control for Rotary Drilling System. *Journal of Computers*, 6(3), pp.564–570.

Liao, C.M., 2011. *Experimental and Numerical Studies of Drill-String Dynamics*.

Lin, Y.Q. & Wang, Y.H., 1991. Stick-Slip Vibration of Drill Strings. *Journal of Engineering for Industry*, 113(1), pp.38–43.

Liu, G., 2012. Breakroom for drilling proffesionals. *Pengasus Vertex*.

Liu, X. et al., 2014. State-dependent delay influenced drill-string oscillations and stability analysis. *Journal of Vibration and Acoustics*, 136(5).

Macpherson, J.D., Mason, J.S. & Kingman, J.E.E., 1993. Surface Measurement and Analysis of Drillstring Vibrations While Drilling. In *Society of Petroleum Engineers, SPE/IADC Drilling Conference*. Amsterdam, Netherlands: Society of Petroleum Engineers.

Majeed, F.A., 2013. *Analysis and control of rotary drilling rigs*. Loughborough University. Available at: https://dspace.lboro.ac.uk/2134/12559.

Majeed, F.A., 2013. *Analysis and control of rotary drilling rigs*. Loughborough University. Available at: https://dspace.lboro.ac.uk/2134/12559.

Mason, J.S. & Sprawls, B.M., 1998. Addressing BHA Whirl: The Culprit in Mobile Bay. In *SPE Drilling & Completion, 1996 SPE/IADC Drilling Conference*. New Orleans, pp. 231–236.

Mihajlovic, N. et al., 2004a. Analysis of friction-induced limit cycling in an experimental drill-string system. *Journal of Dynamic Systems, Measurement, and*

Control, 126(4), pp.709–720.

Mihajlovic, N. et al., 2004b. Analysis of friction-induced limit cycling in an experimental drill-string system Journal of dynamic systems, measurement and control. *Journal of dynamic systems, measurement, and control*, 126(4), pp.709–720.

Mihajlovic, N. et al., 2006. Friction-induced limit cycling in flexible rotor systems: An experimental drill-string set-up. *Nonlinear Dynamics*, 46(3), pp.273–291.

Mihajlović, N. et al., 2007. Interaction between torsional and lateral vibrations in flexible rotor systems with discontinuous friction. *Nonlinear Dynamics*, 50(3), pp.679–699.

Navarro-Lopez, E.M. & Suarez, R., 2004. Practical approach to modelling and controlling stick-slip oscillations in oilwell drillstrings. In *Proceedings of the 2004 IEEE International Conference on Control Applications, 2004*. IEEE, pp. 1454–1460.

Navarro-López, E.M. & Suárez, R., 2004. Practical approach to modelling and controlling stick-slip oscillations in oilwell drillstrings. In *Control Applications, Proceedings of the 2004 IEEE International Conference on. Vol. 2. IEEE,*. IEEE, pp. 1454–1460.

Oliveira, A.R., 2004. The Contribution of Coulomb to Applied Mechanics. *International Symposium on History of Machines and Mechanisms*, pp.217–226.

Olsson, H. et al., 1998. Friction models and friction compensation. *European journal of control*, 4(3), pp.176–195.

Patil, P.A. & Teodoriu, C., 2013. A comparative review of modelling and controlling torsional vibrations and experimentation using laboratory setups. *Journal of Petroleum Science and Engineering*, 112, pp.227–238.

Pavone, D.R. & Desplans, J.P., 1994. Application of High Sampling Rate Downhole Measurements for Analysis and Cure of Stick-Slip in Drilling. In *SPE Annual Technical Conference and Exhibition*. New Orleans, Louisiana: Society of Petroleum Engineers, pp. 335–345.

Petzet, A., 2009. BP's Tiber one of industry's deepest wells. *oil and gas journal*.

Poletto, F. et al., 2014. Drill-bit seismic monitoring while drilling by downhole wired-pipe telemetry. *European Association of Geoscientists & Engineers*, 62(4), pp.702–718.

Popov, V., 2010. *Contact Mechanics and Friction: Physical Principles and Applications*, Berlin, Germany: Springer Science & Business Media.

Puebla, H. & Alvarez-Ramirez, J., 2008. Suppression of stick-slip in drillstrings: A control approach based on modeling error compensation. *Journal of Sound and Vibration*, 310(4–5), pp.881–901.

Ren, F. et al., 2016. Nonlinear Model and Qualitative Analysis for Coupled Axial/Torsional Vibrations of Drill String. *Shock and Vibration*. Available at: http://dx.doi.org/10.1155/2016/1646814.

Runia, D.J., Dwars, S. & Stulemeijer, I.P.J.M., 2013. A brief history of the Shell "Soft Torque Rotary System" and some recent case studies. In *SPE/IADC Drilling Conference*. Netherlands: Society of Petroleum Engineers.

Saldivar, B. et al., 2013. Suppressing Axial-Torsional Coupled Vibrations in Drillstrings. *Control Engineering and Applied Informatics*, 15(1), pp.3–10.

Saldivar, M.B. et al., 2015. *Analysis and control of oilwell drilling vibrations*, Springer.

Santos, H., Placido, J.C.R. & Wolter, C., 1999. Consequences and relevance of drillstring vibration on wellbore stability. In *SPE/IADC drilling conference*. Amsterdam: Society of Petroleum Engineers.

Shokir, E., 2004. A Novel PC Program for drill String Failure Detection and Prevention Before and While Drilling Specially in New Area. *Oil & Gas Business,*, pp.1–14. Available at: http://www.ogbus.com/eng/.

Simon, H.A., 1996. *The sciences of the artificial* 3rd editio., London, England: The MIT Press.

Skaugen, E., 1987. The Effects of Quasi-Random Drill Bit Vibrations Upon Drillstring Dynamic Behavior. In *Society of Petroleum Engineers, SPE Annual Technical Conference and Exhibition*. Dallas, Texas: One Petro.

Slotine, J.J.E. & Li, W., 1991. *Applied Nonlinear Control*, Englewood Cliffs, New

Jersey: Prentice-Hall, Inc.

Spracklen, C.T. & Aslam, T., 2013. Advanced Data Communications for Downhole Data Logging and Control Applications in the Oil Industry. In *Materials Science and Engineering*.

Stribeck, R., 1902. The key qualities of sliding and roller bearings. *Zeitschrift des Vereines Seutscher Ingenieure*, (46), pp.38–39.

Stroud, D.R.H. et al., 2012. Roller Reamer Fulcrum in Point-The-Bit Rotary Steerable System reduces Stick-Slip and Backward Whirl. In *Society of Petroleum Engineers, IADC/SPE Drilling Conference and Exhibition*. San Diego, California, USA: Society of Petroleum Engineers.

Tantos, A., 2011. H-Bridges - the Basics.

Texter, E.C., Irwin, W.A. & Kaump, D.H., 1949. Roentgenologic findings in osteomyelitis following bone marrow infusions in infants; review of literature and report of two cases. *The American journal of roentgenology and radium therapy*, 62(4), p.534.

Tian-shou, M. & Ping, C., 2015. Development and Use of a Downhole System for Measuring Drilling Engineering Parameters. *Chemistry and Technology of Fuels and Oils*, 51(3), pp.294–307.

Tucker, W.R. & Wang, C., 1999. On the Effective Control of Torsional Vibrations in Drilling Systems. *Journal of Sound and Vibration*, 224(1), pp.101–122. Available at: http://dx.doi.org/10.1006/jsvi.1999.2172.

Vaisberg, O. et al., 2002. Fatigue of drillstring: state of the art. *Applied mechanics for the Oil Industry*, 57(1), pp.7–37.

Viguié, R. & Kerschen, G., 2009. Nonlinear vibration absorber coupled to a nonlinear primary system: a tuning methodology. *Journal of Sound and Vibration*, 326(3–5), pp.780–793.

W. Dareing, D. & Joe Livesay, B., 1968. Longitudinal and Angular Drill-String Vibrations With Damping. *Journal of Engineering for Industry*, 90(4).

W. Dykstra, M., C. -K. Chen, D. & M. Warren, T., 1994. Experimental Evaluations of Drill Bit and Drill String Dynamics. *Society of Petroleum Engineers, SPE Annual*

Technical Conference and Exhibition.

Warren, T.M., 1997. Drilling tool.

Wiercigroch, M. et al., 2015. Unveiling Complexities of Drill-String and BHA Dynamics on New Experimental Rig. In *DINAME Proceedings of the XVII International Symposium on Dynamic Problems of Mechanics*. pp. 22–27.

Wu, X. et al., 2010. Decoupling Stick/Slip and Whirl To Achieve Breakthrough in Drilling Performance. In *IADC/SPE Drilling Conference and Exhibition,*. New Orleans, Louisiana, USA: One Petro, pp. 966–978.

Yigit, A.S. & Christoforou, A.P., 1998. Coupled torsional and bending vibrations of drillstrings subject to impact with friction. *Journal of Sound and Vibration*, 215(1), pp.167–181.

Appendices

Appendix A

Experiment drill string design
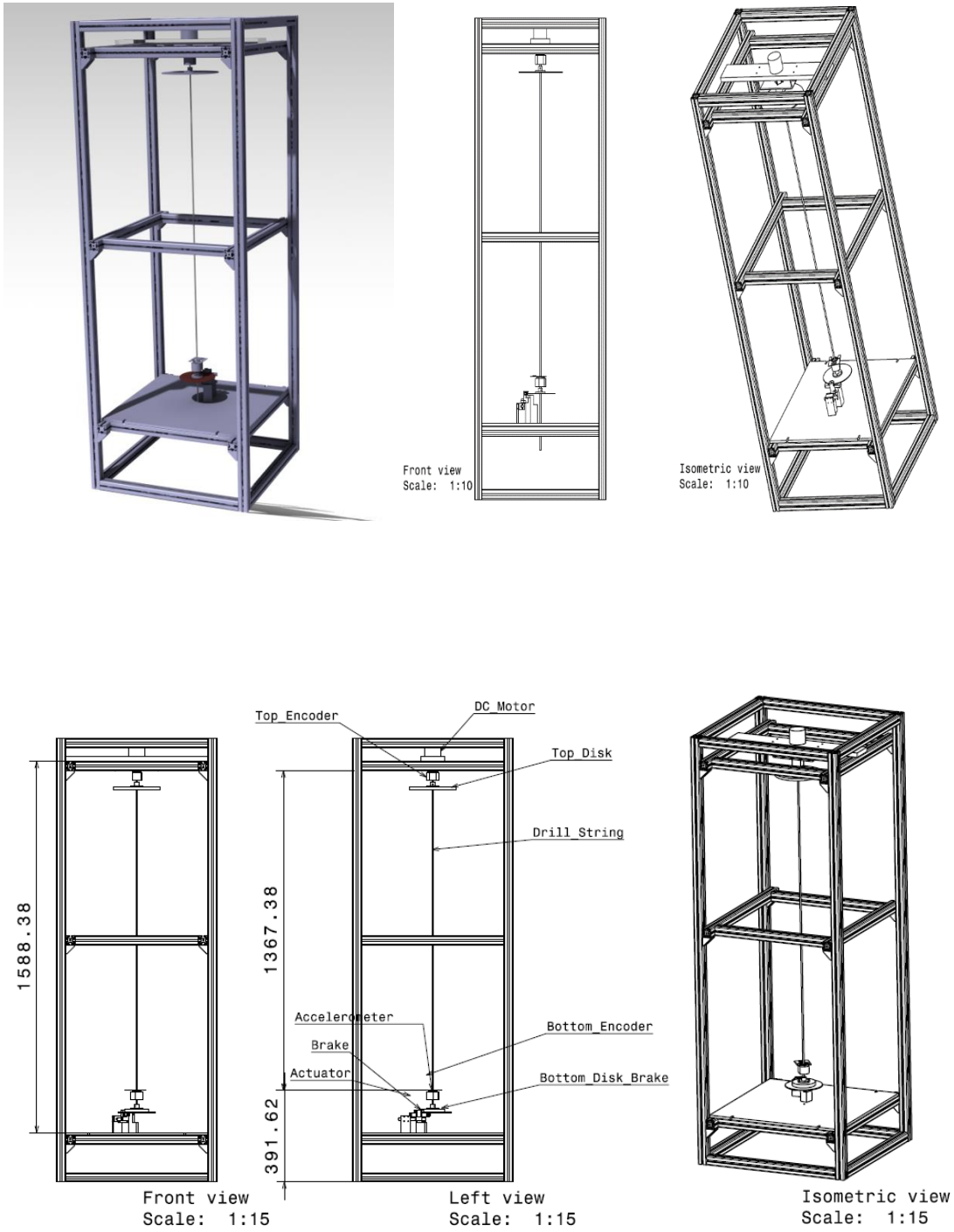
Flange layout
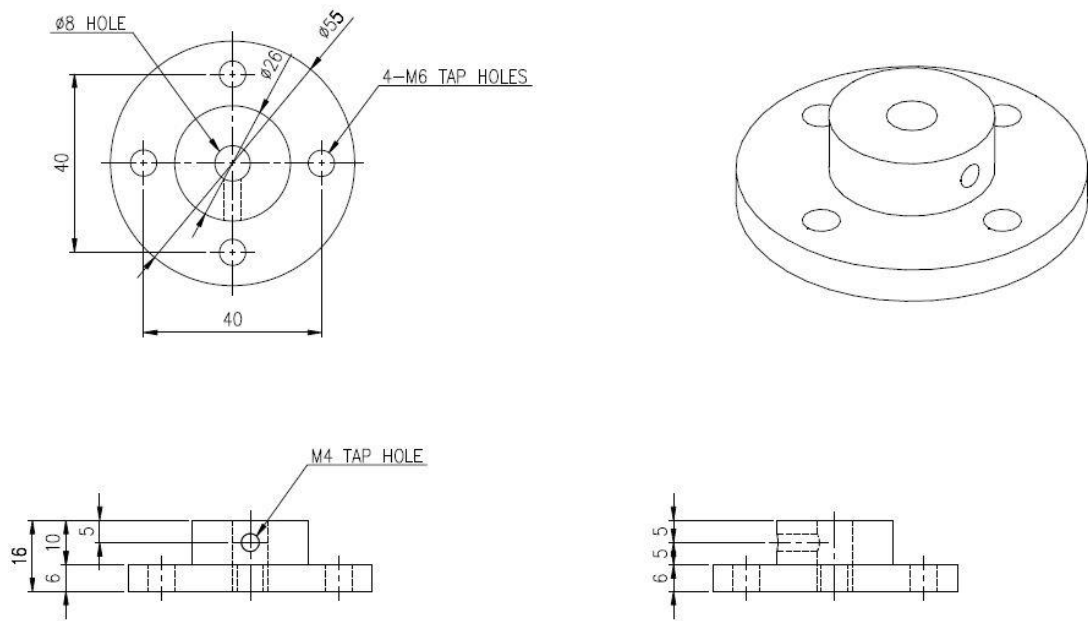
Plate support layout
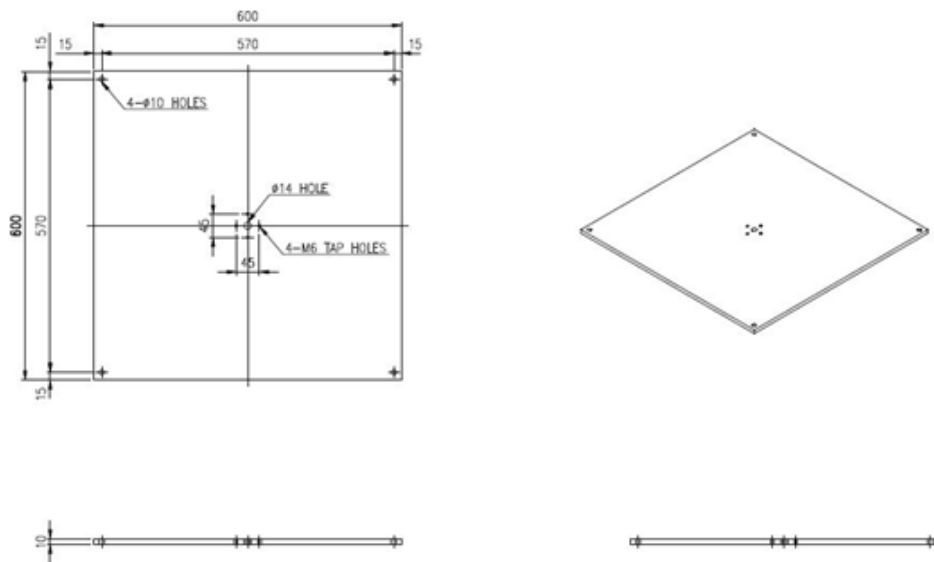
Bearing cover layout
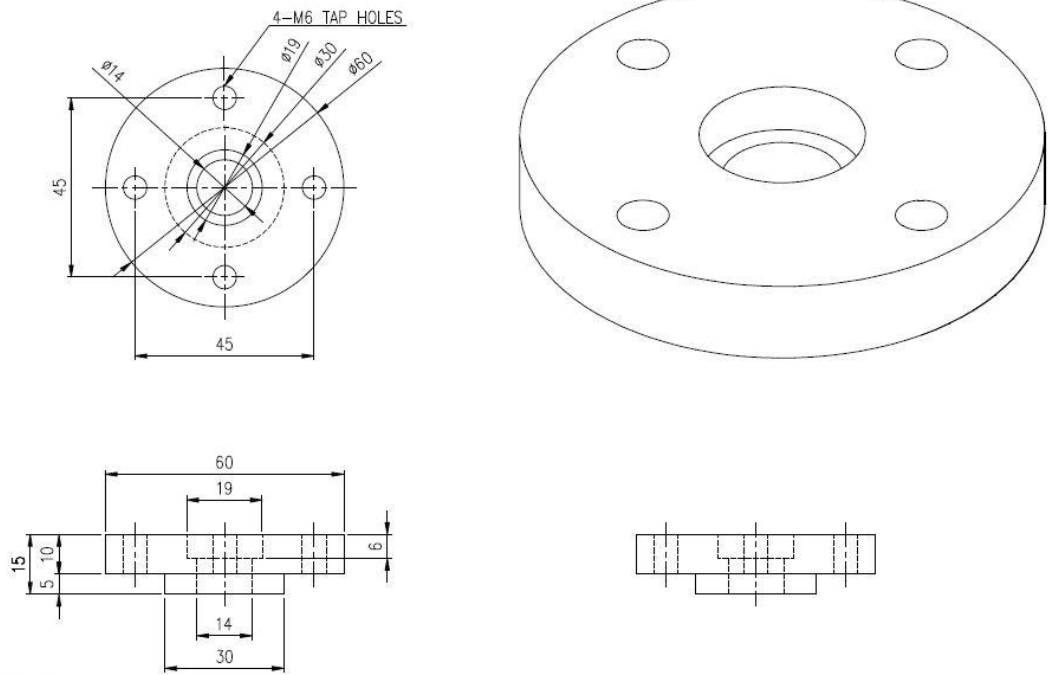
Appendix B

Static simulation -CATIA

Example: 47 RPM

MESH:

Entity	Size
Nodes	1890
Elements	6150

ELEMENT TYPE:

Connectivity	Statistics
TE4	6150 (100.00%)

ELEMENT QUALITY:

Criterion	Good	Poor	Bad	Worst	Average
Stretch	5644 (91.77%)	506 (8.23%)	0 (0.00%)	0.126	0.614
Aspect Ratio	5661 (92.05%)	489 (7.95%)	0 (0.00%)	6.244	2.101

Materials.1

Material	Steel
Young's modulus	2e+011N_m2
Poisson's ratio	0.266
Density	7860kg_m3
Coefficient of thermal expansion	1.17e-005_Kdeg
Yield strength	2.5e+008N_m2

Material	Aluminium
Young's modulus	7e+010N_m2
Poisson's ratio	0.346
Density	2710kg_m3
Coefficient of thermal expansion	2.36e-005_Kdeg
Yield strength	9.5e+007N_m2

Mode number	Frequency Hz	Stability
1	7.1784e-001	1.3971e-015
2	7.3076e-001	4.0444e-015
3	5.9276e+001	1.3908e-010
4	6.0174e+001	2.9460e-010
5	1.6211e+002	1.7728e-007
6	1.6451e+002	2.3273e-007
7	3.1544e+002	8.7486e-006
8	3.1992e+002	1.3575e-005
9	5.1790e+002	2.4578e-005
10	5.2463e+002	2.0514e-004

Frequency Case Solution.2 - Deformed mesh.3

Occurrence: 1 - Value: 0.717837Hz

Figure 2

Occurrence: 2 - Value: 0.730763Hz

Figure 3

Example: 216 RPM

Figure 2

Figure 3

Mode number	Frequency Hz	Stability
1	3.5730e+000	1.1279e-015
2	3.6302e+000	6.5557e-016
3	5.9276e+001	1.3839e-010
4	6.0174e+001	2.9305e-010
5	1.6211e+002	1.7727e-007
6	1.6451e+002	2.3272e-007
7	3.1544e+002	8.7486e-006
8	3.1992e+002	1.3575e-005
9	5.1790e+002	2.4578e-005
10	5.2463e+002	2.0514e-004

Figure 2

Figure 3

Mode number	Frequency Hz	Stability
1	5.6565e+000	7.2001e-016
2	5.7468e+000	5.7550e-015
3	5.9276e+001	1.3840e-010
4	6.0174e+001	2.9302e-010
5	1.6211e+002	1.7727e-007
6	1.6451e+002	2.3272e-007
7	3.1544e+002	8.7486e-006
8	3.1992e+002	1.3575e-005
9	5.1790e+002	2.4578e-005
10	5.2463e+002	2.0514e-004

Appendix C

MSc ADAMS Catalogue

Modeling and Visualization

ADAMS/View

FEATURES

- Model or import geometry in wireframe or 3D solids
- Extensive library of joints and constraints
- Realistic 3D animation
- Visualization of modal forces, stresses, and strains
- Export options to FEA, physical test, and fatigue file formats
- Plot simulation results
- Advanced lighting control with reflections and multiple sources

BENEFITS

- Quickly build and review models for simulation
- Improve efficiency by automating process through customization
- Manually change design parameters and compare iterations to answer what-if questions about your design
- Visually share your design ideas with your product development teammates
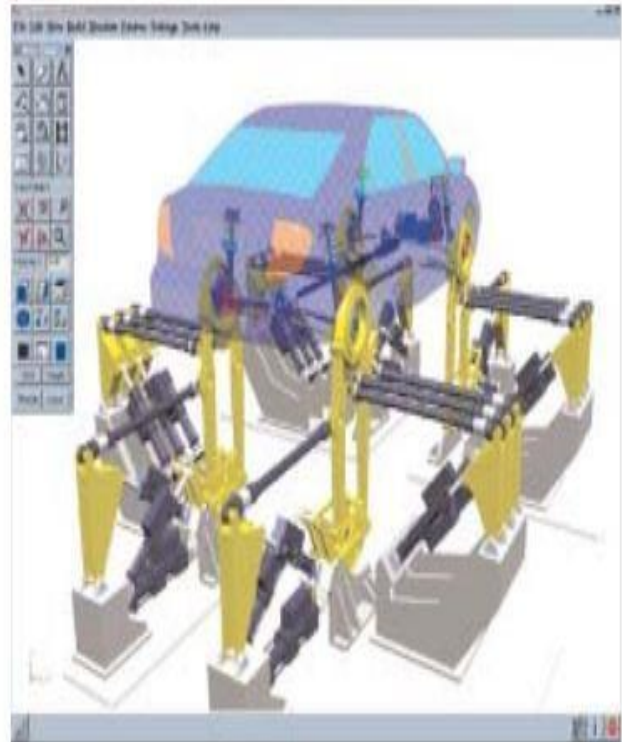
ADAMS/View provides high-end modeling and visualization capabilities in one seamlessly integrated environment. In addition, any element of ADAMS/View's interface – including the toolbox, icons, and menus – can be customized to suit your specific needs.

With ADAMS/View, you build a virtual prototype of a mechanical system just as you would build the physical prototype – creating parts, connecting them with joints, assembling the system, and driving it with physically accurate forces and motions. You can apply springs, dampers, contacts, and friction to improve the fidelity of the simulation. ADAMS/View supports parametric modeling so that the model can be easily modified and used in designed experiments.

For visualization, ADAMS/View provides the ability to animate your models and view key measures of specific simulation data even as your simulation is in progress. This helps you quickly zero in on areas of your model needing refinement. You can apply these capabilities at the very earliest stages of your design, so you can identify and correct problems quickly.

Appendix D

Fast Fourier Transform Algorithm- MATLAB Code

```matlab
%Load data from experiment data for selenoid brake
selenoid_x = load('selenoid_Brake.txt');
N =length(selenoid_x);
fs = 30;
fnyquist = fs/2;

%Load data from experiment data for sudden brake
sudden_x = load('Sudden_Brake.txt');
N1 =length(sudden_x);
fs = 30;
fnyquist = fs/2;

%ftt for selenoid brake
x1_mags = abs(fft(selenoid_x));
bin_vals = [0 : N-1];
N1_2 = ceil(N/2);

%ftt for sudden brake
x2_mags = abs(fft(sudden_x));
bin_vals = [0 : N-1];
N2_2 = ceil(N/2);

fnyquist = fs/2;
fax_Hz = bin_vals*fs/N;

%plotting the graph
plot(fax_Hz(1:N1_2), x1_mags(1:N1_2),'r','LineWidth',1)
hold on
plot(fax_Hz(1:N2_2), x2_mags(1:N2_2),'b:','LineWidth',1)

xlabel('Frequency (Hz)')
ylabel('decibel (dB)');
legend('Solenoid Brake', 'Sudden Brake');
title('Single-sided Magnitude spectrum (Hertz) - 47 rpm');
axis tight
```

Appendix E

C language coding (Arduino MEGA 2560 / ChipKIT Uno32)

```c
#include <stdio.h>
////written by Muhammad Effendy, Guillermo Schkzamian for DAQ encoder 14 bit, acceleromter ADXL 335, Voltage divider sensor, clock-time
////For the purpose of labview DAQ
///////////////////////////////////////////////////////////////////////////////////////

char inComingChar = 0;   // for incoming serial data
// Defining variables for the first Encoder

int s1cw = 0;   // Clockwise MSB, Brown Cable // First Encoder
int s1ccw = 0; // Counter Clockwise MSB Yellow Cable // First Encoder
int s2 = 0;     // White // First Encoder
int s3 = 0;     // Green // First Encoder
int s4 = 0;     //Orange // First Encoder // Changes 0->1 at small angle
int s5 = 0;     //Blue // First Encoder
int s6 = 0;     //Violet // First Encoder
int s7 = 0;     //Grey // First Encoder
int s8 = 0;     //Pink // First Encoder
int s9 = 0;     //Red/Green // First Encoder
int s10 = 0;    //Red-Yellow // First Encoder
int s11 = 0;    //Turquoise // First Encoder
int b = 0;      //binary number created // First Encoder
int b1 =0;      // First Encoder
int b2 = 0;     // First Encoder
int b3 = 0;     // First Encoder
int b4 = 0;     // First Encoder
int b5 = 0;     // First Encoder
int b6 = 0;     // First Encoder
int b7 = 0;     // First Encoder
int b8 = 0;     // First Encoder
int b9 = 0;     // First Encoder
int b10 = 0;    // First Encoder
int b11= 0;     // First Encoder
//////////////////////////////////////////////////////////////////////////
float time = 0.0; // this is the time counting
//////////////////////////////////////////////////////////////////////////
// Defining variables for the Second Encoder
```

```c
int s1cwA = 0;   // Clockwise MSB, Brown Cable // Second Encoder
int s1ccwA = 0; // Counter Clockwise MSB Yellow Cable // Second Encoder
int s2A = 0;     // White // Second Encoder
int s3A = 0;     // Green  // Second Encoder
int s4A = 0;     //Orange // Second Encoder //Changes 0->1 at small angle
int s5A = 0;     //Blue // Second Encoder
int s6A = 0;     //Violet // Second Encoder
int s7A = 0;     //Grey // Second Encoder
int s8A = 0;     //Pink // Second Encoder
int s9A = 0;     //Red/Green
int s10A = 0;    //Red-Yellow // Second Encoder
int s11A = 0;    //Turquoise // Second Encoder
int bA = 0;      //binary number created // Second Encoder
int b1A =0;      // Second Encoder
int b2A = 0;     // Second Encoder
int b3A = 0;     // Second Encoder
int b4A = 0;     // Second Encoder
int b5A = 0;     // Second Encoder
int b6A = 0;     // Second Encoder
int b7A = 0;     // Second Encoder
int b8A = 0;     // Second Encoder
int b9A = 0;     // Second Encoder
int b10A = 0;    // Second Encoder
int b11A = 0;    // Second Encoder
////////////////////////////////////////////////////////////////////////////////////////////////////////////
// Defining variable for accelerometer (x,y,Z)
int numreadingsX = 2;
int numreadingsY = 2;
int numreadingsZ = 2;

int readingX[2];
int readingY[2];
int readingZ[2];
```

```cpp
int y =0;
int z =0;

int X=0;
int Y=0;
int Z=0;

int i =0;

int totalX =0;
int totalY =0;
int totalZ =0;

int averageX =0;
int averageY =0;
int averageZ =0;

const int sampleSize = 10;
// Defining variable for braking voltage
int Val = 0;
int Vol = 0;

// The 11 bits encoder gives a Gray number which must be converted into binary and decimal. using the formula: //
// (b11*1)+(b10*2)+(b9*4)+(b8*8)+(b7*16)+(b6*32)+(b5*64)+(b4*128)+(b3*256)+(b2*512)+(b1*1024)                   //
// b1 =slcw;                                                                                                   //
// b2 = b1^s2;                                                                                                 //
// b3 = b2^s3;                                                                                                 //
// b4 = b3^s4;                                                                                                 //
// b5 = b4^s5;                                                                                                 //
// b6 = b5^s6;                                                                                                 //
// b7 = b6^s7;                                                                                                 //
// b8 = b7^s8;                                                                                                 //
// b9 = b8^s9;                                                                                                 //
// b10 = b9 ^s10;                                                                                              //
// b11 = b10^s11;                                                                                              //
/////////////////////////////////////////////////////////////////////////////////////////////////////////////


void setup()
{
 attachCoreTimerService(MyCallback);
 Serial.begin(9600);   // Set Serial Communication -> sync with labview

  // Encoder 1,  Pin  layout
  pinMode(2,INPUT); //Declare Pin 2 as INPUT
  pinMode(3,INPUT); //Declare Pin 3 as INPUT
  pinMode(4,INPUT); //Declare Pin 4 as INPUT
  pinMode(5,INPUT); //Declare Pin 5 as INPUT
  pinMode(6,INPUT); //Declare Pin 6 as INPUT
  pinMode(7,INPUT); //Declare Pin 7 as INPUT
  pinMode(8,INPUT); //Declare Pin 8 as INPUT
  pinMode(9,INPUT); //Declare Pin 9 as INPUT
  pinMode(41,INPUT); //Declare Pin 10 as INPUT
  pinMode(11,INPUT); //Declare Pin 11 as INPUT
  pinMode(12,INPUT); //Declare Pin 0 as INPUT
  pinMode(13,INPUT); //Declare Pin 1 as INPUT


  // Encoder 2 Pin layout
  pinMode(28,INPUT); //Declare Pin 28 as INPUT
  pinMode(29,INPUT); //Declare Pin 29 as INPUT
  pinMode(30,INPUT); //Declare Pin 30 as INPUT
  pinMode(31,INPUT); //Declare Pin 31 as INPUT
  pinMode(32,INPUT); //Declare Pin 32 as INPUT
  pinMode(33,INPUT); //Declare Pin 33 as INPUT
  pinMode(34,INPUT); //Declare Pin 34 as INPUT
  pinMode(35,INPUT); //Declare Pin 35 as INPUT
  pinMode(36,INPUT); //Declare Pin 36 as INPUT
  pinMode(37,INPUT); //Declare Pin 37 as INPUT
  pinMode(38,INPUT); //Declare Pin 38 as INPUT
  pinMode(39,INPUT); //Declare Pin 39 as INPUT
```

```
  // Accelerometer Pin layout
  pinMode(A0,INPUT); //Declare Pin A0 as INPUT
  pinMode(A1,INPUT); //Declare Pin A1 as INPUT
  pinMode(A2,INPUT); //Declare Pin A2 as INPUT

  // Brake voltage Pin layout
  pinMode(A7,INPUT); //Declare Pin A7 as INPUT

}

void loop()
{
 // Aquiring data from the FIRST Encoder

 s11 = digitalRead(2); // LSB   pin 2  which is the attachInterrupt(0, readings, CHANGE)
 s10 = digitalRead(3);
 s9 = digitalRead(4);
 s8 = digitalRead(5);
 s7 = digitalRead(6);
 s6 = digitalRead(7);
 s5 = digitalRead(8);
 s4 = digitalRead(9); // orange changes 0->1 every small angle
 s3 = digitalRead(41);
 s2 = digitalRead(11); // white changes 0->1 every half cycle
 s1ccw = digitalRead(12);
 s1cw = digitalRead(13);

 // Aquiring data from the SECOND Encoder
 s11A = digitalRead(28); // LSB   pin 2  which is the attachInterrupt(0, readings, CHANGE)
 s10A = digitalRead(29);
 s9A = digitalRead(30);
 s8A = digitalRead(31);
 s7A = digitalRead(32);
 s6A = digitalRead(33);
 s5A = digitalRead(34);
```

```
 b7A = b6A^s7A;
 b8A = b7A^s8A;
 b9A = b8A^s9A;
 b10A = b9A ^s10A;
 b11A = b10A^s11A;

 bA = (b11A*1)+(b10A*2)+(b9A*4)+(b8A*8)+(b7A*16)+(b6A*32)+(b5A*64)+(b4A*128)+(b3A*256)+(b2A*512)+(b1A*1024);

 // calculate at every 2 data [2]
 /// X-Axis
 //totalX =totalX-readingX[i];
 //readingX[i]=x;
 //totalX =totalX+readingX[i];
 //i =i+1;
 ///Y-Axis
// totalY =totalY-readingY[i];
// readingY[i]=y;
 //totalY =totalY+readingY[i];
// i =i+1;
 ///Z-Axis
// totalZ =totalZ-readingZ[i];
// readingZ[i]=z;
 //totalZ =totalZ+readingZ[i];
 i =i+1;
/////////////////////////////////////////////////////////////////////////////////////////////////////////////

 if (Serial.available() > 0) {
      // read the incoming character:
 inComingChar = Serial.read();
 if ( inComingChar == 'r') {   // I arbitrarily used r for a trigger
Serial.print(time,4);
Serial.print(" ");
Serial.print(averageX);
Serial.print(" ");
Serial.print(averageY);
Serial.print(" ");



 s4A = digitalRead(35); // orange changes 0->1 every small angle
 s3A = digitalRead(36);
 s2A = digitalRead(37); // white changes 0->1 every half cycle
 s1ccwA = digitalRead(38);
 s1cwA = digitalRead(39);

 //acquiring data from accelerometer (x,y,z)
 int x = analogRead(A0);
 int y = analogRead(A1);
 int z = analogRead(A2);

 //acquiring data from voltage brake
 int Vol = analogRead(A7);

 // GRAY Code to BINARY Conversion   First Encoder
 b1 =s1cw;
 b2 = b1^s2;
 b3 = b2^s3;
 b4 = b3^s4;
 b5 = b4^s5;
 b6 = b5^s6;
 b7 = b6^s7;
 b8 = b7^s8;
 b9 = b8^s9;
 b10 = b9 ^s10;
 b11 = b10^s11;

 b = (b11*1)+(b10*2)+(b9*4)+(b8*8)+(b7*16)+(b6*32)+(b5*64)+(b4*128)+(b3*256)+(b2*512)+(b1*1024);

 // GRAY Code to BINARY Conversion   Second Encoder
 b1A =s1cwA;
 b2A = b1A^s2A;
 b3A = b2A^s3A;
 b4A = b3A^s4A;
 b5A = b4A^s5A;
 b6A = b5A^s6A;
```

Appendix F

ADXL 335 Data sheet

ANALOG DEVICES

Small, Low Power, 3-Axis ±3 g Accelerometer
ADXL335

FEATURES

3-axis sensing
Small, low profile package
   4 mm × 4 mm × 1.45 mm LFCSP
Low power : 350 μA (typical)
Single-supply operation: 1.8 V to 3.6 V
10,000 g shock survival
Excellent temperature stability
BW adjustment with a single capacitor per axis
RoHS/WEEE lead-free compliant

APPLICATIONS

Cost sensitive, low power, motion- and tilt-sensing
   applications
   Mobile devices
   Gaming systems
   Disk drive protection
   Image stabilization
   Sports and health devices

GENERAL DESCRIPTION

The ADXL335 is a small, thin, low power, complete 3-axis accelerometer with signal conditioned voltage outputs. The product measures acceleration with a minimum full-scale range of ±3 g. It can measure the static acceleration of gravity in tilt-sensing applications, as well as dynamic acceleration resulting from motion, shock, or vibration.

The user selects the bandwidth of the accelerometer using the C_X, C_Y, and C_Z capacitors at the X_{OUT}, Y_{OUT}, and Z_{OUT} pins. Bandwidths can be selected to suit the application, with a range of 0.5 Hz to 1600 Hz for the X and Y axes, and a range of 0.5 Hz to 550 Hz for the Z axis.

The ADXL335 is available in a small, low profile, 4 mm × 4 mm × 1.45 mm, 16-lead, plastic lead frame chip scale package (LFCSP_LQ).

FUNCTIONAL BLOCK DIAGRAM

Figure 1.

SPECIFICATIONS

$T_A = 25°C$, $V_S = 3$ V, $C_X = C_Y = C_Z = 0.1$ μF, acceleration = 0 g, unless otherwise noted. All minimum and maximum specifications are guaranteed. Typical specifications are not guaranteed.

Table 1.

Parameter	Conditions	Min	Typ	Max	Unit
SENSOR INPUT	Each axis				
Measurement Range		±3	±3.6		g
Nonlinearity	% of full scale		±0.3		%
Package Alignment Error			±1		Degrees
Interaxis Alignment Error			±0.1		Degrees
Cross-Axis Sensitivity[1]			±1		%
SENSITIVITY (RATIOMETRIC)[2]	Each axis				
Sensitivity at X_{OUT}, Y_{OUT}, Z_{OUT}	$V_S = 3$ V	270	300	330	mV/g
Sensitivity Change Due to Temperature[3]	$V_S = 3$ V		±0.01		%/°C
ZERO g BIAS LEVEL (RATIOMETRIC)					
0 g Voltage at X_{OUT}, Y_{OUT}	$V_S = 3$ V	1.35	1.5	1.65	V
0 g Voltage at Z_{OUT}	$V_S = 3$ V	1.2	1.5	1.8	V
0 g Offset vs. Temperature			±1		mg/°C
NOISE PERFORMANCE					
Noise Density X_{OUT}, Y_{OUT}			150		μg/√Hz rms
Noise Density Z_{OUT}			300		μg/√Hz rms
FREQUENCY RESPONSE[4]					
Bandwidth X_{OUT}, Y_{OUT}[5]	No external filter		1600		Hz
Bandwidth Z_{OUT}[5]	No external filter		550		Hz
R_{FILT} Tolerance			32 ± 15%		kΩ
Sensor Resonant Frequency			5.5		kHz
SELF-TEST[6]					
Logic Input Low			+0.6		V
Logic Input High			+2.4		V
ST Actuation Current			+60		μA
Output Change at X_{OUT}	Self-Test 0 to Self-Test 1	−150	−325	−600	mV
Output Change at Y_{OUT}	Self-Test 0 to Self-Test 1	+150	+325	+600	mV
Output Change at Z_{OUT}	Self-Test 0 to Self-Test 1	+150	+550	+1000	mV
OUTPUT AMPLIFIER					
Output Swing Low	No load		0.1		V
Output Swing High	No load		2.8		V
POWER SUPPLY					
Operating Voltage Range		1.8		3.6	V
Supply Current	$V_S = 3$ V		350		μA
Turn-On Time[7]	No external filter		1		ms
TEMPERATURE					
Operating Temperature Range		−40		+85	°C

[1] Defined as coupling between any two axes.
[2] Sensitivity is essentially ratiometric to V_S.
[3] Defined as the output change from ambient-to-maximum temperature or ambient-to-minimum temperature.
[4] Actual frequency response controlled by user-supplied external filter capacitors (C_X, C_Y, C_Z).
[5] Bandwidth with external capacitors = $1/(2 × \pi × 32$ kΩ $× C)$. For C_X, $C_Y = 0.003$ μF, bandwidth = 1.6 kHz. For $C_Z = 0.01$ μF, bandwidth = 500 Hz. For C_X, C_Y, $C_Z = 10$ μF, bandwidth = 0.5 Hz.
[6] Self-test response changes cubically with V_S.
[7] Turn-on time is dependent on C_X, C_Y, C_Z and is approximately 160 × C_X or C_Y or $C_Z + 1$ ms, where C_X, C_Y, C_Z are in microfarads (μF).

USE WITH OPERATING VOLTAGES OTHER THAN 3 V

The ADXL335 is tested and specified at $V_S = 3$ V; however, it can be powered with V_S as low as 1.8 V or as high as 3.6 V. Note that some performance parameters change as the supply voltage is varied.

The ADXL335 output is ratiometric, therefore, the output sensitivity (or scale factor) varies proportionally to the supply voltage. At $V_S = 3.6$ V, the output sensitivity is typically 360 mV/g. At $V_S = 2$ V, the output sensitivity is typically 195 mV/g.

The zero g bias output is also ratiometric, thus the zero g output is nominally equal to $V_S/2$ at all supply voltages.

The output noise is not ratiometric but is absolute in volts; therefore, the noise density decreases as the supply voltage increases. This is because the scale factor (mV/g) increases while the noise voltage remains constant. At $V_S = 3.6$ V, the X-axis and Y-axis noise density is typically 120 μg/√Hz, whereas at $V_S = 2$ V, the X-axis and Y-axis noise density is typically 270 μg/√Hz.

Self-test response in g is roughly proportional to the square of the supply voltage. However, when ratiometricity of sensitivity is factored in with supply voltage, the self-test response in volts is roughly proportional to the cube of the supply voltage. For example, at $V_S = 3.6$ V, the self-test response for the ADXL335 is approximately −560 mV for the X-axis, +560 mV for the Y-axis, and +950 mV for the Z-axis.

At $V_S = 2$ V, the self-test response is approximately −96 mV for the X-axis, +96 mV for the Y-axis, and −163 mV for the Z-axis.

The supply current decreases as the supply voltage decreases. Typical current consumption at $V_S = 3.6$ V is 375 μA, and typical current consumption at $V_S = 2$ V is 200 μA.

AXES OF ACCELERATION SENSITIVITY
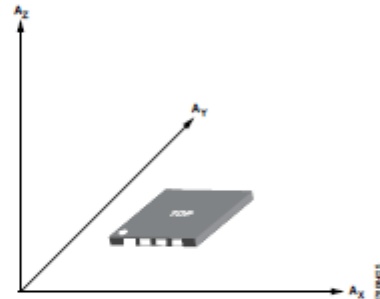
Figure 23. Axes of Acceleration Sensitivity; Corresponding Output Voltage Increases When Accelerated Along the Sensitive Axis.
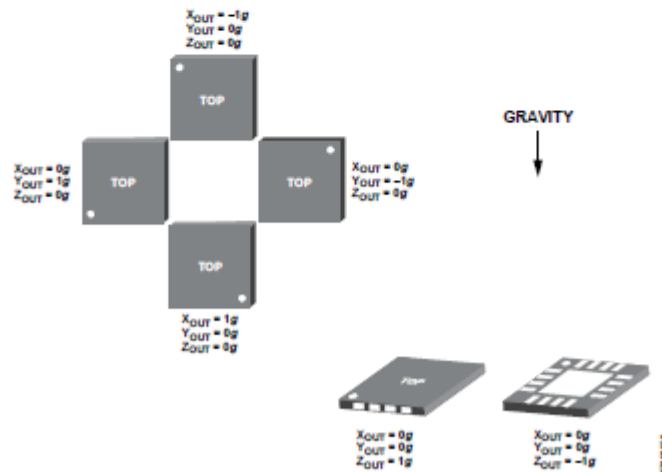

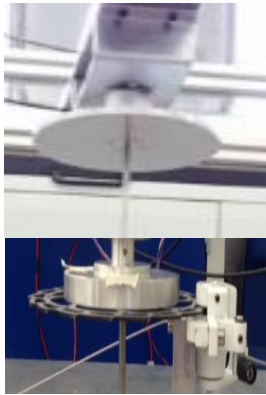Figure 24. Output Response vs. Orientation to Gravity
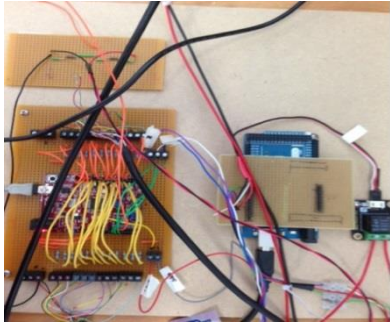
Appendix G

No	Item	Description	Image
1	DC Motor BL58 EB 50 W	A DC motor as the main driving device to stimulate the system. Brushless DC motor features: i) Maximum speed of 4000rpm ii) Flexible/adjustable speed loop iii) Directional control input (forward / backward) iv) Thermal motor protection	
2	Rotating Discs (upper and lower)	• Upper disc (12 inches) represents to the actual rotary table of the drill string. • Lower disc (6 inches) represents to the BHA bottom hole assembly which is combination of the drill collar and drill bits.	
3	Encoder 960 Single Turn	Absolute rotary encoders are to be used to measure the rotation angles of the discs. The revolution of this encoder is 2047bits per revolution. The single-turn Model 960 Absolute series provides an unique solution to a wide variety of industrial applications requiring absolute position information. By providing a low profile package of just 40mm, a variety of thru-bore and blind-	

		bore sizes, and an easy to use flexible mounting system, the Model 960 goes where traditional absolute encoders do not fit. In addition, its innovative Opto-ASIC circuitry, coupled with its digital output, make it an excellent choice in those applications plagued by an unusually high level of electrical noise. The Model 960 can easily be mounted directly on a motor shaft, bringing the advantage of absolute positioning in an all metal housing while eliminating the fixtures, couplers, and adapters required by other absolute encoder designs.	
4	Drill string	• Stainless steel grade-303 • Diameter: 6mm • Length:1500 mm • Modulus of elasticity :193 Mpa • Tensile strength, ultimate: 620 Mpa • Tensile strength, yield : 240 Mpa • Shear Modulus :77.2 Gpa • Poisson's ratio: 0.25	
5	Microcontroller	1. Microcontroller (chipKIT Uno32) Acquiring data feedback from 2 sensors (encoder and Accelerometer) 2. Microcontroller (Arduino MEGA2560) angular speed of drilling string and hard	

|		brake solenoid actuator Details:
		• Microchip® PIC32MX320F128 processor
		  i) 80 Mhz 32-bit MIPS
		  ii) 128K Flash, 16K SRAM
		• Compatible with many existing Arduino™ code examples, reference materials and other resources.
		• (OPEN SOURCE)Arduino™ "Uno" form factor
		• Connects to a PC using a USB	

6	Accelerometer	GY-61 ADXL335 3-Axis Analog Output Details: • 3-axis sensing (X,Y and Z) • Small, low profile package 4 mm × 4 mm × 1.45 mm LFCSP • Single-supply operation: 1.8 V to 3.6 V • 10,000 g shock survival	
7	Power supply	Run motor connected to drill string up to desired speed (low, medium, fast). Detail: • Dual adjustable outputs: 0-30V and 0-5A • Fixed output: 5V and 3A • Display reading accuracy: +/-1% for voltage and +/-2% for current • Dual adjustable outputs: 0-30V and 0-5A • Fixed output: 5V and 3A • Display reading accuracy:	

		+/-1% for voltage and +/-2% for current	
8	Labview NI	Tool to integrate with all measurement hardware, existing legacy software, and IP while capitalizing on the latest computing technologies.	
9	Solenoid actuator	1kg Force 10mm Stroke Push Solenoid Electromagnet DC 12V. Rated Voltage : DC 12V;Resistance : 5.6Ohm;Action Form : Push	
10	Linear actuator	Linear actuator brake used to pull a string that attach to the brake for braking system.	
11	40 x 40 aluminium profile	As main based for the equipment and string.- entire frame support	

12	Microcontroller chipkit UNO32	As a data acquisition – sensors installed and stored (accelerometer and encoder are recorded continuously during the operation)	

Appendix H

BL58 EB — Brushless DC motor — **50 Watt**

Dimensional drawing
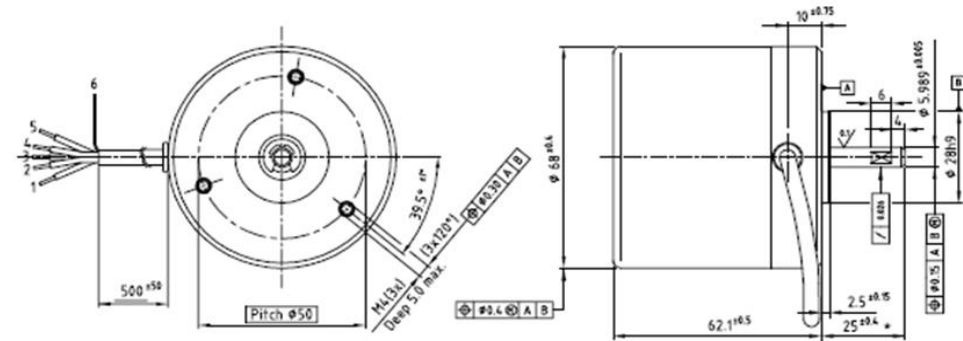
Motor data

| Motor order number | Shaft length 25 mm | 4322 016 58011 |
| | Shaft length 20 mm | 4322 016 58012 * |

Nominal Voltage	[V]	24
No load Speed (V in > 4V)	[rpm]	5050
No load Current (V in > 4V)	[mA]	380
Nominal Current limitation (V in > 4V)	[A]	3.1
Maximum torque	[mNm]	114
Maximum output power	[W]	50
Operating temperature range	[°C]	0 to 90
Thermal resistance from housing to ambient	[K/W]	3.7
Rotor inertia	[kgm²]	120x10⁻⁶
Mass of motor	[g]	550

Maximum radial load 20 mm from mounting front (no axial load towards flange)	[N]	40
Maximum axial load		
– towards flange (no radial load)	[N]	18
– from flange	[N]	10

Thermal motor protection :

Motor shuts down if the motor flange temperature reaches approx. 90°C
Motor restarts if the flange temperature is cooled down to approx. 80°C

For thermal reasons it is advised to mount the motor on a heat conducting frame if high output power is desired.

* Shaft 20 mm for combination with gearboxes.

Electrical Connection

Lead no.	Lead colour	Function	Description
1	brown	FW/RV	Direction control input : 'High' CW, 'Low' CCW (shaftside) (do not leave this lead floating)
2	white	V in	Input voltage (setpoint) for speed loop. Resulting speed approx. 1000 rpm/V. V in > 4 V : motor at full speed, speedloop off (open loop)
3	green	FG	Frequency generator output, 36 ppr ; R out = 4k Ohm (approx)
4	black	GND	Motor return, ground (0 V)
5	red	Vp	Motor supply voltage +24 V (min. 14 V – max 30 V)
6	bare	shield	Shield for cable and connected to motor housing

		min.	typ.	max.
Lead 1				
input 'high'	[V]	4.1	5	
input 'low'	[V]		0	1.9
abs. max/min. input	[V]			±30
Lead 2				
abs. max./min. input	[V]			±30
Lead 3				
output 'high', not loaded	[V]	4.0	4.5	5.0
output 'low', not loaded	[V]	0	0.1	0.2

Performance curve
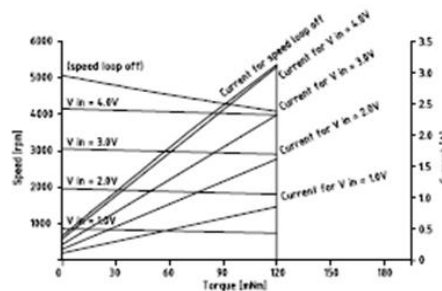
Product combinations

- Gearbox S64A
- Gearbox S69A
- Gearbox P50A
- Gearbox P59A

Options

- Square mounting flange
- Shaft diameter, 7 or 8 mm
- Speed loop with frequency input
- Protection class upto IP67DS

Features

- Adjustable speed loop
- Direction control input (forward / reverse)
- Frequency Generator output (speed sensing)
- Thermal motor protection
- Long life (20.000 hours)
- Low EMI
- Protection class IP54

Appendix I

Block diagram - LabVIEW